Real-time Personalized Tolling with Long-term Objectives

by

Yifei Xie

B.Sc., Technion - Israel Institute of Technology (2017)
S.M., Massachusetts Institute of Technology (2019)

Submitted to the Department of Civil and Environmental Engineering
in partial fulfillment of the requirements for the degree of

Doctor of Philosophy

at the

MASSACHUSETTS INSTITUTE OF TECHNOLOGY

February 2022

Author .....
Department of Civil and Environmental Engineering
January 14, 2022

Certified by .....
Moshe Ben-Akiva
Edmund K. Turner Professor of Civil and Environmental Engineering
Thesis Supervisor

Certified by .....
Ravi Seshadri
Assistant Professor, Technical University of Denmark
Thesis Supervisor

Accepted by .....
Colette L. Heald
Professor of Civil and Environmental Engineering
Chair, Graduate Program Committee

Real-time Personalized Tolling with Long-term Objectives

by

Yifei Xie

Submitted to the Department of Civil and Environmental Engineering
on January 14, 2022, in partial fulfillment of the
requirements for the degree of
Doctor of Philosophy

Abstract

Managed lanes are separate tolled lanes adjacent to free general-purpose lanes. The key real-time operation problem is how to set the toll for both effective network management and revenue generation, jointly considering the objectives of the operator, the travelers and the regulator. Based on a comprehensive analysis of travel behavior, this thesis develops a solution with adaptive personalized pricing.

Travelers are observed to either predominantly use managed lanes or almost never. This could be attributed to two competing latent behavioral factors: *preference heterogeneity*, and *state dependence*—not switching between options causally yields positive utility. Their econometric quantifications have crucial implications on pricing, but are challenging due to endogeneity known as the initial condition problem. We begin by proposing a Control Function solution under a general setting, which is shown to improve a commonly used solution by Wooldridge. Then, through applying the developed solutions to empirical data, we discovered heterogeneity and state dependence to be both significant in explaining the usage decision. It is further shown that when ignoring unobserved heterogeneity or the initial condition problem, state dependence will be largely overstated. Price endogeneity caused by dynamic pricing is also discovered and corrected.

The developed behavioral model is integrated into an online personalized tolling system that incorporates prediction, optimization and personalization. In addition to optimizing the toll adaptively, an online bi-level optimization problem is formulated to jointly offer personalized discounts. A flexible multi-component objective is designed to consider not only short-term revenue and social welfare, but also the impact on future revenue based on the state-dependent choice behavior. The online personalized tolling system is deployed to a microscopic traffic simulator calibrated with real data. The results show simultaneous improvements of revenue, traffic conditions and social welfare. Equity improvement is also discovered as travelers with lower values of time are presented lower tolls.

The developed methodologies for behavioral analysis and personalized pricing could be directly adapted for other applications in transportation and beyond.

Thesis Supervisor: Moshe Ben-Akiva
Title: Edmund K. Turner Professor of Civil and Environmental Engineering

Thesis Supervisor: Ravi Seshadri
Title: Assistant Professor, Technical University of Denmark

Acknowledgments

I would like to thank my advisor Prof. Moshe Ben-Akiva for his continuous and irreplaceable guidance and for being a great inspiration, and my co-advisor Prof. Ravi Seshadri for working closely with me, encouraging me and providing detailed insights.

I would like to thank my committee members Prof. Jinhua Zhao, Prof. Carolina Osorio, and Prof. Tomer Toledo for their valuable comments and suggestions on my thesis.

I would like to thank my friends and colleagues at the ITS lab, which include Mazen Danaf, Siyu Chen, Youssef Medhat Aboutaleb, Yundi Zhang, Haizheng Zhang, Peiyu Jing, Xiang Song and many others. I collaborated with Mazen Danaf and Yundi Zhang on different parts of this thesis and enjoyed the process.

I would like to thank Cintra/Ferrovial for sponsoring this research and their team, including John Brady, Wei He, Thu Hoang, and Ricardo Sanchez, for their insights and feedbacks.

Last but not the least, special thanks go to my parents who have always been supportive of all the decisions I made, and my girlfriend Shuyan Wang for her unconditional support.

Contents

List of Figures

List of Tables

Chapter 1

Introduction

1.1 Background

1.1.1 Managed Lanes

Transportation networks worldwide are plagued by congestion and inefficient usage of existing infrastructure, which lead to increased energy consumption, emissions, and economic costs. In 2019, the congestion in U.S. is estimated to cost travelers in total $88 billion [5]. Despite the COVID-19 pandemic that caused a significant drop in traffic in 2020 [6], it has been widely observed that congestion has gradually returned to pre-pandemic levels [1, 7, 8].

Among various solutions to mitigate congestion, road pricing schemes have attracted the most attention. In the U.S., road pricing is commonly implemented on highway corridors in urban areas, in the form of managed lanes (henceforth referred as ML) that are separate and tolled lanes in parallel to free general-purpose lanes (henceforth referred as GP) [107]. Figure 1-1 shows an example of such a facility near the Atlanta metropolitan area [4].

ML are often constructed and operated through concessions between private operators and the regulator [3]. The private operator is responsible for the ML's construction and the maintenance of the highway corridor, in return for the right to collect toll revenue over a long period of time, commonly several decades.

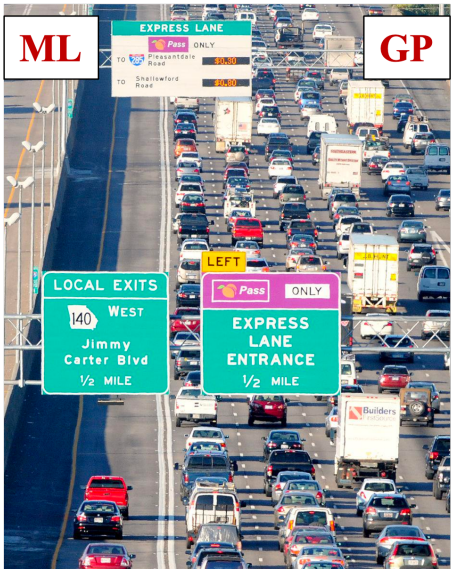

Figure 1-1: Managed Lanes near Atlanta, GA

For network management and revenue generation, the operator typically adjusts the toll on ML dynamically according to the demand and traffic conditions, commonly every 5 minutes. The toll in effect are communicated to the travelers via dynamic message signs (e.g., the white board in Figure 1-1). A single toll is often applied to all travelers, sometimes with pre-determined group-level discounts and exemptions.

Commonly, the concession agreement includes regulations on how frequent the toll is allowed to change, target level of service on the ML (e.g., minimum speed), and the maximum toll. When excessive demand is encountered, the maximum toll constraint is relaxed to guarantee that no congestion appears on the managed lanes.

In terms of benefits, ML provide additional capacity to the corridor and actively manage the induced demand with tolling. They are therefore expected to reduce congestion, allow more efficient usage of system capacity, and provide a faster, safer and more reliable travel option. The partnership with private sectors on construction investment and toll revenue also serves as an effective financing mechanism for network capacity expansions and renovations.

1.1.2 Tolling Challenges

As exepected, setting the toll is not a simple task. In addition to the traffic uncertainties, a key fundamental challenge is how to align the interests among the operator, the travelers, and the regulator, summarized in Table 1.1. On ML, toll is the critical economic instrument determining how these interests are balanced and satisfied. The tolling algorithm affects the total benefits to the society as a whole, but also how they are distributed between the operator and the travelers, as well as among the travelers.

Stakeholders	**Primary interests**
operator	revenue
travelers	travel time cost
regulator	congestion utilization energy and emission equity

Table 1.1: Primary interests of different stakeholders in managed lanes projects

A tolling algorithm to make everyone happy is very challenging, if not impossible. For instance, some managed lanes projects are criticized for creating "Lexus lanes" that mainly serve wealthy travelers, as it is sometimes observed that ML is underutilized while the majority of drivers are stuck in the GP congestion. In this case, the toll is set high to ensure ML condition and earn sufficient revenue from the highly inelastic travelers, yet unfortunately reject the elastic travelers as a by-product. While the operator and the wealthy travelers are winning, other travelers are relatively at loss which causes equity concerns. The GP congestion that could have been reduced also yields more emission and energy consumption.

1.1.3 Typical Tolling Algorithms

On operational ML facilities, typical tolling algorithms reactively adjust the toll as rule-based functions of traffic metrics based on the real-time sensor measurements

(typically from the ML, sometimes also the GP) [31, 111]. These algorithms are designed with objectives in mind, for example the conditions on ML and revenue, yet do not have the capabilities for their explicit optimization. Further, no personalization is considered.

In the literature, the state-of-the-art algorithms distinguish themselves by determining the toll through solving explicitly defined optimization problems formulated on real-time short-term traffic predictions, hence being proactive rather than reactive and are more adaptive in dealing with traffic uncertainties. They also have the potential to be equipped with multi-component objectives for balancing the interests of different stakeholders, although it has been rarely considered and developed. More details are reviewed later in this thesis.

1.2 Proactive Personalized Pricing as a Solution

How could we improve the status quo, and resolve the conflicts of interests among the operator, the travelers, and the regulator? This thesis is going to show that proactive personalized pricing—done intelligently with a multi-component objective—is a promising answer.

Building on the literature of proactive toll optimization, our algorithm first considers a multi-component objective that incorporates the interests of different stakeholders. The algorithm's proactiveness refers to considerations of not only short-term traffic predictions (common in the literature), but also long-term revenue predictions based on a dynamic choice model for how a traveler's future usage would be affected by current toll levels (because of habit and loyalty). Further, more importantly, the tolling algorithm provide travelers with personalized discounts. These discounts are optimized based on individual-specific preferences, and jointly with the optimization of proactive toll aiming for the same system-level objective. The system interacts with the travelers as Figure 1-2.

With a properly designed objective, personalized discounts are expected to attract travelers who always use GP to ML, which lead to five potential benefits:

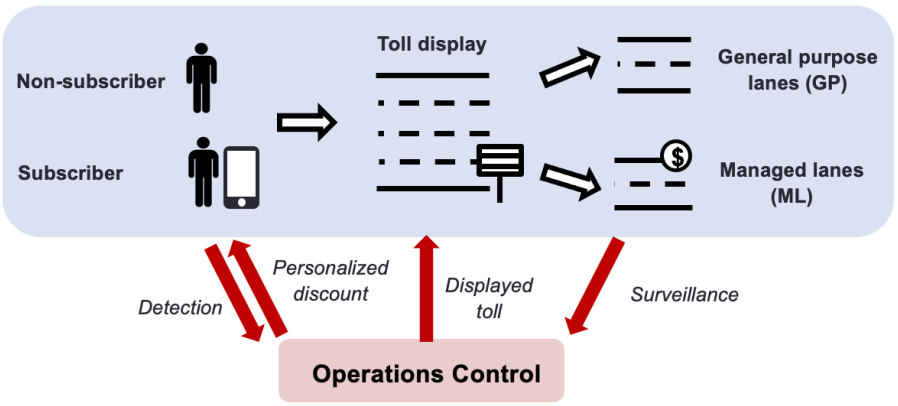

Figure 1-2: Proposed personalized tolling system

1. **Capacity utilization** (increased ML volume)
2. **Reduced congestion** on GP
3. **Increased revenue** from the increased ML volume
4. **Customer acquisition and retention**: if the usage of ML cultivates habit and loyalty, the attracted travelers would be more likely to continue using ML, leading to future revenue potential.
5. **Improved equity**: as the attracted travelers are likely of lower income in the population, personalized discounts alleviate the equity concerns around the ML.

In the general literature beyond transportation, some concerns are raised against the application of personalized pricing, arguing that some customers might feel being treated unequally. We respond it from the perspectives of fairness and equity:

1. **Fairness**: the proposed algorithm treats everyone fairly in the sense that the same personalized pricing algorithm will be applied to all travelers based on their preferences. Two travelers with the same characteristics and conditions will receive the same price.
2. **Perceived fairness**: the proposed algorithm practices personalized pricing in the form of discounts, which should only cause minimal perceived unfairness, as could be seen from the e-commerce space where targeted promotions are widely applied and accepted.
3. **Equity**: the proposed algorithm is expected to improve equity as it would offer

cheaper tolls for travelers who would not want or afford to use ML otherwise.

These points are further supported by a recent review [71] that classifies personalized pricing based on willingness to pay—like ours—as *value-based*, in contrast to *risk-based pricing* based on estimated costs such as in lending, and summarizes that fairness concerns mainly appear in risk-based personalized pricing.

The implementation feasibility of a personalized tolling system is supported by the emergence of mobile tolling that collects tolls through mobile apps. For example, a mobile tolling app, GoToll, is available in more than 50 tolled facilities across 6 states as of Dec, 2021 [9]. More broadly in the transportation industry, thanks to the advancements in Information and Communications Technologies, various personalized app-based on-demand mobility services have been proposed, implemented, and widely used [110]. There is therefore no good reason to believe that the implementation of personalized tolling would be prevented by any technological barriers.

1.3 Research Questions and Gaps

To design a personalized tolling algorithm that delivers the expected benefits, we need to address two key research questions:

1. ***Behavioral modeling of managed lanes choices***: How do travelers decide whether to use ML or GP? How do their choices correlate over time?
2. ***Personalized tolling algorithm design***: How should the toll and discounts be optimized considering travelers' preferences and real-time traffic condition? What objectives should we consider?

Now we provide an overview of what has been done in addressing these questions, and the identified research gaps. A more detailed literature review will be provided in chapter 2.

1.3.1 Behavioral Modeling of Managed Lanes Choices

To analyze the choice between ML and GP, classical models specify it to be primarily based on a simplified trade-off between cost and time saving, where the heterogeneity among individuals is assumed to be mostly accounted for with observed characteristics. Interestingly, empirical data often suggest unexpected high serial correlations among choices made by the same traveler, even after conditioning on the attributes and observed characteristics, as if the travelers were not making deliberate and rational decisions. Specifically, from 24 million trip records, [38] discovered that most travelers only used either GP or ML in a 3-month period. This observation is not well-understood in managed lanes, yet has been analyzed extensively in other fields of applied econometrics. Two competing latent behavioral factors could be in play: (1) *preference heterogeneity*: unobserved individual-specific preferences dominate the range of attributes variation in the data so that switchings are seldom observed; (2) *state dependence*: people prefer sticking to the previous choices because of brand loyalty, habit, perceived reliability and switching cost [65].

The quantification of state dependence and preference heterogeneity is crucial for personalized pricing. Consider under a simple example of revenue maximization; an operator offers large discounts to travelers as they think significant effects of state dependence are in play and would like to invest for future revenue. If the actual effects of state dependence is minimal, such investments will return nothing, as the attracted travelers will stop purchasing once the discounts are removed.

To model the choice between ML and GP, the other issue is the quantification of price elasticity under dynamic pricing. A number of previous studies found counter-intuitive positive price response from empirical data [70, 74]. Explanations have been given that some travelers use price as an indicator for congestion. However, it is hard to believe the pervasiveness of such behavior under the high penetration of real-time travel information system like Google Maps, especially to flip the sign of price response. [34] first identified it as an endogeneity problem caused by dynamic pricing, yet has remained the only work to the best of my knowledge. The importance

of treating price endogeneity is obvious in pricing analysis.

There has been no previous work addressing these econometric issues for the development of a choice model that is suitable for personalized pricing analysis.

1.3.2 Personalized Tolling Algorithm Design

There exists an extensive literature of tolling algorithms [82]. Progressing from fixed toll schedules, the common existing tolling algorithms in research and practice focus on dynamic pricing models that modify tolls in real time, as they have greater flexibility in coping with traffic uncertainties.

With more details to be provided in chapter 2, we identify four research gaps in the existing literature:

1. **Simplified travel behavior**: most studies focus on the optimization side of the problem and traffic dynamics, with simplified travel behavior. A number of studies assume simple choice models that only consider the trade-off between cost and travel time with insufficient considerations of heterogeneity.
2. **Single-component objective**: most studies use single-component objectives, such as revenue or throughput maximizations. The literature lacks a discussion of how to design the objective to balance the interests among different stakeholders identified in Table 1.1.
3. **Considerations of long-term performance**: no study considers the probable state-dependent choice behavior and its impact on pricing decisions. Under state dependence, myopic objectives will lead to sub-optimal long-term performance.
4. **Personalization**: studies regarding personalized tolling has been scarce. The only previous work is [115] that shares the three above-mentioned gaps.

1.4 Research Approach and Thesis Outline

First, we start out with a detailed literature review regarding the above-mentioned research gaps in chapter 2.

Second, with the end goal of developing a personalized tolling algorithm, chapter 3 and chapter 4 develop a comprehensive managed lanes choice model to understand how travelers decided whether to use ML, highlighting the proper quantifications of heterogeneity and state dependence. These two chapters are organized as follows:

- Chapter 3: the workhorse for quantifying unobserved heterogeneity and state dependence is the dynamic choice model with random parameters. Unfortunately, these models are challenging to estimate. Because we often do not observe the individual's time-ordered choice sequence from an exogenous starting point, special econometric treatment is needed in constructing the likelihood, without which large biases would appear in parameter estimates. This is an endogeneity problem, well known as the initial condition problem. Therefore, chapter 3 investigates the performance of existing solutions to the initial condition problem, and proposes an alternative solution based on the Control Function method that is commonly used for endogeneity problems in choice models [109]. The proposed and existing solutions are compared through theoretical analysis and Monte Carlo studies. The study considers the general case of dynamic models with random parameters instead of the ones with only random intercept which are widely analyzed in the literature.

- Chapter 4: building on the analysis of chapter 3, through modeling trip records from an existing managed lanes facility, chapter 4 develops a comprehensive dynamic model for the choice of whether to use ML or GP. The model is estimated with methods analyzed in chapter 3 for initial condition, as well as correction of price endogeneity caused by dynamic pricing.

Then, the thesis culminates with the development and testing of a dynamic personalized tolling algorithm in chapter 5. Leveraging our comprehensive behavior analysis in previous chapters, the algorithm is designed based on an online bi-level optimization paradigm termed *Tri-POP* that stands for prediction, optimization and personalization [19]. Specifically, we focus on the joint optimization of personalized discounts and system-level toll, as well as the design of a multi-component objective

that includes considerations for long-term performance and the interest reconciliation among the operator, the travelers, and the regulator. The pricing system is tested with closed-loop simulation experiments where the simulation laboratory is calibrated with real-world data.

Finally, chapter 6 concludes the thesis and discuss future directions of research.

1.5 Thesis Contributions

The proposed research has the following contributions to three research areas:

- The initial condition problem in dynamic model estimation
  - analyzed the widely used correction methods under the case of dynamic models with random parameters, instead of with only random intercepts
  - proposed a Control Function solution that is general and applicable to multinomial choice
  - compared the Control Function method with common methods analytically and through Monte Carlo studies where the recoveries of random parameters' population distribution are considered, and showed improvement of Control Function over Wooldridge's method in [108]
- Managed lanes travel behavior modeling
  - quantified significant unobserved heterogeneity and state dependence from empirical data on the managed lanes travel behavior
  - demonstrated largely overstated state dependence when unobserved heterogeneity is not modeled or the initial condition is not corrected
  - discovered and corrected price endogeneity caused by dynamic pricing
  - provided a modeling manual for managed lanes trip records that have limited characteristics and potential price endogeneity
- Personalized toll optimization

- formulated a scalable real-time optimization problem with personalization, based on a multi-component objective function that includes the interests of the operator, the travelers and the regulator, and future revenue considerations based on state-dependent choice behavior
- demonstrated that the proposed personalized tolling algorithm could improve operator revenue, improve managed lanes usage, reduce congestion, and improve traveler's benefit all at the same time
- demonstrated that the proposed personalized tolling algorithm would give more benefit to travelers with lower values of time and hence improve equity

Chapter 2

Literature Review

2.1 Dynamic Choice Model

Panel discrete choice data, especially the ones from real-life situations, often exhibit strong correlations among choices made by the same individual, even after properly conditioning on observed alternative attributes and characteristics. Nobel laureate James Heckman, attributed such correlations of intricate causes to two latent factors: *structural state dependence* and *unobserved heterogeneity* [65]. Commonly, dynamic discrete choice models with random parameters are used to capture and identify both factors. The discussions on this topic may appear abstract to readers without previous exposure, but will become clear in chapter 3 where detailed equations are provided.

2.1.1 State Dependence and Unobserved Heterogeneity

State dependence exists when past choices or experience structurally affect future choices as they alter the associated preferences, attributes, or constraints. Supporting behavior theories include learning, inertia, habit formation, and switching costs [12, 102]. State dependence has been discovered and studied in a variety of fields, such as consumer behavior [48], labor participation [65, 98], and public health [95]. Mathematically, structural state dependence is represented by including the lagged choices of the same individual into the utility equation as explanatory variables. The

constructed choice models are hence dynamic, distinguished from the common static ones. For simplification, a first-order Markovian assumption is typically invoked that specifies the utility at time period m to only directly depend on the most recent choice at time period $m-1$, but not the choices even before. Other studies have used the number of times an alternative has been chosen in the past [11] or the attributes of previously chosen alternatives [53, 59].

On the other hand, unobserved heterogeneity refers to the latent features of an individual that affects choices. These features are not affected by the individual's previous choices. Unobserved heterogeneity is handled by including individual-specific effects in the utility equation, either through alternative-specific constants or more generally the vector of preference parameters. These effects can be estimated either as fixed or random. Fixed effects models consider the individual-specific parameters as fixed parameters, but have been shown to give inconsistent estimates for finite samples with a limited choice history because of the incidental parameter problem [80]. Random effects models consider the individual-specific parameters as random variables whose specified distribution contains unknown parameters, and are commonly adopted (e.g., logit mixture). We consider random effects models as the default way to estimate unobserved heterogeneity.

To successfully identify state dependence, one must first properly consider heterogeneity. Failing to do so will cause spurious state dependence in parameter estimates that overstates the structural state dependence effect, in which case past choices statistically serve as proxies for the uncaptured heterogeneity [65].

2.1.2 The Initial Condition Problem

If no unobserved heterogeneity is present, consistent estimation of dynamic choice models is simple with standard procedures for static models [102]. However, no unobserved heterogeneity is a strong and often unrealistic assumption, as it implies heterogeneity is sufficiently explained by observed variables.

The consistent estimation of state dependence with unobserved heterogeneity—dynamic choice models with random parameters—has long been recognized as a chal-

lenging problem due to endogeneity known as the initial condition problem. This problem occurs when the individuals' time-ordered choices are not observed from exogenous starting point, as is often the case in empirical datasets where the analyst often only observes a limited period of a person's choice history. In this case, the first observed choice (initial condition) is endogenous because it correlates with the random parameters for unobserved heterogeneity. Ignoring this correlation—using standard approach for estimating static models with random parameters—causes largely biased estimates.

Two methods for dynamic choice models with random parameters have been widely adopted in the literature. The first method, commonly referred as the Heckman's method, is to construct the joint likelihood of the initial condition and subsequent choices [66]. The second method, commonly referred as the Wooldridge's method, is to construct the conditional likelihood of subsequent choices on the initial condition with proper treatment of the correlation between the initial condition and unobserved heterogeneity, namely the endogeneity of the initial condition [108]. Both methods involve analytically intractable elements in the likelihoods they considered respectively, which are resolved by different forms of approximations in their original works and the following research [13, 14, 18, 55, 77, 81, 88, 95]. More details are provided in chapter 3.

2.1.3 Summary

In quantifying state dependence, the importance of capturing unobserved heterogeneity and the need for initial condition correction have been widely acknowledged and analyzed. Widely adopted solutions for the initial condition problem look at ways for constructing (approximating) the correct likelihoods.

Although initial condition problem is a special form of endogeneity, the Control Function—a common tool for endogeneity in choice models—has rarely been applied. We found that [81] developed a method that is essentially the Control Function method, without using the term Control Function.

Further, previous works commonly consider dynamic binary choice models with

random intercepts, instead of the general case of (multinomial) choice models with random parameters.

2.2 Managed Lanes Travel Behavior Modeling

Managed lanes travel behavior modeling considers the choice between managed lanes (ML) and general purpose lanes (GP).

The most common data source is stated preference (SP) surveys, as many studies investigate responses to infrastructures and policies that have not yet been implemented [67, 85]. In general, SP studies have the limitation of hypothetical bias, which can be alleviated by combining SP with revealed preference (RP) data of the existing situation [24, 27, 28, 69]. On managed lanes, the actual behaviors found in RP are especially different from the presumptions and conclusions of many SP studies [38, 101]. This motivates the use of RP data, which is also becoming increasingly available as more operational managed lanes come to existence. In contrast to traditional RP data collected with travel surveys [33, 35], the electrification of tolling facilities has made a massive amount of directly collected RP trip records available, presenting new opportunities. Behavior studies based on this type of RP data are mainly limited to exploratory analysis, but not econometric modeling [37]. One main challenge of using these trip records is the absence of travelers' characteristics. In addition, compared to SP experiments, RP data could be subject to different forms of endogeneity. Despite these challenges, RP data are more relevant to dynamic pricing as they are constantly observed by toll operators and could be pipelined into online pricing systems.

In the following sections, we review existing choice models for managed lanes and other related applications from three crucial aspects to personalized pricing: how they capture and learn heterogeneity, how they consider state dependence, and how they treat price endogeneity.

2.2.1 Heterogeneity

In the general econometric literature, while traditional models have put their primary focus on estimating average preferences towards (effects of) service level and policy variables, recent efforts have emerged to elicit heterogeneity and learn individual preferences [15]. Two types of preference heterogeneity are commonly considered: inter-consumer heterogeneity that accounts for preference variations among individuals, and intra-consumer heterogeneity for preference variations of the same individual among choice situations (trips, for example). Intra-consumer heterogeneity has received less attention in the literature, but its importance has nonetheless been acknowledged [28, 32, 68]. Both types of heterogeneity could be incorporated in two ways. First, they could be specified as a function of observed socio-economic characteristics and attributes. Further, unexplained (i.e., unobserved) variations in preferences could be accounted for with random parameters, commonly by using a logit mixture.

Inter-consumer preference heterogeneity has been widely considered in the context of managed lanes [96, 101], which has become a standard procedure in dealing with panel data that is crucial for welfare analysis and a basis for individual-level parameter inference [27]. Intra-consumer heterogeneity has been considered when it is observed [32] and unobserved [68]. However, as these literatures are limited to SP, it is unclear to what degree the discovered intra-consumer heterogeneity exists in real choice situations.

For a model that captures heterogeneity with random parameters, their conditional (posterior) distribution on past choices—individual-speicific parameters—could be acquired by Bayesian inference. This idea initially attracted attention in marketing applications, as marketers are often interested in determining consumer preference at individual and household levels for the purpose of differentiating product offerings [15, 16]. In transportation, as real-time communications between travelers and service operators are becoming more efficient, ideas have been proposed to learn individual preferences online and use them to tailor products and services to different travelers

with varied preferences to maximize profit or welfare [44, 110].

In the context of managed lanes, capturing heterogeneity and learning individual preference are of obvious importance for personalized pricing. It's hard to imagine a useful personalization strategy based on models that only measure the average effects in the population.

2.2.2 State Dependence

Although it has been hypothesized that state dependence plays a role in managed lanes choices [38], barely any efforts have been put to identify its magnitude, with the exception of [115] who specifies a flat logit model that includes personal trip history as explanatory variables but not considering unobserved heterogeneity. As reviewed previously, the drawback of using flat logit to identify state dependence is being susceptible to *spurious state dependence*—the past choices would statistically serve as proxies for the omitted unobserved heterogeneity and exaggerate the actual state dependence effects [65]. A model with spurious state dependence might predict as well under the existing pricing policy if the data distribution in prediction remains the same as in training, but it will fail miserably under new policies [10, 52].

2.2.3 Price Endogeneity

Modern managed lanes facilities often practice dynamic pricing that modifies tolls in response to real-time demand. Regardless of the specific algorithms, tolls are commonly raised as the demand for managed lanes increases. This presents a typical case of price endogeneity caused by the simultaneity between price and demand. In fact, a number of previous studies discovered positive price elasticities and simply explained them with price being congestion indicators [70, 74].

To the best of my knowledge, [34] is the first and only publication that deals with the endogeneity issue in RP data from dynamically priced managed lanes. With first differencing and using downstream traffic as instruments, [34] estimated the aggregate toll elasticity on Seattle SR16 HOT lanes to be -0.16 to -0.21, which is in similar ranges

from relevant natural experiments that avoid endogeneity concerns [36, 54, 56]. For example, [36] estimated the elasticity on toll bridges in Florida to be -0.076 to -0.15, and [56] estimated the price elasticity under congestion pricing to be -0.304 in Milan, Italy.

2.2.4 Summary

There is clearly a scarcity of literature in rigorous econometric modeling for managed lanes behavior based on RP data, with proper considerations of heterogeneity, state dependence and price endogeneity.

2.3 Road Pricing and Toll Optimization

The idea of road pricing traces back at least to Adam Smith who considers toll on a facility as a way to defray its own expenses [73, 97]. The concept was then revolutionized by Pigou who views road charges as a tax that would help achieve economic efficiency [87]. With increasing traffic congestion, modern road pricing has become an essential tool for travel demand management. The application of pricing measures is expected to modify temporal and spatial dimensions of travel [92]. As toll roads directly generate revenue, they are also considered as a classic model for public-private partnerships to finance highway projects.

2.3.1 Dynamic Pricing

Leveraging real-time information, dynamic pricing constantly modifies prices [17, 91]. It could be classified as proactive or reactive based on whether prices are functions of future predictions [45].

Reactive strategies determine price solely based on just observed network condition. To name a few, [112] outlined a simple feedback-control approach where the toll is adjusted as a function of observed occupancy from loop detectors and the desired occupancy. [75] presented a reactive self-learning approach where a homogeneous de-

mand model based on value of time is learned online and coupled with a multi-lane kinematic wave supply model to maximize corridor throughput. More recent work [84] developed a deep reinforcement learning approach where states are defined as network cells and a deep neural network is trained to learn the optimal toll rates (policy) given states, building on their earlier formulations in [83]. Other examples of reactive pricing algorithm include [40] and [113].

As suggested by [31, 111], typical state-of-the-practice tolling algoritms on managed lanes are mainly simple reactive algorithms that modify toll based on real-time traffic metrics measured on the managed lanes to keep them from congestion.

Compared to reactive pricing strategies, proactive ones have been investigated less frequently as they involve complex prediction models. [46] compared a reactive and a proactive strategy for maintaining link density and showed the superior performance of the latter. [100] presented a proactive tolling framework supported by a dynamic traffic assignment (DTA) model. [116] showed that more accurate prediction by online calibration of DTA yields better revenue performance. [115] advanced [116] to formulate a bi-level optimization problem to offer personalized prices based on system and individual-level prediction. [62] used the same DTA platform as [115, 116], and formulated a genetic algorithm-based solution approach for toll optimization. The same DTA platform is also used in [72] to investigate systematic definitions of tolling zones.

Clearly, if the supporting prediction models are accurate, proactive strategies would have superior performance compared to reactive methods as they price the future based on predictions of it. Reactive approaches are widely adopted because they are easy to implement. However, a salient limitation of previous proactive pricing literature is the use of simplified supply and choice models that ignore heterogeneity to different extent, which limits the benefit of being proactive and especially hampers the potential of personalized pricing. This could be seen from a summary of the above-mentioned literature in Table 2.1, where a "VOT model" refers to a homogeneous choice model with only price and time saving.

Reference	Objective	Method	Supply Model	Demand Model
Reactive strategies				
[112]	occupancy	localized freedback-control	\	\
[75]	throughput	(VOT) learning with Kalman filter	kinetic wave	VOT model
[84]	revenue or travel time	deep reinforcement learning	cell transmission	\
Proactive strategies				
[46]	target link density	toll as a function of predicted density	DTA simulation	VOT model
[100]	revenue, welfare or throughput	simulation-based optimization	cell transmission	VOT model
[115]	revenue	online bi-level optimization	DTA simulation	dynamic logit with observed heterogeneity

Table 2.1: Selected references on managed lanes dynamic pricing

2.3.2 Considerations for Long-term Performance

Moreover, existing ML pricing strategies are myopic in that they only consider immediate returns. This is a natural result of neglecting state dependence in choice modeling. On the other hand, pricing strategies for long-term benefits appeared in marketing literature. For example, [49] formulated it as a dynamic programming problem and concluded that considering brand loyalty motivates price reductions. The research context was then extended by [42] to consider the case of multiple manufacturers. Other contexts of pricing considering long-run dynamics include continued borrowing and preventive health interventions [71].

In practice, to price for long-term performance, many firms consider customer lifetime value (CLV) that measures the return over a customer's lifetime [63]. See [39] for CLV considered in airline industry, and [2] for that in transportation network companies.

2.3.3 Personalized Pricing

Personalized pricing strategies have been barely explored in ML except [115] that shows personalized pricing could improve operator's revenue. In transportation, [106] explored air fare personalized pricing, and [21] investigated personalizing sustainable

travel incentives. In addition, Airline, car rental, and transportation network companies often offer targeted promotions that are common marketing strategies nowadays.

Driven by advancements in technology, algorithmic personalized pricing based on big data is especially gaining popularity in online applications such as e-commerce [93].

While traditional personalized pricing literature takes on the viewpoint of revenue-maximizing firms and illustrates revenue improvements [90, 94], a hot ongoing debate is found regarding how personalized pricing would affect consumer benefits and related ethical and legal issues [103]. For instance, based on experiments with a large digital firm, [50] shows that while personalized pricing would yield 19% extra profit compared to uniform optimal price, total consumer surplus declines 23%. On the other hand, over 60% of consumers benefited from lower prices under personalization so total welfare could as well increase under inequity-averse welfare functions. These findings suggest cautions need to be taken for the benefit analysis of personalized pricing, and the potential advantages of incorporating welfare components into the objective.

The other related issue in personalized pricing is fairness and equity. [71] differentiates *value-based* personalized pricing based on willingness to pay from *risk-based* personalized pricing based on estimated cost such as in lending and insurance. Although some may argue that personalized pricing introduces perceived unfairness for charging different price for the same product, value-based personalized pricing actually improves access and equity because lower income people tend to have lower willingness to pay. As transportation systems are public resources, we would argue access and equity to be more important and relevant to consider compared to perceived fairness.

In the general literature of personalization, various strategies based on consumer behavior theory have been proposed [79]. In applications such as personalized online recommendation, data-driven methods are widely used to personalize service based on the revealed preferences of similar customers, with collaborative filtering being a typical example [44].

2.3.4 Summary

In summary, four limitations are identified in the dynamic pricing literature:

1. **Simplified travel behavior**: most studies focus on the optimization side of the problem and traffic dynamics, with simplified travel behavior. A number of studies assume simple choice models that only consider the trade-off between cost and travel time with insufficient considerations of heterogeneity.
2. **Single-component objective**: most studies use single-component objectives, such as revenue or throughput maximizations. The literature lacks a discussion of how to design the objective to balance the interests among different stakeholders identified in Table 1.1.
3. **Considerations of long-term performance**: no study considers the probable state-dependent choice behavior and its impact on pricing decisions. Under state dependence, myopic objectives will lead to sub-optimal long-term performance.
4. **Personalization**: studies regarding personalized tolling has been scarce. The only previous work is [115] that shares the three above-mentioned gaps.

Chapter 3

The Initial Condition Problem in Dynamic Choice Models

3.1 Introduction

Dynamic models with random parameters are widely adopted for quantifying unobserved heterogeneity and state dependence, and we are going to use them to understand managed lanes choice behavior in chapter 4. However, it is well-known that these models' consistent estimations are challenging due to endogeneity known as the initial condition problem [66]. Therefore, this chapter analyzes the initial condition problem from a general context and proposes an alternative solution with the Control Function method [109]. The proposed method is applicable to multinomial choice models in addition to the commonly considered binary ones. This chapter advances previous literature also through the considerations of dynamic models with general random parameters instead of only random intercepts.

This chapter starts with mathematical explanations of the initial condition problem, followed by popular solutions, namely the one by Heckman [66] and the one by Wooldridge [108]. Then, the proposed Control Function solution is outlined and compared with the Heckman's and Wooldridge's methods, both from an analytical view and Monte Carlo experiments. Control Function is shown to be closely related to the Wooldridge's method, and Monte Carlo experiments suggest its improvements.

3.2 Mathematical Background

3.2.1 The Initial Condition Problem

We consider the working example to be a simple dynamic binary choice model with a first-order Markovian assumption as shown in Equation 3.1. The generalization to multinomial choice is discussed in subsection 3.3.5.

$$\begin{aligned} U_{nm} &= \zeta_n^{ASC} + \zeta_n^d d_{n(m-1)} + \zeta_n^{X\prime} X_{nm} + \varepsilon_{nm} \\ d_{nm} &= 1[U_{nm} > 0] \end{aligned} \tag{3.1}$$

A decision-maker is indexed n and a choice situation is indexed with m. The choice is denoted with $d_{nm} \in \{0, 1\}$. The utility corresponding to $d_{nm} = 1$ is denoted with U_{nm}, and the utility corresponding to $d_{nm} = 0$ is normalized to zero. X_{nm} is a vector of exogenous explanatory variables. ζ_n^{ASC} is a scalar alternative-specific constant. ζ_n^d is a scalar random dynamic parameter reflecting the extent of state dependence. ζ_n^X is a random vector compatible with the dimension of X_{nm}. The parameter vector $\zeta_n = (\zeta_n^{ASC}, \zeta_n^d, \zeta_n^X)$ is individual-specific and follows a population distribution G whose parameters are to be estimated. In this work, we consider G being a gaussian distribution with mean μ and covariance matrix Ω. Note that we consider a full random parameter vector compared to previous studies that limit their random parameter to only the alternative-specific constant.

Following random utility theory, ε_{nm} is a random error term specified with independent and identical (i.i.d.) logistic distributions with location zero and unit scale. The resulting choice probability is logit as shown in Equation 3.2.

$$P(d_{nm} = 1 | \zeta_n, X_{nm}, d_{n(m-1)}) = \frac{exp(\zeta_n^{ASC} + \zeta_n^d d_{n(m-1)} + \zeta_n^{X\prime} X_{nm})}{1 + exp(\zeta_n^{ASC} + \zeta_n^d d_{n(m-1)} + \zeta_n^{X\prime} X_{nm})} \tag{3.2}$$

For a given individual, we observe the choices $d_n = (d_{n0}, d_{n1}, ..., d_{nM_n})$, as well as exogenous variables $X_n = (X_{n0}, ..., X_{nM_n})$. As the model has a first-order state depen-

dence, the initial condition is d_{n0}. The likelihood of all observed choices conditional on X_n is shown in Equation 3.3.

$$L(d_{n0}, d_{n1}, ..., d_{nM_n}|X_n) = \int \Pi_{m=1}^{M_n} P(d_{nm}|\zeta_n, X_{nm}, d_{n(m-1)}) P(d_{n0}|\zeta_n, X_n) g(\zeta_n) d\zeta_n \tag{3.3}$$

The difficulty in computing this expression comes from the fact that $P(d_{n0}|\zeta_n, X_n)$ is generally unknown. Except the rare case where d_{n0} is the actual first choice made in the stochastic process, this probability depends on the information regarding the pre-sample period (e.g., distribution of exogenous attributes) that is unknown to the analyst. Commonly used alternative estimation methods instead consider the likelihood conditional on d_{n0} as shown in Equation 3.4.

$$L(d_{n1}, ..., d_{nM_n}|X_n, d_{n0}) = \int \Pi_{m=1}^{M_n} P(d_{nm}|\zeta_n, X_{nm}, d_{n(m-1)}) f(\zeta_n|X_n, d_{n0}) d\zeta_n \tag{3.4}$$

However, as shown in Equation 3.5, the conditional distribution $f(\zeta_n|X_n, d_{n0})$ is hard to compute and depends on $P(d_{n0}|\zeta_n, X_n)$ that causes difficulty with Equation 3.3 from the first place.

$$f(\zeta_n|X_n, d_{n0}) = \frac{P(d_{n0}|\zeta_n, X_n) g(\zeta_n)}{\int P(d_{n0}|\zeta_n, X_n) g(\zeta_n) d\zeta_n} \tag{3.5}$$

If $P(d_{n0}|\zeta_n, X_n)$ is known, it is easier to directly use it in the joint likelihood. Therefore, methods with the conditional likelihood seek to directly approximate $f(\zeta_n|X_n, d_{n0})$. A naive approach is to directly use $g(\zeta_n)$, as if d_{n0} is exogenous. Unfortunately, this replacement is only valid if d_{n0} is indeed exogenous and hence independent from ζ_n, i.e., $g(\zeta_n)$ equals $f(\zeta_n|X_n, d_{n0})$.

Naturally, solutions to the initial condition problem construct (often approximate)

either the joint likelihood (Equation 3.3) or the conditional likelihood (Equation 3.4). [95] refers to them accordingly as joint likelihood solutions and conditional likelihood solutions.

3.2.2 Joint Likelihood Solutions

Straightforward estimation with the joint likelihood (Equation 3.3) is prevented by the unknown quantity $P(d_{n0}|\zeta_n, X_n)$. Its computation is prohibitive for requiring marginalizing (integrating) the choice model over the pre-sample period where distributional assumptions of exogenous attributes also need to be made.

Heckman proposed a useful approximation solution [66]. He considered a special case of our model where the preference parameters are not distributed, and serial correlation is captured by scalar i.i.d. deviates $\Delta\zeta_n^{ASC}$ as in Equation 3.6—this is equivalent to only keeping ζ_n^{ASC} distributed, but we use this deviation form for consistency with [66]. This model is often analyzed and used in the literature and we refer it as the dynamic binary choice model with a random intercept.

$$U_{nm} = \zeta^{ASC} + \zeta^{d} d_{n(m-1)} + \zeta^{X\prime} X_{nm} + \Delta\zeta_n^{ASC} + \varepsilon_{nm} \tag{3.6}$$

A choice model is used to approximate the probability of the initial condition as Equation 3.7. Fixed parameters c_{ASC} and c_X can differ from those of the following choices (ζ^{ASC} and ζ^X). The error term (e_{n0}) can be freely correlated with those of the following choices ($\Delta\zeta_n^{ASC} + \varepsilon_{nm}, \forall m \in \{1, ..., M_n\}$).

$$U_{n0} = c_{ASC} + c_X' X_{n0} + e_{n0} \tag{3.7}$$

This approach was sometimes considered to be computationally intensive because it requires M_n dimensional integration. This challenge has been much alleviated with recent advances in estimation software and computation. On the other hand, other approaches have been proposed to restrict the way in which total errors are correlated to improve statistical efficiency and simplify computation [13, 18]. Specifically, e_{n0}

is restricted to follow the same i.i.d. distribution as ε_{nm}, and the correlation of total errors is captured by including $\Delta\zeta_n^{ASC}$ also into the initial condition model as a common factor with a new scaling parameter r_ζ (Equation 3.8). A similar approach was adopted by [55, 81] in which two correlated random intercepts were used for the initial choice and subsequent choices.

$$U_{n0} = c_{ASC} + c_X' X_{n0} + r_\zeta \Delta\zeta_n^{ASC} + \varepsilon_{n0} \tag{3.8}$$

This restricted form is generally preferred and used in the literature [14, 95]. It could as well be easily generalized to account for preference heterogeneity in all parameters as shown in Equation 3.9. $\Delta\zeta_n^X$ and $\Delta\zeta_n^d$ respectively denote deviations of ζ_n^X and ζ_n^d from population mean. Additional parameters c_{ASC}, c_X, r_{ASC}, r_X and r_d need to be estimated for the initial condition model.

$$\begin{aligned} U_{nm} &= \zeta_n^d d_{n(m-1)} + \zeta_n^{X\prime} X_{nm} + \varepsilon_{nm}; \forall m > 0 \\ U_{n0} &= c_{ASC} + r_{ASC}\Delta\zeta_n^{ASC} + (c_X + r_X\Delta\zeta_n^X)' X_{n0} + r_d\Delta\zeta_n^d + \varepsilon_{n0} \end{aligned} \tag{3.9}$$

3.2.3 Conditional Likelihood Solutions

As overviewed, conditional likelihood solutions to the initial condition problem use Equation 3.4 with approximated $f(\zeta_n|X_n, d_{n0})$. We denote the density function approximation as $\hat{f}(\zeta_n|X_n, d_{n0})$.

Wooldridge proposed a popular method, in which $\hat{f}_{Wool}(\zeta_n|X_n, d_{n0})$ is specified as the sum of the conditional expectation $E[\zeta_n|X_n, d_{n0}]$ and a random i.i.d. error v_n^{Wool} as Equation 3.10 [108]. v_n^{Wool} is specified to follow a normal distribution $N(0, \Omega^{Wool})$ to be estimated. The conditional expectation is often specified as a linear function but could potentially incorporate more flexible forms.

$$\zeta_n = E[\zeta_n|X_n, d_{n0}] + v_n^{Wool} \tag{3.10}$$

The performance of this approach depends on how well Equation 3.10 approximates $f(\zeta_n|X_n, d_{n0})$ [95]. [18] found that the Wooldridge's method produced smaller

biases for short panels than common factor models, and similar, insubstantial bias for longer panels. [77] suggested constraining this model by using the means of exogenous attributes across all observations of individual n, denoted $\bar{X}_n$. However, [14, 88] showed that such a model will be overly constrained, leading to noticeable bias. In Monte Carlo experiments, [14] showed that this approach worked very well for panels longer than 5-8 periods, but was inferior to Heckman's reduced-form approximation for shorter panels. Similarly, [78] showed that Heckman's method is hardly subject to any bias, while the constrained Wooldridge's method and [81] deliver estimators that can be subject to substantial bias and low precision. In these two methods, the bias does not seem to decrease as sample size increases. To reduce this bias, [88] proposed including the initial period explanatory variables as additional regressors in the auxiliary model proposed by [77]. This specification is shown in Equation 3.11, where the exogenous attributes of initial condition denoted as X_{n0}. We consider it as our working model for the Wooldridge's method. k denotes the dimension of the random parameter vector.

$$\zeta_n^k = \alpha_0^k + \alpha_d^k d_{n0} + \alpha_X^{k\prime} X_{n0} + \alpha_{\bar{X}}^{k\prime} \bar{X}_n + v_n^{Wool,k}; \forall k \in \{1, ..., K\} \tag{3.11}$$

The popularity of the Wooldridge's method largely comes from its ease of application with canned software, especially when the unobserved heterogeneity is only considered in the random intercept of a binary model as Equation 3.6.

3.3 Methodology

In this paper, we propose a Control Function (CF) solution to the well-known initial condition problem. First, the initial condition problem is analyzed from an endogeneity perspective. Then the CF solution is presented and analyzed. A similar method is proposed by [81], which applies to the case of binary choice model with a random intercept. This work extends [81] to the general case of random parameters, compares it closely with the Wooldridge's method, and at the end extends it to the case

of multinomial choice in subsection 3.3.5.

3.3.1 Endogeneity of the Initial Conditions

Endogeneity occurs when some explanatory variables are correlated with the unobserved factors of utility [86]. In our working example Equation 3.1, the random parameter ζ_n and lagged choice $d_{n(m-1)}$ are correlated as $d_{n(m-1)}$ was driven by the same ζ_n. Note that this is different from the common case where some explanatory variables are correlated with the error term ε_{nm} in utility as the problematic random component is the random parameter ζ_n.

For choices driven by a dynamic model, endogeneity occurs for all observations—$corr(d_{n(m-1)}, \zeta_n) \neq 0$, $\forall m \in \{1, ..., M_n\}$—but only that of the second observed choice ($m = 1$) requires correction because the endogeneity of following choices are automatically treated by including the probability of their previous choice into the likelihood function.

The Heckman's method corrects the endogeneity by including the probability of initial condition. Using the conditional likelihood with a marginal distribution of random parameters incurs bias due to the ignorance of endogeneity. The Wooldridge's method solves the endogeneity from a rather uncommon approach by considering the distribution of unobserved factors (i.e., random parameters) conditional on their correlated explanatory variable (i.e., the initial condition).

3.3.2 A Control Function Solution

The Control Function (CF) method addresses endogeneity by using extra variables—controls—in the utility specification that are obtained using exogenous instruments. Such methods have been applied extensively in the literature [30, 58, 60, 61, 86, 104, 109].

This method consists of two steps. In the first step, the endogenous variable is fitted as a function of exogenous instruments to acquire controls (residuals in the case of continuous endogenous variable). Then in the second step, these controls are

added as explanatory variables to the model of interests to capture the correlation between the endogenous variables and unobserved factors, such that the endogeneity is removed.

To apply Control Function for the initial condition, we first need to find valid instruments. The two requirements of valid instruments are: (1) exogeneity—they have to be uncorrelated with the random components of the utility (ζ_n and ε_{nm}), and (2) relevance—they have to be sufficiently correlated with d_{n0}. The exogenous attributes associated with the initial condition (X_{n0}) naturally meet these requirements. As the exogenous attributes across observations of the same individual are commonly correlated, the average exogenous attributes ($\bar{X}_n$) are also expected to be a valid instrument as it reflects conditions in pre-sample period. Unsurprisingly, these instruments have also been used in applications with the Wooldridge's method, although not being explicitly referred as instruments.

With the Control Function method, the first step is to fit a choice model predicting the initial condition (choice) as a function of the instruments as Equation 3.12. Like Heckman's method, this step considers an initial condition model, but the involved computation is much simpler as it is estimated separately from the choice model of interest and does not contain any random parameters. The intuition is that as $\tilde{V}_{n0}$ only contains fixed parameters, so the correlation of d_{n0} and ζ_n is encapsulated in the error term δ_n.

$$\begin{aligned} d_{n0} &= 1[\tilde{U}_{n0} > 0] \\ \tilde{U}_{n0} &= \tilde{V}_{n0} + \delta_n \\ \tilde{V}_{n0} &= \tau_{ASC} + \tau'_X X_{n0} + \tau'_{\bar{X}} \bar{X}_n \end{aligned} \tag{3.12}$$

Given the estimated first step model, and the observed initial condition d_{n0}, we define the control as the posterior conditional mean of δ_n that is $\hat{\delta}_n = E[\delta_n | d_{n0}]$. This treatment of discrete endogenous variable with Control Function follows [109].

The computation of $E[\delta_n | d_{n0}]$ depends on the distribution specification for δ_n. The most well-known result is that when δ_n follows a standard normal distribution (a

probit initial condition model), $E[\delta_n|d_{n0}]$ could be computed with the inverse Mills ratio as Equation 3.13 [109]. λ denotes the inverse Mills ratio, defined as the ratio between the standard normal density function ϕ and the standard cumulative density function Φ. In estimation, $\tilde{V}_{n0}$ is computed from the estimated Equation 3.12. A related more general result is by [81] who derived a general expression for censored normal linear models.

$$\begin{aligned}
\hat{\delta}_n &= E[\delta_n|d_{n0}] \\
\hat{\delta}_n &= d_{n0}E[\delta_n|d_{n0}=1] + (1-d_{n0})E[\delta_n|d_{n0}=0] \\
\hat{\delta}_n &= d_{n0}E[\delta_n > -\tilde{V}_{n0}] + (1-d_{n0})E[\delta_n < -\tilde{V}_{n0}] \\
\hat{\delta}_n &= d_{n0}\lambda(\tilde{V}_{n0}) - (1-d_{n0})\lambda(-\tilde{V}_{n0}) \\
&\text{where } \lambda(x) = \frac{\phi(x)}{\Phi(x)}
\end{aligned} \tag{3.13}$$

When δ_n follows an extreme value distribution (in a logit initial condition model), $E[\delta_n|d_{n0}]$ could be computed with results from [51]. Their results are also applicable to the case of multinomial choice where we have one error term corresponding to each alternative, to be detailed in subsection 3.3.5.

Further, arguably the most general approach for computing $E[\delta_n|d_{n0}]$ is to use simulations. In principal, it is applicable to any error distribution and number of choice alternatives. Taking any estimated first step model, we can simulate T draws of the utility error(s), and correspondingly T choices. Then we can select the simulations that generated the observed d_{n0} and compute the average simulated error term(s) among them, which serves as an unbiased estimator of $E[\delta_n|d_{n0}]$. The computation here is quite manageable as the model has already been estimated. This method could also be used to validate any derived closed-form expressions.

Then, the second step of Control Function considers the conditional likelihood of Equation 3.4, assuming that conditional on $\hat{\delta}_n$, the actual random parameter now denoted as $v_n^{CF,k}$ in Equation 3.14 is independent from the initial condition d_{n0}. $v_n^{CF,k}$ across k is denoted as v_n^{CF} and specified to follow a normal distribution $N(0, \Omega^{CF})$.

$$\zeta_n^k = \gamma_0^k + \gamma_h^k \hat{\delta}_n + v_n^{CF,k}; \forall k \in \{1, ..., K\} \tag{3.14}$$

The modified conditional likelihood to use is presented in Equation 3.15, where density $\hat{f}_{CF}(\zeta_n|\hat{\delta}_n)$ replaces $f(\zeta_n|X_n, d_{n0})$. It implies the assumption that the dependence between d_{n0} and ζ_n is fully encapsulated in the residuals $\hat{\delta}_n$.

$$\begin{aligned} &L(d_{n1}, ..., d_{nM_n}|X_n, d_{n0}) = \\ &\int \Pi_{m=1}^{M_n} P(d_{nm}|\zeta_n, X_{nm}, d_{n(m-1)}) \hat{f}_{CF}(\zeta_n|\hat{\delta}_n) d\zeta_n \end{aligned} \tag{3.15}$$

To summarize, the Control Function solution to the initial condition problem consists of two steps as follows:

- Step 1: estimate an auxiliary model for the initial condition as Equation 3.12, and then acquire the control $\hat{\delta}_n$ as Equation 3.13.
- Step 2: plug the acquired $\hat{\delta}_n$ into the choice model through ζ_n as Equation 3.14, such that the resulted new random component of v_n^{CF} could be more justifiably assumed to be independent from d_{n0}.

Essentially, compared to the Wooldridge's method, it models the conditional density $f(\zeta_n|X_n, d_{n0})$ with only controls from d_{n0}, instead of d_{n0} itself. By bringing in the additional structural equation (the first step) that reflects our understandings of the initial condition problem, the proposed method is expected to offer comparable or improved performance in terms of consistency and efficiency. Compared to the Heckman's, this method is simpler to apply as it doesn't require joint estimation with the auxiliary model.

3.3.3 Estimates of Population Distribution

One issue of the conditional likelihood methods, namely the Wooldridge's and the Control Function, is that they only directly estimate the conditional distribution

$\hat{f}(\zeta_n|X_n, d_{n0})$, but not the population (marginal) distribution $g(\zeta_n)$ as in the joint likelihood approach. Despite the conditional distribution could be directly used for prediction, the population distribution might be still of interest for some applications. As the previous literature often look at dynamic models with only random intercepts, the recovery of population distribution is commonly not discussed.

Through our Monte Carlo studies, we found that estimates of $g(\zeta_n)$ could be acquired through a post processing procedure as follows. After applying the Control Function method to a sample of N individuals, we first acquire estimates of $\hat{\gamma}_0^k, \hat{\gamma}_h^k \ \forall k \in \{1, ...K\}$. Then for each individual in the sample, we can compute the fitted value of conditional mean $E[\zeta_n^k|\hat{\delta}_n]$ as $\hat{\gamma}_0^k + \hat{\gamma}_h^k\hat{\delta}_n$. An estimate of $Mean(\zeta_n)$ could be then acquired from the sample average of $\hat{\gamma}_0^k + \hat{\gamma}_h^k\hat{\delta}_n$. Combining with the estimates of the conditional variance $\hat{\Omega}^{CF}$, an estimate of the population covariance matrix $Cov(\zeta_n)$ could be acquired by computing the sample covariance matrix of the fitted conditional expectation $Cov(\hat{\gamma}_0^k + \hat{\gamma}_h^k\hat{\delta}_n)$ plus $\hat{\Omega}^{CF}$.

The same trick could be applied for the Wooldridge's method as well. With Equation 3.11, denote the estimates of α's as $\hat{\alpha}$'s, and Ω^{Wool} as $\hat{\Omega}^{Wool}$. An estimate of population mean would be the sample average of $\hat{\alpha}_0^k + \hat{\alpha}_d^k d_{n0} + \hat{\alpha}_X^{k\prime} X_{n0} + \hat{\alpha}_{\bar{X}}^{k\prime}\bar{X}_n$, and an estimate of population variance would be the sample covariance matrix $Cov(\hat{\alpha}_0^k + \hat{\alpha}_d^k d_{n0} + \hat{\alpha}_X^{k\prime} X_{n0} + \hat{\alpha}_{\bar{X}}^{k\prime}\bar{X}_n)$ plus $\hat{\Omega}^{Wool}$.

3.3.4 An Analytical Comparison to the Wooldridge's Method

As the Control Function and the Wooldridge's method both use the conditional likelihood $L(d_{n1}, ..., d_{nM_n}|X_n, d_{n0})$, in this section we analyze how they are connected and how they differ.

As the Wooldridge's method commonly uses a linear function for $\hat{f}(\zeta_n|X_n, d_{n0})$, and for the sake of more straightforward intuition, in this comparison we specify the first step of Control Function to also be a linear function (Equation 3.16) instead of a choice model.

$$d_{n0} = \tau_{ASC} + \tau'_X X_{n0} + \tau'_{\bar{X}} \bar{X}_n + \delta_n \tag{3.16}$$

We can then write the residual as $\delta_n = d_{n0} - \tau_{ASC} - \tau'_X X_{n0} - \tau'_{\bar{X}} \bar{X}$, and plug it into the expression for $\hat{f}_{CF}(\zeta_n|\hat{\delta}_n)$, as Equation 3.17.

$$\begin{aligned} \zeta_n^k &= \gamma_0^k + \gamma_h^k (d_{n0} - \tau_{ASC} - \tau'_X X_{n0} - \tau'_{\bar{X}} \bar{X}) + v_n^{CF,k}; \forall k \in \{1, ..., K\} \\ \zeta_n^k &= \gamma_0^k - \gamma_h^k \tau_{ASC} + \gamma_h^k d_{n0} - \gamma_h^k \tau'_X X_{n0} - \gamma_h^k \tau'_{\bar{X}} \bar{X} + v_n^{CF,k}; \forall k \in \{1, ..., K\} \end{aligned} \tag{3.17}$$

Comparing Equation 3.17 with Equation 3.11, we can establish the following equalities in Equation 3.18.

$$\begin{aligned} \gamma_0^k - \gamma_h^k \tau_{ASC} &= \alpha_0^k \\ \gamma_h^k &= \alpha_d^k \\ -\gamma_h^k \tau_X &= \alpha_X^k \\ -\gamma_h^k \tau_{\bar{X}} &= \alpha_{\bar{X}}^k \end{aligned} \tag{3.18}$$

Therefore, for a given set of parameters γ and τ with the CF method, there exists a unique set of parameters α with the Wooldridge's method.

On the other hand, given a set of Wooldridge parameters α, we might not always be able to find a set of equivalent γ and τ with the CF method. To see this, we can substitute the second equality from Equation 3.18 into the third and forth equalities, which gives $\tau_X = -\alpha_X^k / \alpha_d^k$ and $\tau_{\bar{X}} = -\alpha_{\bar{X}}^k / \alpha_d^k$ across all the random parameters $k = \{1, ..., K\}$. For $K > 1$, we cannot guarantee to always find values for γ_X and $\gamma_{\bar{X}}$. Therefore, coincided with our intuition, the CF method imposes additional structural theory-driven constraints compared to the Wooldridge's method.

The constraints by Control Function are not only expected to reduce the standard errors, but also crucial for identification under an extreme case where for each

individual only one choice is observed after the initial condition. To illustrate this, consider a simple true model with one exogenous attribute x_{nm} as in Equation 3.19 and we only observe 2 choices per individual.

$$U_{nm} = \zeta_n^{ASC} + \zeta_n^d d_{n(m-1)} + \zeta_n^x x_{nm} + \varepsilon_{nm} \tag{3.19}$$

The Wooldridge's method fits the conditional likelihood of d_{n1} with Equation 3.20.

$$\begin{aligned} U_{n1} =& (\alpha_0^{ASC} + \alpha_d^{ASC} d_{n0} + \alpha_x^{ASC} x_{n0} + \alpha_{\bar{x}}^{ASC} \bar{x}_n + v_n^{Wool,ASC}) + \\ & (\alpha_0^d + \alpha_d^d d_{n0} + \alpha_x^d x_{n0} + \alpha_{\bar{x}}^d \bar{x}_n + v_n^{Wool,d}) d_{n0} + \\ & (\alpha_0^x + \alpha_d^x d_{n0} + \alpha_x^x x_{n0} + \alpha_{\bar{x}}^x \bar{x}_n + v_n^{Wool,x}) x_{n1} \end{aligned} \tag{3.20}$$

Note that α_d^{ASC} and α_0^d enter U_{n1}—hence the likelihood—exactly the same way, and therefore cannot be identified. This is not merely a nuance of normalization because α_0^d is the important policy parameter that is subject to bias in the first place. This also explains why the Wooldridge's method is only applicable to common initial condition problems where the panel is not extremely short, but not to general endogeneity problems in other contexts.

3.3.5 Extension to Multinomial Choice

In this section, we extend the previously developed Control Function solution to the case of multinomial choice.

The considered multinomial choice model is presented in Equation 3.21. The alternatives in choice set $\mathbb{C}_n$ for individual n is indexed with i. $\zeta_n^{i,ASC}$ and ζ_n^d are scalars and ζ_n^X is a vector. Denote ζ_n as the vector collecting $(\zeta_n^{i,ASC}\, \forall i, \zeta_n^d, \zeta_n^X)$. The choice at situation m is denoted with indicators y_{inm} collected into a vector d_{nm}.

$$\begin{aligned} U_{inm} &= \zeta_n^{i,ASC} + \zeta_n^d y_{in(m-1)} + \zeta_n^{X\prime} X_{inm} + \varepsilon_{inm} \quad \forall i \in \mathbb{C}_n \\ y_{inm} &= 1[U_{inm} = max(U_{jnm} \forall j \in \mathbb{C}_n)] \end{aligned} \tag{3.21}$$

Same as before, observing a sequence of choices (d_{n0},d_{n1},...,d_{nM_n}), the initial condition is d_{n0}. Endogeneity known as the initial condition problem occurs because d_{n0} is correlated with ζ_n. The Control Function uses a two-step procedure to capture this correlation. The difference is that now d_{n0} is no longer a binary scalar, but a vector of choice indicators.

Naturally, a multinomial choice model could be specified as the initial condition model, outlined in Equation 3.22. The instruments in this model are the same as the binary case—exogenous attributes of the initial condition and average attributes across all observations of n, and they enter the utility of their associated alterantives. In this model, the error term δ_{in} captures the individual-specific random parameters. The coefficients of instruments could be further made alternative-specific.

$$\begin{aligned} y_{in0} &= 1[\tilde{U}_{in0} = max(\tilde{U}_{jn0} \forall j \in \mathbb{C}_n)] \\ \tilde{U}_{in0} &= \tilde{V}_{in0} + \delta_{in} \\ \tilde{V}_{in0} &= \tau_{i,ASC} + \tau'_X X_{in0} + \tau'_{\bar{X}} \bar{X}_{in} \end{aligned} \tag{3.22}$$

Different from the binary case where we would just acquire a scalar control, in this case, we have one control for each alternative $\hat{\delta}_{in} = E[\delta_{in}|d_{n0}] \ \forall i \in \mathbb{C}_n$. To compute these expectations, in addition to the previously outlined general simulation method, closed-form results are directly available when δ_{in} follows i.i.d. extreme value distributions $EV(-\gamma, 1)$ where γ is the Euler's constant ≈ 0.577 to make the unconditional mean of δ_{in} zero. The results from [51] are shown in Equation 3.23 where $P_{n0}(i)$ is the predicted probability of alternative i by the initial condition model.

$$\hat{\delta}_{in} = E[\delta_{in}|d_{n0}] = \begin{cases} -lnP_{n0}(i), & \text{if } y_{in0} = 1 \\ \frac{P_{n0}(i)}{1-P_{n0}(i)} lnP_{n0}(i), & \text{if } y_{in0} = 0 \end{cases} \tag{3.23}$$

Denote $\hat{\delta}_n$ the vector collecting $\hat{\delta}_{in} \ \forall i \in \mathbb{C}_n$. The second step is to specify ζ_n as a function of $\hat{\delta}_n$ with the assumption that ζ_n conditional on $\hat{\delta}_n$ is no longer correlated with d_{n0}. One specification is provided in Equation 3.24 where k index the dimension of ζ_n. Compared to the binary case, as $\hat{\delta}_n$ becomes a vector, γ_h^k also becomes a vector.

$v_n^{CF,k}$ is the new random components that are assumed to be uncorrelated with d_{n0}.

$$\zeta_n^k = \gamma_0^k + \gamma_h^{k\prime}\hat{\delta}_n + v_n^{CF,k}; \forall k \in \{1, ..., K\} \tag{3.24}$$

Normalizations of the specification for $\zeta_n^{i,ASC}$ are required. For example, one of the $\gamma_0^{i,ASC}$ needs to be fixed to zero, and any element of control cannot enter all the $\zeta_n^{i,ASC}$. One sparser specification of the $\zeta_n^{i,ASC}$ could be $\zeta_n^{i,ASC} = \gamma_0^{i,ASC} + \gamma_h^{i,ASC}\hat{\delta}_{in} + v_n^{CF,i,ASC}$ which makes an alternative-specific constant only a function of that alternative's expected error in the auxiliary initial condition model.

3.4 Monte Carlo Experiment

3.4.1 Experimental Setup

We consider a choice between two routes, each of which is associated with a cost and travel time. The utility of route 1 for individual n and choice situation m is specified in Equation 3.25 where x_{nm}^{time} denotes the travel time saving of route 1 compared to route 2, and the x_{nm}^{cost} denotes for extra cost of route 1 compared to route 2. The cost coefficient is normalized to -1 to make the utility money metric and a scale parameter is estimated. ζ_n^{scale} and ζ_n^{time} enter the utility with exponentiation to ensure logical sign constraints. The utility of route 2 is normalized to zero.

$$U_{nm} = \zeta_n^d d_{n(m-1)} + \zeta_n^{ASC} - x_{nm}^{cost} + exp(\zeta_n^{time}) x_{nm}^{time} + \varepsilon_{nm}/exp(\zeta_n^{scale}) \tag{3.25}$$

For each person, we first generate 100 unobserved choice situations as the pre-sample period. For the utility of the first-ever choice, its lagged choice $d_{n(m-1)}$ is valued zero. As explained, the existence of these unobserved choices realistically mimics the actual situation of empirical datasets, and is the source of the initial condition problem. Then, we further generate M following choices for each individual and these comprise the observed data. Following our notation, these are denoted from

d_{n0} to $d_{n(M-1)}$.

We generate two datasets with different distributions specified for exogenous attributes x_{nm}^{cost} and x_{nm}^{time} and for the individual-specific random parameters $\zeta_n = (\zeta_n^d, \zeta_n^{scale}, \zeta_n^{ASC}, \zeta_n^{time})$ as follows:

- Dataset 1: ζ_n follows a normal distribution with a diagonal covariance matrix. The exogenous attributes are generated from i.i.d. standard normal distribution (i.e., N(0,1)).

- Dataset 2: ζ_n follows a normal distribution with a full covariance matrix. The exogenous attributes are generated with respective individual-specific mean to incorporate serial correlation in the exogenous attributes. We first draw $x_n^{cost} \sim N(0, 0.5)$ and $x_n^{time} \sim N(0, 0.5)$, and then for each choice situation draw $x_{nm}^{cost} \sim N(x_n^{cost}, 0.5)$ and $x_{nm}^{time} \sim N(x_n^{time}, 0.5)$.

3.4.2 Estimation Methods

Four previously explained estimation methods are respectively deployed. Additional specifications of the Wooldridge's Method and Control Function are tested for dataset 2, to be introduced later:

1. *No Correction*: it considers the conditional likelihood in Equation 3.4, but uses a marginal density $\breve{f}(\zeta_n)$ in place of $f(\zeta_n|X_n, d_{n0})$.

2. *Heckman's Method*: it considers the joint likelihood in Equation 3.3 with the model for initial condition as Equation 3.26 where $\Delta\zeta$ denotes the difference between ζ_n and the population mean.

$$\begin{aligned} U_{n0} =& r_0\Delta\zeta_n^d + (c_1 + r_1\Delta\zeta_n^{ASC}) - x_{n0}^{cost} + exp(c_2 + r_2\Delta\zeta_n^{time})x_{n0}^{time} \\ &+ \varepsilon_{n0}/exp(c_3 + r_3\Delta\zeta_n^{scale}) \end{aligned} \tag{3.26}$$

3. *Wooldridge's Method*: it considers the conditional likelihood with $f(\zeta_n|X_n, d_{n0})$

approximated by $\hat{f}_{Wool}$ as Equation 3.27, where $k \in \{d, scale, ASC, time\}$.

$$\zeta_n^k = \alpha_0^k + \alpha_1^k d_{n0} + \alpha_2^k x_{n0}^{cost} + \alpha_3^k x_{n0}^{time} + \alpha_4^k \bar{x}_n^{cost} + \alpha_5^k \bar{x}_n^{time} + v_n^{Wool,k} \tag{3.27}$$

4. *Control Function*: it considers the conditional likelihood with $f(\zeta_n|X_n, d_{n0})$ approximated by $\hat{f}_{CF}$ as Equation 3.28, where $k \in \{d, scale, ASC, time\}$.

$$\begin{aligned} d_{n0} &= 1[\tau_0 + \tau_1 x_{n0}^{cost} + \tau_2 x_{n0}^{time} + \tau_3 \bar{x}_n^{cost} + \tau_4 \bar{x}_n^{time} + \delta_n > 0], \delta_n \sim N(0,1) \\ \hat{\delta}_n &= E[\delta_n|d_{n0}] \\ \zeta_n^k &= \gamma_0^k + \gamma_1^k \hat{\delta}_n + \nu_n^{CF,k} \end{aligned} \tag{3.28}$$

For dataset 1, as the true population distribution of random parameters has a diagonal covariance matrix, for the No Correction and Heckman's Method, diagonal covariance matrices are directly specified for ζ_n. For the Wooldridge's Method and Control Function, because they approximate the conditional distribution of random parameters on the initial condition, we first estimate full covariances matrices for ν_n^{Wool} and ν_n^{CF} where the covariances are then found to be insignificant, so we change to diagonal covariance matrices. Results of the Wooldridge's Method and Control Function with full covariance matrices are available in Table A.1 and Table A.2 of Appendix A.

For dataset 2, as the true population distribution of random parameters has a full covariance matrix, full covariance matrices are directly specified for the random paramters in all methods.

3.4.3 Computation

To estimate the model with the listed methods, we use the Hierarchical Bayes procedure described in [102] that uses Gibbs Sampling and an embedded Metropolis-Hastings (MH) step. For a model with random parameters $\zeta_n \sim N(\mu, \Omega)$, the algorithm generates draws from the posterior distribution of the parameters by iterating the following steps:

- Step 1: drawing from the conditional posterior of the population mean $\mu|\Omega, \zeta_n$ using the posterior formula for a Normal distribution with unknown mean and known variance.

- Step 2: drawing from the conditional posterior of the covariance matrix $\Omega|\mu, \zeta_n$ using the posterior formula for a Normal distribution with known mean and unknown variance.

- Step 3: drawing from the conditional posterior of the individual-specific parameters $\zeta_n|\mu, \Omega$ using the Metropolis-Hastings (MH) algorithm.

Then, estimates of population mean and variances are acquired by averaging the generated draws, excluding draws generated from the beginning *burn-in* iterations. The Bayesian method is used to replicate maximum simulated likelihood estimates with a lower computation cost. With uninformative priors and a large sample, Bayesian estimates should be identical to the classical method [27].

For the No Correction method, the outlined Sampler could be directly used. As the Heckman's Method involves additional fixed (non-random) parameters that appear in the auxiliary Equation 3.9, these fixed parameters are drawn using an additional separate MH step as in [22], where the jumping distribution's covariance is also adapted during the burn-in stage to facilitate convergence. For the Wooldridge's Method and Control Function, as the ζ_n follows conditional distributions whose means are linear functions of regressors, the Step 1 is replaced with drawing from the posterior formula of multivariate regression in [89]. The first step of Control Function is performed with the standard *glm* package in R as it doesn't involve random parameters.

3.4.4 Results

Dataset 1: 5 observed choices, 5000 individuals

The estimation results on dataset 1 is shown in Table 3.1, with RMSE of the estimators in Table 3.2. Standard errors from the Monte Carlo repetitions are shown in brackets. In terms of performance, the No Correction significantly overestimates the

state dependence effect ζ_n^d. The three correction methods offer overall similar performance in bias reduction. The proposed Control Function yields smaller standard errors compared to the Wooldridge's Method, thanks to its incorporation of additional structural knowledge. Comparing the RMSE, the Control Function is slightly better than the Wooldridge's Method and comparable to the Heckman's Method.

	True Value	**No Correction**	**Heckman's Method**	**Wooldridge's Method**	**Control Function**
Population mean					
ζ_n^{scale}	1	0.866 (0.0632)	0.992 (0.0741)	1.01 (0.0789)	1.00 (0.0724)
ζ_n^{d}	1.5	2.14 (0.0531)	1.48 (0.0504)	1.48 (0.0526)	1.47 (0.0476)
ζ_n^{ASC}	-0.5	-0.836 (0.0309)	-0.487 (0.0374)	-0.493 (0.0330)	-0.495 (0.0326)
ζ_n^{time}	0	-0.00173 (0.0338)	0.00389 (0.0321)	0.0118 (0.0384)	0.0135 (0.0331)
Population variance					
ζ_n^{scale}	0.5	0.458 (0.0928)	0.506 (0.112)	0.570 (0.121)	0.544 (0.112)
ζ_n^{d}	0.5	1.14 (0.111)	0.485 (0.109)	0.472 (0.0936)	0.427 (0.0922)
ζ_n^{ASC}	1	0.419 (0.0519)	1.06 (0.0983)	1.03 (0.0977)	0.989 (0.0860)
ζ_n^{time}	1	1.16 (0.0841)	1.00 (0.0716)	0.986 (0.0808)	0.951 (0.0756)
60 repetitions, 5 observed choices, 5,000 individuals					

Table 3.1: Dataset 1 estimates (5,000 individuals)

	No Correction	Heckman's Method	Wooldridge's Method	Control Function
Population mean				
ζ_n^{scale}	0.148	0.0746	0.0794	0.0725
ζ_n^{d}	0.643	0.0541	0.0569	0.0558
ζ_n^{ASC}	0.337	0.0397	0.0337	0.0329
ζ_n^{time}	0.0339	0.0323	0.0401	0.0358
Population variance				
ζ_n^{scale}	0.102	0.113	0.140	0.121
ζ_n^{d}	0.651	0.110	0.0978	0.118
ζ_n^{ASC}	0.584	0.115	0.101	0.0867
ζ_n^{time}	0.181	0.0716	0.0820	0.0903
60 repetitions, 5 observed choices, 5,000 individuals				

Table 3.2: Dataset 1 RMSE (5,000 individuals)

Dataset 2: 5 observed choices, 5000 individuals

To further investigate their performance under more involved situations, we move on to dataset 2 where the true distribution of ζ_n has nonzero covariances and the exogenous attributes have individual-specific mean.

The results are shown in Table 3.3 and Table 3.4. It is first worth noting that under this setting the Heckman's Method shows convergence problems, likely due to the joint estimation with the initial condition model and specifying a full covariance matrix. Out of 60 repetitions, only 16 have converged for the Heckman's approach and the results for the Heckman's approach are based on these converged repetitions. This convergence issue disappears when the number of observations per individual or the number of individuals increases.

As expected, bias of the No Correction method increases, as the past choices could also capture correlations in the exogenous attributes. The three correction methods all reduce the bias. For population mean of the random parameters, all these methods provide estimates close to the true value considering the standard errors. For population variances and covariances, Wooldridge's Method and Control Function have larger biases compared to the Heckman's Method, likely due to the approxima-

tions of ζ_n's conditional distribution are not good enough and that the population distributions are computed from post-processing as described in subsection 3.3.3.

	True Value	**No Correction**	**Heckman's Method**	**Wooldridge's Method**	**Control Function**
Population mean					
ζ_n^{scale}	1	0.839 (0.0974)	1.00 (0.0980)	0.967 (0.102)	0.982 (0.0932)
ζ_n^{d}	1.5	2.50 (0.0780)	1.52 (0.0549)	1.57 (0.0882)	1.49 (0.0629)
ζ_n^{ASC}	-0.5	-0.899 (0.0367)	-0.505 (0.0453)	-0.523 (0.0554)	-0.482 (0.0449)
ζ_n^{time}	0	0.00826 (0.0434)	0.00617 (0.0507)	0.0764 (0.0550)	0.0567 (0.0436)
Population variance					
ζ_n^{scale}	0.5	0.539 (0.149)	0.648 (0.165)	0.670 (0.172)	0.662 (0.158)
ζ_n^{d}	0.5	3.18 (0.275)	0.637 (0.122)	0.693 (0.208)	0.505 (0.169)
ζ_n^{ASC}	1	0.476 (0.0909)	1.07 (0.139)	0.894 (0.165)	0.918 (0.119)
ζ_n^{time}	1	0.962 (0.0974)	1.07 (0.0835)	0.788 (0.0992)	0.785 (0.0879)
Population covariance					
$\zeta_n^{scale}, \zeta_n^{d}$	0.1	0.268 (0.128)	0.0123 (0.102)	0.00354 (0.101)	0.0111 (0.0916)
$\zeta_n^{scale}, \zeta_n^{ASC}$	0.3	-0.0500 (0.0876)	0.347 (0.141)	0.316 (0.124)	0.348 (0.116)
$\zeta_n^{scale}, \zeta_n^{time}$	0.2	0.180 (0.0819)	0.0822 (0.0846)	0.0895 (0.0859)	0.0621 (0.0784)
$\zeta_n^{d}, \zeta_n^{ASC}$	-0.1	-0.831 (0.111)	-0.0862 (0.0953)	-0.0180 (0.123)	-0.0116 (0.104)
$\zeta_n^{d}, \zeta_n^{time}$	-0.15	-0.759 (0.109)	-0.132 (0.0855)	-0.217 (0.0917)	-0.179 (0.0785)
$\zeta_n^{ASC}, \zeta_n^{time}$	-0.5	0.0265 (0.0610)	-0.550 (0.0912)	-0.328 (0.101)	-0.364 (0.0700)
60 repetitions, 5 observed choices, 5,000 individuals					

Table 3.3: Dataset 2 estimates (5,000 individuals)

	No Correction	Heckman's Method	Wooldridge's Method	Control Function
Population mean				
ζ_n^{scale}	0.188	0.0981	0.108	0.0950
ζ_n^{d}	1.01	0.0592	0.112	0.0642
ζ_n^{ASC}	0.401	0.0456	0.0598	0.0485
ζ_n^{time}	0.0442	0.0511	0.0941	0.0715
Population variance				
ζ_n^{scale}	0.154	0.221	0.242	0.226
ζ_n^{d}	2.69	0.184	0.284	0.169
ζ_n^{ASC}	0.531	0.155	0.196	0.144
ζ_n^{time}	0.105	0.112	0.234	0.232
Population covariance				
$\zeta_n^{scale}, \zeta_n^{d}$	0.211	0.134	0.140	0.128
$\zeta_n^{scale}, \zeta_n^{ASC}$	0.361	0.148	0.125	0.126
$\zeta_n^{scale}, \zeta_n^{time}$	0.0844	0.145	0.140	0.159
$\zeta_n^{d}, \zeta_n^{ASC}$	0.740	0.0963	0.148	0.137
$\zeta_n^{d}, \zeta_n^{time}$	0.619	0.0874	0.114	0.0837
$\zeta_n^{ASC}, \zeta_n^{time}$	0.530	0.104	0.200	0.153
60 repetitions, 5 observed choices, 5,000 individuals				

Table 3.4: Dataset 2 RMSE (5,000 individuals)

Dataset 2: 5 observed choices, 10,000 individuals

As significant biases of population variances are observed with the Wooldridge's Method and Control Function on dataset 2 with 5,000 individuals, we increase the number of individuals to 10,000 to check whether the bias would decrease as sample size increases. Unfortunately, based on results in Table 3.5 and Table 3.6, no noticeable bias reductions of these two methods are observed as sample size increases. Therefore, the advantage of Heckman's Method in estimating population variances becomes clearer.

Dataset 2: flexible correction specifications

Attempting to improve the Wooldridge's Method and Control Function, we performed further experiments with the specifications listed below:

- *Flexible Wooldridge*: add to Equation 3.27 the polynomials and interactions of the instruments x_{n0}^{cost2}, x_{n0}^{time2}, $\bar{x}_n^{cost2}$, $\bar{x}_n^{time2}$, $x_{n0}^{cost}x_{n0}^{time}$, $\bar{x}_n^{cost}\bar{x}_n^{time}$, and interactions between the instrument and initial condition $x_{n0}^{cost}d_{n0}$, $x_{n0}^{time}d_{n0}$, $\bar{x}_n^{cost}d_{n0}$, $\bar{x}_n^{time}d_{n0}$.

- *Flexible Control Function*: add to the first step of Equation 3.28 the polynomials and interactions of the instruments listed in *Flexible Wooldridge*, and add to the second step $\hat{\delta}_n^2$, $\hat{\delta}_n/x_{n0}^{cost}$, $\hat{\delta}_n/x_{n0}^{time}$, $\hat{\delta}_n/\bar{x}_n^{cost}$, $\hat{\delta}_n/\bar{x}_n^{time}$. The inclusions of these ratios are motivated by that the random parameter ζ_n^{time} is expected to enter the error term δ_n in the initial condition model as a product with attributes, and the variance of ζ_n^{time} is especially biased under the previous simpler specification. When computing these ratios, for numerical stability, constants are added to the instruments such that their minimum values are one in the dataset.

20 repetitions are done for these methods and compared with the previously presented simpler specifications under 5,000 and 10,000 individuals. The results are shown in Table 3.7 and Table 3.8. Compared to the previous simple specifications, these flexible specifications reduce the large bias in $var(\zeta_n^{time})$, but seem to incur

	True Value	No Correction	Heckman's Method	Wooldridge's Method	Control Function
Population mean					
ζ_n^{scale}	1	0.846 (0.0546)	0.992 (0.0500)	0.978 (0.0650)	0.991 (0.0567)
ζ_n^{d}	1.5	2.48 (0.0619)	1.53 (0.0601)	1.58 (0.0667)	1.51 (0.0575)
ζ_n^{ASC}	-0.5	-0.897 (0.0364)	-0.508 (0.0399)	-0.533 (0.0447)	-0.497 (0.0396)
ζ_n^{time}	0	0.0102 (0.0243)	0.0116 (0.0241)	0.0731 (0.0341)	0.0560 (0.0222)
Population variance					
ζ_n^{scale}	0.5	0.533 (0.109)	0.601 (0.0918)	0.651 (0.120)	0.650 (0.113)
ζ_n^{d}	0.5	3.22 (0.262)	0.597 (0.143)	0.751 (0.159)	0.591 (0.138)
ζ_n^{ASC}	1	0.491 (0.0615)	1.06 (0.0649)	0.882 (0.0927)	0.915 (0.0747)
ζ_n^{time}	1	0.903 (0.0732)	1.04 (0.0754)	0.743 (0.0652)	0.751 (0.0672)
Population covariance					
$\zeta_n^{scale}, \zeta_n^{d}$	0.1	0.243 (0.114)	-0.0137 (0.0783)	-0.0258 (0.102)	-0.0124 (0.0912)
$\zeta_n^{scale}, \zeta_n^{ASC}$	0.3	-0.0173 (0.0613)	0.345 (0.0765)	0.336 (0.0906)	0.369 (0.0854)
$\zeta_n^{scale}, \zeta_n^{time}$	0.2	0.217 (0.0547)	0.152 (0.0568)	0.136 (0.0556)	0.102 (0.0555)
$\zeta_n^{d}, \zeta_n^{ASC}$	-0.1	-0.860 (0.105)	-0.0759 (0.0885)	-0.0567 (0.102)	-0.0439 (0.0915)
$\zeta_n^{d}, \zeta_n^{time}$	-0.15	-0.774 (0.0751)	-0.163 (0.0480)	-0.250 (0.0435)	-0.212 (0.0453)
$\zeta_n^{ASC}, \zeta_n^{time}$	-0.5	0.0311 (0.0445)	-0.535 (0.0504)	-0.298 (0.0553)	-0.343 (0.0453)
30 repetitions, 5 observed choices, 10,000 individuals					

Table 3.5: Dataset 2 estimates (10,000 individuals)

	No Correction	Heckman's	Wooldridge's	Control Function
Population mean				
ζ_n^{scale}	0.163	0.0506	0.0687	0.0575
ζ_n^{d}	0.983	0.0672	0.103	0.0578
ζ_n^{ASC}	0.398	0.0407	0.0554	0.0397
ζ_n^{time}	0.0264	0.0267	0.0807	0.0602
Population variance				
ζ_n^{scale}	0.114	0.137	0.193	0.188
ζ_n^{d}	2.73	0.173	0.297	0.165
ζ_n^{ASC}	0.512	0.0884	0.150	0.113
ζ_n^{time}	0.122	0.0873	0.266	0.257
Population covariance				
$\zeta_n^{scale}, \zeta_n^{d}$	0.183	0.138	0.162	0.145
$\zeta_n^{scale}, \zeta_n^{ASC}$	0.323	0.0888	0.0977	0.110
$\zeta_n^{scale}, \zeta_n^{time}$	0.0572	0.0742	0.0851	0.112
$\zeta_n^{d}, \zeta_n^{ASC}$	0.767	0.0917	0.111	0.107
$\zeta_n^{d}, \zeta_n^{time}$	0.629	0.0498	0.109	0.0765
$\zeta_n^{ASC}, \zeta_n^{time}$	0.533	0.0612	0.210	0.164
30 repetitions, 5 observed choices, 10,000 individuals				

Table 3.6: Dataset 2 RMSE (10,000 individuals)

larger bias in the other variances. Further, the biases still persist when the number of individuals increases. Therefore, these results indicate no significant further improvements over the previously presented simpler specifications.

	True Value	**Flexible Wooldridge (5,000 ind.)**	**Flexible Wooldridge (10,000 ind.)**	**Flexible Control Function (5,000 ind.)**	**Flexible Control Function (10,000 ind.)**
Population mean					
ζ_n^{scale}	1	1.04 (0.121)	1.02 (0.0698)	1.03 (0.0868)	1.02 (0.0484)
ζ_n^{d}	1.5	1.54 (0.103)	1.57 (0.919)	1.54 (0.0730)	1.55 (0.0671)
ζ_n^{ASC}	-0.5	-0.539 (0.0700)	-0.563 (0.0706)	-0.513 (0.0415)	-0.530 (0.0469)
ζ_n^{time}	0	0.0567 (0.0695)	0.0517 (0.0230)	0.0518 (0.0437)	0.0541 (0.0226)
Population variance					
ζ_n^{scale}	0.5	0.810 (0.241)	0.710 (0.121)	0.723 (0.188)	0.680 (0.0996)
ζ_n^{d}	0.5	0.762 (0.259)	0.771 (0.131)	0.619 (0.213)	0.652 (0.142)
ζ_n^{ASC}	1	0.901 (0.154)	0.834 (0.0931)	0.861 (0.131)	0.879 (0.0648)
ζ_n^{time}	1	1.11 (0.125)	1.01 (0.0816)	0.963 (0.106)	0.919 (0.0629)
Population covariance					
$\zeta_n^{scale}, \zeta_n^{d}$	0.1	-0.0384 (0.113)	-0.0209 (0.116)	-0.0123 (0.117)	-0.0242 (0.104)
$\zeta_n^{scale}, \zeta_n^{ASC}$	0.3	0.281 (0.137)	0.282 (0.0859)	0.283 (0.125)	0.318 (0.0744)
$\zeta_n^{scale}, \zeta_n^{time}$	0.2	0.133 (0.119)	0.196 (0.0705)	0.118 (0.101)	0.168 (0.0594)
$\zeta_n^{d}, \zeta_n^{ASC}$	-0.1	-0.0307 (0.120)	-0.0638 (0.115)	-0.0868 (0.112)	-0.115 (0.114)
$\zeta_n^{d}, \zeta_n^{time}$	-0.15	-0.218 (0.143)	-0.250 (0.0745)	-0.183 (0.105)	-0.199 (0.548)
$\zeta_n^{ASC}, \zeta_n^{time}$	-0.5	-0.441 (0.131)	-0.386 (0.0533)	-0.402 (0.0809)	-0.401 (0.0428)
20 repetitions , 5 observed choices					

Table 3.7: Dataset 2 estimates (Flexible correction specifications)

	Flexible Wooldridge (5,000 ind.)	**Flexible Wooldridge (10,000 ind.)**	**Flexible Control Function (5,000 ind.)**	**Flexible Control Function (10,000 ind.)**
Population mean				
ζ_n^{scale}	0.127	0.0738	0.0911	0.0513
ζ_n^{d}	0.113	0.113	0.0836	0.0831
ζ_n^{ASC}	0.0800	0.0945	0.0435	0.0557
ζ_n^{time}	0.0897	0.0566	0.0678	0.0586
Population variance				
ζ_n^{scale}	0.393	0.242	0.291	0.206
ζ_n^{d}	0.368	0.301	0.244	0.208
ζ_n^{ASC}	0.183	0.190	0.192	0.138
ζ_n^{time}	0.166	0.0820	0.112	0.103
Population covariance				
$\zeta_n^{scale}, \zeta_n^{d}$	0.178	0.168	0.162	0.162
$\zeta_n^{scale}, \zeta_n^{ASC}$	0.138	0.0877	0.126	0.0766
$\zeta_n^{scale}, \zeta_n^{time}$	0.136	0.0706	0.130	0.0676
$\zeta_n^{d}, \zeta_n^{ASC}$	0.139	0.121	0.113	0.115
$\zeta_n^{d}, \zeta_n^{time}$	0.159	0.125	0.111	0.0734
$\zeta_n^{ASC}, \zeta_n^{time}$	0.144	0.126	0.127	0.108
20 repetitions, 5 observed choices				

Table 3.8: Dataset 2 RMSE (Flexible correction specifications)

3.5 Conclusions

In this chapter, a Control Function solution is proposed to the well-known initial condition problem in the estimation of dynamic choice model with random parameters. The proposed method is compared with existing solutions, namely the one by Heckman [66] and the one by Wooldridge [108], both from an analytical view and Monte Carlo experiments. Instead of dynamic models with only random intercepts that are commonly considered in the literature, our analysis considers the general case of random parameters and the estimation of their population distributions. Further, the Control Function solution is extended for dynamic multinomial choice models.

Compared to the Wooldridge's method, Control Function provides similar bias reductions with smaller standard errors as it incorporates more structural knowledge regarding the source of endogeneity. Compared to the Heckman's Method, Control Function has similar performance in estimating the population mean of random parameters, but gives considerably larger bias in estimating population covariance matrix (similar to Wooldridge's method). This covariance matrix bias does not seem to decrease as the number of individual increases. More flexible modeling assumptions could potentially alleviate this problem, for example trying to use semi-parametric distribution specifications (for example [43]) for the conditional distributions.

The impact of the covariance matrix bias on personalized pricing is not immediately clear and requires further investigation. Nevertheless, the corrected models should at least be much better to use than the uncorrected model with largely biased population mean. Further, as will be introduced in chapter 5, to predict a new choice by a given individual, our personalized pricing methodology uses the posterior distribution of individual-specific parameters (ζ_n) on previous choices from that person. In this case, the population distribution only serves as a prior, and hence its influence should decrease to none when a large amount of observations from the individual becomes available.

Chapter 4

Managed Lanes Travel Behavior Modeling

4.1 Introduction

This chapter develops a comprehensive choice model for whether a traveler uses the managed lanes (ML), as opposed to general purpose lanes (GP). The choice situation is shown in Figure 4-1. A corridor consists of tolled ML and free GP that run in parallel. Travelers who opt to use ML are required to pay a toll. The study is based on empirical data that are detailed in section 4.2.

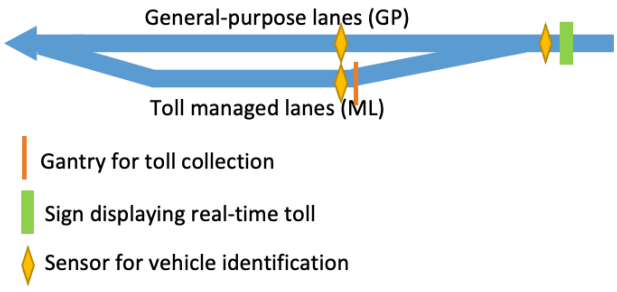

Figure 4-1: Choice situation between ML and GP

Aiming to develop a useful choice model for personalized pricing analysis, we have two main objectives. The first objective is to quantify the extent of unobserved heterogeneity and state dependence. Incorporations of unobserved heterogeneity allow estimation of individual-level parameters that better predict choices of specific individuals. Quantification of state dependence is particularly important when the price is determined considering future returns (for example, a discount program that tries to cultivate travel habit or brand loyalty). The second objective is to correctly estimate the price elasticity, the importance of which is obvious.

In this study, we extend the model specification developed by [115] which used the same data to estimate a flat logit model with a comprehensive list of state-dependent variables that capture past choices and their interactions with past experience. We build on their work first by including random parameters to capture unobserved heterogeneity. This incurs the initial condition problem we analyzed in chapter 3, and the Wooldridge's and Control Function corrections are applied and compared. In addition, we analyze the price endogeneity problem caused by dynamic pricing, and find suitable instruments for its correction.

In this chapter, we start by describing the data. Then the choice model is specified, followed by methods for correcting the initial condition problem and price endogeneity. The chapter concludes with a discussion of estimation results and implications.

4.2 Data Description

The study is based on empirical trip records from an operational ML facility near the Dallas/Fort Worth Airport, which is a 13.3-mile corridor on I-635 and I-35E in Dallas, Texas (Figure 4-2). The toll on ML is adjusted dynamically according to demand.

We acquired the data of westbound trips that start before U.S. Route 75 (east of toll segment 3) and continue beyond I-35E (west of toll segment 2). These trips are recorded by Automatic Vehicle Identification (AVI) sensors. Each trip record includes anonymized unique transponder IDs, trip start time, actual travel time on the chosen paths, pre-trip travel time (processed by the data provider to approximate

Figure 4-2: Case study network

Google Maps predictions), the displayed toll, and the traffic condition (flow, speed and density) at the decision point. Unlike common choice datasets in transportation or applied econometrics, our data have no observed characteristics of the traveler (e.g., income, occupation), but only trip attributes including toll, travel time, and time of day, which highlights the need for considering unobserved heterogeneity. Five months of data from Sep, 2017 is available. The trips during holiday and weekends are excluded as the study focuses on typical weekdays. The range of toll in our data is between \$1.9 to \$8.25.

4.3 Model Specification

A traveler n makes trip m and considers a binary choice between ML and GP. We normalize the utility of GP to zero and specify the utility of ML as Equation 4.1.

$$
\begin{aligned}
U_{ML,nm} = \beta_{nm}^{ASC} &- exp(\beta_{nm}^{toll}) x_{nm}^{toll\,(boxcox)} + exp(\beta_{nm}^{time}) x_{nm}^{timeSaving} \\
&- exp(\beta_{nm}^{DPspeed}) x_{nm}^{DPspeed} + \varepsilon_{nm} \qquad (4.1) \\
\text{where } x_{nm}^{toll\,(boxcox)} &= \frac{(x_{nm}^{toll}+1)^{b^{boxcox}} - 1}{b^{boxcox}}
\end{aligned}
$$

The utility has four components constructed by trip-specific sensitivity functions denoted with β_{nm} and trip attributes denoted with x_{nm}. $x_{nm}^{toll(boxcox)}$ denotes box cox transformed toll rates with fixed parameter b^{boxcox}. $x_{nm}^{timeSaving}$ denotes the time saving of managed lanes. $x_{nm}^{DPspeed}$ denotes personalized decision point speed that equals the decision point speed minus the average of traveler's past experienced ones in the previous 90 days.

In estimating heterogeneous preferences towards the attributes, it is important to place logical sign restrictions. A rational traveler should perceive toll to generate negative utility, time saving to generate positive utility, and higher decision point speed to generate negative utility of ML relative to GP. These sign restrictions are specified through the exponential function, which is convenient for Bayesian estimation [27].

To capture the state dependence effects, we allow the current choice to depend on previous 90 days' trip history denoted as set $\mathcal{D}_{n(m-1)}$. State-dependent variables are considered as characteristics and denoted with letter s, in contrast to the attributes denoted by x. $\mathcal{D}_{n(m-1)}$ enters β_{nm} with transformations that map it to a vector of state-dependent variables listed in Table 4.1. Each of these variables is generated from one of the three time spans of previous history: (a) previous 90 days, (b) previous 30 days, and (c) last choice in the previous 90 days. These variables are either purely based on past choices, or are interactions of past choices with past travel time for measuring previous experiences of the traveler.

To capture the unobserved heterogeneity among individuals (inter-consumer heterogeneity), β_{nm} includes individual-specific random parameter $\zeta_n = (\zeta_n^{ASC}, \zeta_n^{toll}, \zeta_n^{time}, \zeta_n^{DPspeed}) \sim N(\mu, \Omega_b)$. To capture unobserved heterogeneity among trips made by the same individual (intra-consumer heterogeneity), β_{nm} includes trip-

Variable	Definition
Based on choices in the previous 90 days	
$s_{nm}^{loyal90}$	$ln((1+s_{nm}^{MLtrips90})/(1+s_{nm}^{GPtrips90}))$ where $s_{nm}^{MLtrips90}$ and $s_{nm}^{GPtrips90}$ are respectively the numbers of ML and GP trips in the previous 90 days
$s_{nm}^{hadMLtrip90}$	1 if had ML trips in the previous 90 days, 0 otherwise
$s_{nm}^{hadGPtrip90}$	1 if had GP trips in the previous 90 days, 0 otherwise
Based on choices in the previous 30 days	
$s_{nm}^{loyal30}$	similar to $s_{nm}^{loyal90}$ except based on the previous 30 days
$s_{nm}^{hadMLtrip30}$	similar to $s_{nm}^{hadMLtrip90}$ except based on the previous 30 days
$s_{nm}^{hadGPtrip30}$	similar to $s_{nm}^{hadGPtrip90}$ except based on the previous 30 days
Based on the last choice in previous 90 days	
$s_{nm}^{lastChoiceML}$	1 if had trip in the previous 90 days and the last choice was ML
$s_{nm}^{lastChoiceGP}$	1 if had trip in the previous 90 days and the last choice was GP
Based on experiences in previous 90 days	
$s_{nm}^{histMLtimeDiff}$	Experience on ML trips in the previous 90 days, which is measured by the average difference between actual travel time and the expected travel time. 0 if the traveler didn't have ML trips in the previous 90 days
$s_{nm}^{histGPtimeDiff}$	similar to $s_{nm}^{histMLtimeDiff}$ except based on GP trips
Based on experience of the last trip in previous 90 days	
$s_{nm}^{lastTripMLDiff}$	Difference between actual travel time and the expected travel time for the last trip, if that trip was ML. 0 for travelers whose last trip is GP or didn't travel in previous 90 days
$s_{nm}^{lastTripGPDiff}$	Similar to $s_{nm}^{lastTripMLDiff}$ if the traveler's last choice was GP

Table 4.1: State-dependent variables

specific random parameter $\eta_{nm} = (\eta_{nm}^{ASC}, \eta_{nm}^{toll}, \eta_{nm}^{time}, \eta_{nm}^{DPspeed}) \sim N(0, \Omega_w)$. ζ_n and η_{nm} enter β_{nm} linearly, as specified in Equation 4.2, Equation 4.4, Equation 4.5, and Equation 4.6.

We specify β_{nm}^{ASC} as Equation 4.2. It includes β_{nm}^{H} which is a function of the listed state-dependent variables (to be further specified in Equation 4.3). The time of day ranging between 0 (00:00) and 1 (24:00) is denoted as x_{nm}^{tod} and enters utility through a Fourier series as introduced in [23]. In estimation, η_{nm}^{ASC} is normalized to zero, as the alternative-specific variance of a binary choice model could not be identified from the scale of ε_{nm} [105].

$$\begin{aligned}\beta_{nm}^{ASC} =& \beta_{nm}^{H} + \sum_{k=1}^{6}[b_k^{sin} sin(2k\pi x_{nm}^{tod}) + b_k^{cos} cos(2k\pi x_{nm}^{tod})] + \\ & \zeta_n^{ASC} + \eta_{nm}^{ASC}\end{aligned} \tag{4.2}$$

As in Equation 4.3, β_{nm}^{H} includes the full list of state-dependent variables in Table 4.1. Further, the effects of the last choice and experience is specified to diminish as the last trip is more distant from the current choice. This is reflected by $exp(-b^{memory}) s_{nm}^{daysSinceLastTrip}$ where $s_{nm}^{daysSinceLastTrip}$ is the number of days since the last trip in previous 90 days and we expect b^{memory} to be positive.

$$\begin{aligned}\beta_{nm}^{H} =& b^{loyal90} s_{nm}^{loyal90} + b^{hadMLtrip90} s_{nm}^{hadMLtrip90} + b^{hadGPtrip90} s_{nm}^{hadGPtrip90} + \\ & b^{loyal30} s_{nm}^{loyal30} + b^{hadMLtrip30} s_{nm}^{hadMLtrip30} + b^{hadGPtrip30} s_{nm}^{hadGPtrip30} + \\ & b^{histMLtimeDiff} s_{nm}^{histMLtimeDiff} + b^{histGPtimeDiff} s_{nm}^{histGPtimeDiff} + \\ & (b^{lastChoiceML} + b^{lastChoiceMLMemory} s_{nm}^{memory}) s_{nm}^{lastChoiceML} + \\ & b^{lastChoiceGPMemory} s_{nm}^{memory} s_{nm}^{lastChoiceGP} + \\ & b^{lastTripMLDiff} s_{nm}^{memory} s_{nm}^{lastTripMLDiff} + \\ & b^{lastTripGPDiff} s_{nm}^{memory} s_{nm}^{lastTripGPDiff} \\ s_{nm}^{memory} =& exp(-b^{memory}) s_{nm}^{daysSinceLastTrip}\end{aligned} \tag{4.3}$$

We specify β_{nm}^{toll} as Equation 4.4, a function of the traveler's trips per day in previous 90 days (denoted as s_{nm}^{freq}), $s_{nm}^{loyal90}$ (defined in Table 4.1), and whether the traveler had any trip in the previous 90 days (denoted as s_{nm}^{noTrip} that equals 1 if the person did not). Note that s_{nm}^{freq} and s_{nm}^{noTrip} are in fact not state-dependent because they are independent from previous choices.

$$\begin{aligned}\beta_{nm}^{toll} =& b^{toll,freq} s_{nm}^{freq} + b^{toll,loyal90} s_{nm}^{loyal90} + b^{toll,noTrip} s_{nm}^{noTrip} + \\ & \zeta_n^{toll} + \eta_{nm}^{toll}\end{aligned} \tag{4.4}$$

We specify β_{nm}^{time} as Equation 4.5, a function of s_{nm}^{freq}, $s_{nm}^{loyal90}$ and s_{nm}^{noTrip} that appeared in β_{nm}^{toll}, as well as time period indicators x_{nm}^{night}, x_{nm}^{AM} and x_{nm}^{PM} that respectively represent time periods 7 PM to 5:30 AM, 5:30 AM to 10 AM, and 3 PM to 7 PM. The time-of-day effect during midday (10AM to 3PM) is normalized to zero.

$$\begin{aligned}\beta_{nm}^{time} =& b^{time,freq} s_{nm}^{freq} + b^{time,loyal90} s_{nm}^{loyal90} + b^{time,noTrip} s_{nm}^{noTrip} + \\ & b_{nm}^{time,night} x_{nm}^{night} + b_{nm}^{time,AM} x_{nm}^{AM} + b_{nm}^{time,PM} x_{nm}^{PM} + \\ & \zeta_n^{time} + \eta_{nm}^{time}\end{aligned} \tag{4.5}$$

We specify $\beta_{nm}^{DPspeed}$ as Equation 4.6, a simple function that does not involve interactions. Based on the prevalence of real-time traffic information systems, we expect most travelers make their choice based on travel time rather than the decision point speed.

$$\beta_{nm}^{DPspeed} = \zeta_n^{DPspeed} + \eta_{nm}^{DPspeed} \tag{4.6}$$

Finally, we specify the error term of utility ε_{nm} to follow a logistic distribution that makes the model a logit mixture with inter- and intra-consumer heterogeneity.

To make the notation succinct, we use X_{nm} to denote the vector of all attributes relevant to individual n and trip m. The probability of choosing ML conditional on

ζ_n and η_{nm} is shown in Equation 4.7, as a function of X_{nm} and $\mathcal{D}_{n(m-1)}$.

$$P(d_{nm}|X_{nm}, \mathcal{D}_{n(m-1)}, \zeta_n, \eta_{nm}) = \frac{1}{1 + e^{-V(X_{nm}, \zeta_n, \eta_{nm}, \mathcal{D}_{n(m-1)})}} \tag{4.7}$$

We can integrate out η_{nm} with its marginal distribution $N(0, \Omega_w)$ as it's by definition independent from X_{nm}, $\mathcal{D}_{n(m-1)}$, and ζ_n. This gives Equation 4.8. Then, as ζ_n and $\mathcal{D}_{n(m-1)}$ are not independent, we encounter the initial condition problem. Solutions under this context are outlined in subsection 4.4.1.

$$P(d_{nm}|X_{nm}, \mathcal{D}_{n(m-1)}, \zeta_n) = \int P(d_{nm}|X_{nm}, \mathcal{D}_{n(m-1)}, \zeta_n, \eta_{nm}) f(\eta_{nm}) d\eta_{nm} \tag{4.8}$$

4.4 Model Estimation

In estimating the specified model, we face two econometric issues. The first is the initial condition problem, and the second is price endogeneity from dynamic pricing.

4.4.1 The Initial Condition Problem

In this application, the state dependence effects are not only on the previous choice, but the previous 90 days. Denote d_{n1} the first choice of individual n made after the beginning 90 days of the observed sample, then the initial condition is $\mathcal{D}_{n0}$—the 90 days previous to d_{n1}. Note that for different individuals, the initial condition is always defined as the previous 90 days to that person's first trip after the beginning 90 days of the data. For example, for a traveler whose first trip after the beginning 90 days is at day 93, their initial condition would be day 3 to day 92.

With $P(d_{nm}|X_{nm}, \mathcal{D}_{n(m-1)}, \zeta_n)$ derived in Equation 4.8, the probability of observing the choices of individual n after the initial condition is expressed in Equation 4.9, where M_n denotes the number of observations from individual n after the first 90

days, and X_n denotes the collection of X_{nm} across all the observations of n.

$$P(d_{n1}, ..., d_{nM_n}|X_n, \mathcal{D}_{n0}, \zeta_n) = \prod_{m=1}^{M_n} P(d_{nm}|X_{nm}, \mathcal{D}_{n(m-1)}, \zeta_n) \tag{4.9}$$

The initial condition problem occurs when we integrate out ζ_n during estimation, for its correlation with $\mathcal{D}_{n0}$. In chapter 3, we discussed three ways of addressing the initial condition. The Heckman's method considers the joint likelihood of the initial condition and following choices is as Equation 4.10. In this case, a model needs to be constructed for set $\mathcal{D}_{n0}$ and jointly estimated with the choice model of interest. We have not pursued this idea and adopt the simpler Wooldridge's method and Control Function.

$$L(\mathcal{D}_{n0}, d_{n1}, ..., d_{nM_n}|X_n) = \int \prod_{m=1}^{M_n} P(d_{nm}|X_{nm}, \mathcal{D}_{n(m-1)}, \zeta_n) P(\mathcal{D}_{n0}|\zeta_n, X_n) g(\zeta_n) d\zeta_n \tag{4.10}$$

The Wooldridge's method and Control Function consider the conditional likelihood in Equation 4.11.

$$L(d_{n1}, ..., d_{nM_n}|X_n, \mathcal{D}_{n0}) = \int \prod_{m=1}^{M_n} P(d_{nm}|X_{nm}, \mathcal{D}_{n(m-1)}, \zeta_n) f(\zeta_n|X_n, \mathcal{D}_{n0}) d\zeta_n \tag{4.11}$$

The Wooldridge's approach models $f(\zeta_n|X_n, \mathcal{D}_{n0})$ directly, and we specify it as Equation 4.12. The variables are described in Table 4.2. $\mathcal{D}_{n0}$ is summarized in a parsimonious manner based on the observed log odds ($s_{n0}^{logOdds}$), which should approximate the average utility (and hence the individual-specific parameter) for n during the initial condition well (as when $p = \frac{1}{1+e^{-v}}$, $ln\frac{p}{(1-p)} = v$). The instruments are the ratios of time saving over toll, averaged across the initial condition ($x_{n0}^{avgTSoverToll}$) and across all observations of n ($x_n^{avgTSoverTollAll}$). They should be strong indicators for the worthiness of using ML during the initial condition and overall. For travelers who had no trip during the initial condition, we allow a different intercept reflected by $\alpha^{k,noTrip}$ for their joint considerations with other travelers.

$$\zeta_n^k = \alpha^{k,0} + \alpha^{k,logOdds} s_{n0}^{logOdds} + \alpha^{k,onlyML} s_{n0}^{onlyML} + \alpha^{k,onlyGP} s_{n0}^{onlyGP} + \alpha^{k,noTrip} s_{n0}^{noTrip} + \alpha^{k,avgTSoverToll} x_{n0}^{avgTSoverToll} + \alpha^{k,avgTSoverTollAll} x_n^{avgTSoverTollAll} + v_n^{k,Wool}$$

where $k \in \{ASC,\ toll,\ time,\ DPspeed\}$

$$v_n^{Wool} = [v_n^{ASC,Wool}, v_n^{toll,Wool}, v_n^{time,Wool}, v_n^{DPspeed,Wool}] \sim N(0, \Omega^{Wool}) \tag{4.12}$$

Variable	Definition
$s_{n0}^{logOdds}$	$\begin{cases} 0 & \text{if } s_{n0}^{MLtrips90} = 0 \text{ or } s_{n0}^{GPtrips90} = 0, \\ ln(s_{n0}^{MLtrips90} / s_{n0}^{GPtrips90}) & \text{otherwise} \end{cases}$ where $s_{n0}^{MLtrips90}$ and $s_{n0}^{GPtrips90}$ are respectively the number of ML and GP trips in $\mathcal{D}_{n0}$.
s_{n0}^{onlyML}	1 if had and only had ML trip in $\mathcal{D}_{n0}$
s_{n0}^{onlyGP}	1 if had and only had GP trip in $\mathcal{D}_{n0}$
s_{n0}^{noTrip}	1 if no trip in $\mathcal{D}_{n0}$
$x_{nm}^{TSoverToll}$	ratio of time saving over toll
$x_{n0}^{avgTSoverToll}$	the average of $x_{nm}^{TSoverToll}$ across all trips in the initial condition
$x_n^{avgTSoverTollAll}$	the average of $x_{nm}^{TSoverToll}$ across all trips of n

Table 4.2: Variables for initial condition correction

Then the Control Function method has two steps: in the first step we acquire controls from an auxiliary model predicting the initial condition $\mathcal{D}_{n0}$ with the instrument, then in the second step these controls are used to specify ζ_n to capture its correlation with $\mathcal{D}_{n0}$ for solving endogeneity.

In the first step, we specify the model for each choice in the initial condition $\mathcal{D}_{n0}$

to be a probit model of the instruments as Equation 4.13. $\tau^{TSoverToll}$ is estimated to be 0.271 with standard error 0.00581, and $\tau^{avgTSoverTollAll}$ is estimated to be 0.735 with standard error 0.0106. These estimates indicate that the instruments are very strong and the signs of their effects are intuitive. For this first-step model, more instruments could be easily incorporated, but we keep using the same instruments as Wooldridge's method for their direct comparison.

$$\begin{aligned} &\forall m \in \mathcal{D}_{n0} \qquad \delta_{nm} \sim N(0,1) \\ &d_{nm} = [\tau^0 + \tau^{TSoverToll} x_{nm}^{TSoverToll} + \tau^{avgTSoverTollAll} x_n^{avgTSoverTollAll} + \delta_{nm}] \end{aligned} \tag{4.13}$$

Then, the control $\hat{\delta}_{nm}$ is computed with the inverse Mills ratio as discussed in chapter 3. The structural equation for ζ_n is specified as Equation 4.14, where we use the average $\hat{\delta}_{nm}$ across $\mathcal{D}_{n0}$ denoted as $\bar{\delta}_n$. Similar to the specification of Wooldridge, for travelers who had no trip during the initial condition, we allow a different intercept $r^{k,noTrip}$ and their $\bar{\delta}_n$'s are zero.

$$\begin{aligned} \zeta_n^k =& \gamma^{k,0} + \gamma^{k,control}\bar{\delta}_n + \gamma^{k,noTrip} s_{n0}^{noTrip} + v_n^{k,CF} \\ \text{where } k \in& \{ASC,\ toll,\ time,\ DPspeed\} \\ & v_n^{CF} = [v_n^{ASC,CF}, v_n^{toll,CF}, v_n^{time,CF}, v_n^{DPspeed,CF}] \sim N(0, \Omega^{CF}) \end{aligned} \tag{4.14}$$

In addition to the Wooldridge's method and Control Function, we also directly estimate the model with no correction for comparison in section 4.5.

4.4.2 Price Endogeneity from Dynamic Pricing

As reviewed in subsection 2.2.3, low elasticity or even positive price response are often discovered on empirical managed lanes studies, with [34] being the only work that viewed it as an endogeneity problem and corrected it with instrumental variables in the case of aggregate demand models.

The speculated source of endogeneity is that the dynamic pricing schemes on managed lanes cause the error term of utility to be correlated with price. The demand

and pricing system under the case of dynamic pricing is shown in Figure 4-3. The toll at interval t is determined as a function of the demand just observed at interval $t-1$ (each time interval corresponds to a toll change, in our case 5 minutes). We denote this relationship by $toll_t = f_{price}(demand_{t-1})$, where $toll_t$ denotes the toll at t, f_{price} denotes the pricing function that should have a positive derivative with respect to demand, and $demand_{t-1}$ denotes the total demand to ML at the previous interval. Now suppose that the demand is affected by unobserved factors that are not captured by the attributes in the demand model (examples in next paragraph). These factors would affect $toll_t$ through their influence on $demand_{t-1}$ and f_{price}, as well as appear in the utility error terms of people who travel at time t. Because the pricing function has a positive derivative, a positive correlation would appear between $toll_t$ and the error term of demand, which makes the estimated toll sensitivity less negative or even positive.

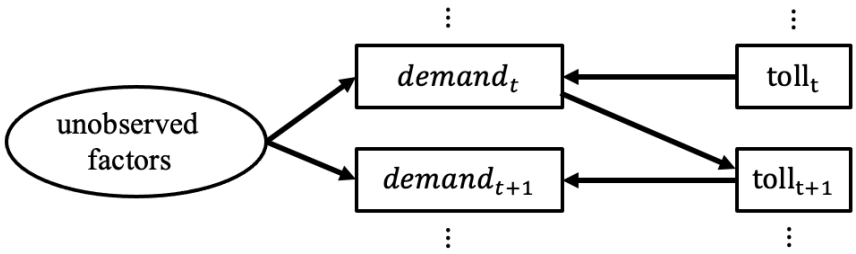

Figure 4-3: Interactions between demand and toll in dynamic pricing

In essence, under dynamic tolls that depend on ML demand, if there exist unobserved factors (factors that are not in the demand model) that affect demand and persist more than one time interval (5 minutes), endogeneity exists and gives positive bias to toll sensitivity. These unobserved factors could be of multiple sources. A first example is the incidents and traffic disruptions upstream to the ML entrance. These incidents make the travelers perceive high congestion, or in more rush, and hence increase ML demand, but would not be captured by the specified demand model. A second example is the unobserved variations in trip purpose at a given time and day. As in Figure 4-2, the westbound trips we have are heading towards Dallas/Fort Worth International Airport. When there are more departure flights, or disruptions

in those flights, the ML demand is expected to increase as it offers shorter and much more reliable travel time for people to catch their flights.

To fix the endogeneity problem, we apply the Control Function method. Unlike the case of initial condition problem where instruments are readily available from the attributes, the challenge here is to find instruments that are correlated with $toll_t$, but uncorrelated with the unobserved factors that affect demand. A common type of instruments for price endogeneity is the Hausman type that uses the price of the same or similar product in other markets as instruments [60, 64]. Following this idea, we tested the toll rate from the opposite direction of the corridor at the same interval, denoted as $toll_t^*$. $toll_t^*$ should correlate with the endogenous $toll_t$, as they are set by the same operator under various considerations of historical patterns and same rules. Further, it is reasonable to assume $toll_t^*$ being uncorrelated with the error term of the demand model, as it is on the opposite direction of the modeled demand. Specifically, going back to the facility map in Figure 4-2, the $toll_t$ is the toll associated with gantry 7 plus gantry 10, and the $toll_t^*$ we selected is the toll associated with gantry 1A. Intentionally, $toll_t^*$ is not exactly associated with the opposite origin-destination pair of the demand we are modeling, which further supports its exogeneity. To statistically test the exogeneity of $toll_t^*$, overidentification tests could be used, but they require at least one other instrument of a different nature [57]. This could be further investigated if other potential instruments are identified.

The control function is applied in two steps. In the first step, we use a linear regression model to fit the endogenous variable x_{nm}^{toll} on the instrument $x_{nm}^{toll^*}$ and other exogenous variables already in the choice model (time saving, decision point speed, and time-of-day Fourier series). The adjusted R^2 of this regression model is 0.933, suggesting that the instrument and exogenous attributes explain most of the variations in x_{nm}^{toll}. The estimated coefficient for $x_{nm}^{toll^*}$ is 1.28 with a standard error of 0.0107, indicating that the instrument is strong and has a positive correlation with the endogenous variable x_{nm}^{toll}, which coincides with our intuition. The estimates of this model is presented in Appendix B.

The second step of control function uses the fitted model of the first step to com-

pute residuals $\hat{w}_{nm}$ that capture the endogenous part of the toll. These residuals are used as an additional variable (a control) in the choice model estimation as Equation 4.15. The assumption is that the original error term ε_{nm} that is correlated with x_{nm}^{toll} is decomposed into the control function $b^w\hat{w}_{nm}$ that is correlated with x_{nm}^{toll}, and a new error term $\tilde{\varepsilon}_{nm}$ that is no longer correlated with x_{nm}^{toll}. This therefore solves the endogeneity problem. $\tilde{\varepsilon}_{nm}$ is specified to still follow a logistic distribution for keeping the model a logit mixture.

$$\begin{aligned} U_{ML,nm} = \beta_{nm}^{ASC} &- exp(\beta_{nm}^{toll})x_{nm}^{toll\,(boxcox)} + exp(\beta_{nm}^{time})x_{nm}^{timeSaving} \\ &- exp(\beta_{nm}^{DPspeed})x_{nm}^{DPspeed} + b^w\hat{w}_{nm} + \tilde{\varepsilon}_{nm} \\ \text{where } x_{nm}^{toll\,(boxcox)} &= \frac{(x_{nm}^{toll}+1)^{b^{boxcox}}-1}{b^{boxcox}} \end{aligned} \tag{4.15}$$

4.5 Estimation Results

4.5.1 Overview

This section presents the estimated logit mixture model with three methods of treating the initial condition problem:

- **No correction**: assume that the initial condition is exogenous and directly estimating the model by integrating Equation 4.8 on the marginal (population) distribution of ζ_n.
- **Wooldridge's method**: use the correction specified in Equation 4.12.
- **Control Function**: use the correction specified in Equation 4.13 and Equation 4.14.

In addition, to compare the estimated state dependence effects under different considerations of heterogeneity, we also present a flat logit model which differs from the logit mixture specification only in that it does not include unobserved heterogeneity ($\Omega_b = 0, \Omega_w = 0$).

As the specified state dependence is of previous 90 days, the first 90 days of the data are only used as the initial condition, and the day 91 to day 120 are used as the

training data. Data from day 121 to 144 are used as the testing data.

Similar to subsection 3.4.3, the Hierarchical Bayes procedure is used to estimate the outlined logit mixture model under different treatements for the initial condition problem. The difference here is that we have fixed parameters in addition to random parameters, and unobserved intra-heterogeneity in addition to inter-heterogeneity. Therefore, a 5-step Gibbs Sampling procedure developed in [22, 44] is used. The flat logit model is estimated with Biogeme [29].

All the models are corrected for price endogeneity. As shown by Table 4.3, the estimated coefficients (b^w) of the control for price endogeneity are always positive and significant. This confirms our theory that the control should capture the positive correlation between toll and the error term of utility. Because if there was no endogeneity, the coefficients of the control should not appear to be significantly different from zero. Further, to validate the effects of correction, a flat logit model without price endogeneity correction is estimated for comparison. The uncorrected model has a price elasticity of -0.227 whereas the corrected flat logit has a price elasticity of -0.428. This clearly indicates a significant price endogeneity problem and that our method addresses it. Under no price endogeneity correction, the specified logit mixture for price endogeneity shows convergence issues as the distribution of toll sensitivity is constrained to be negative in the utility specification Equation 4.1.

Parameter	**Flat Logit**	**Logit Mixture No Correction**	**Logit Mixture Wooldridge**	**Logit Mixture Control Function**
b^w	0.242 (0.0336)	0.306 (0.0388)	0.300 (0.0483)	0.311 (0.0434)

Table 4.3: Coefficient estimates of the price endogeneity control

The fit of the four estimated models is shown in Table 4.4. The training data contains 120,193 observations from 53,966 individuals. The logit mixture models with corrections perform the best. The Wooldridge's correction fits slightly better than the Control Function. A comparison of predictions on the testing data is discussed in subsection 4.5.3.

Despite that the fit is not very different across the 4 models, it is not correct to

say that the four models are of similar qualities, as we know that the Wooldridge's and the Control Function corrections address endogeneity, and in the next section we will show that the flat logit and uncorrected logit mixture estimated very different state dependence effects compared to the corrected mixture models.

	Flat Logit	**Logit Mixture No Correction**	**Logit Mixture Wooldridge**	**Logit Mixture Control Function**
Number of parameters	41	54	78	62
Log-likelihood	-40,073	-39,655	-39,382	-39,519
AIC	80,228	79,418	78,919	79,161
BIC	80,625	79,941	79,676	79,762
$\bar{\rho}^2$	0.5185	0.5234	0.5264	0.5249

Table 4.4: Model fit and comparison

4.5.2 Parameter Estimates

In the following paragraphs, we present, analyze and discuss parameter estimates in four groups that exhaustively include all the parameters in the utility specifications:

- State dependence effects
- Unobserved heterogeneity
- Time of day effects
- Toll, time and decision point speed sensitivities

State dependence effects

As previously listed in Table 4.1, each state-dependent variable is specified either based on the previous 90 days history, the previous 30 days history, or the last trip in the previous 90 days. Parameter estimates are shown in Table 4.5, which will be discussed block by block in the following paragraphs. A comparison of the overall estimated state dependence effects across models will be provided at the end.

The main effects of choices in previous 90 days and 30 days have intuitive signs, except for Wooldridge's estimate of $b^{hadMLtrip90}$ that is negative and more than two

Parameter	Flat Logit	Logit Mixture No Correction	Logit Mixture Wooldridge	Logit Mixture Control Function
Main effects of choices in the previous 90 days				
$b^{loyal90}$	0.626 (0.0311)	0.943 (0.0572)	0.799 (0.102)	0.701 (0.0851)
$b^{hadMLtrip90}$	0.708 (0.0809)	0.514 (0.134)	-0.629 (0.234)	-0.182 (0.186)
$b^{hadGPtrip90}$	-0.711 (0.0474)	-0.713 (0.0786)	0.142 (0.173)	-0.280 (0.112)
Main effects of choices in the previous 30 days				
$b^{loyal30}$	0.452 (0.0308)	0.279 (0.0602)	0.297 (0.0767)	0.227 (0.0723)
$b^{hadMLtrip30}$	-0.0686 (0.0533)	-0.0610 (0.0927)	0.204 (0.126)	0.232 (0.116)
$b^{hadGPtrip30}$	-0.0207 (0.0500)	-0.0802 (0.0765)	-0.133 (0.0949)	-0.226 (0.0910)
Main effects of last choice in the previous 90 days				
$b^{lastChoiceML}$	-0.0841 (0.0875)	0.00937 (0.118)	-0.126 (0.149)	-0.228 (0.150)
$b^{lastChoiceMLMemory}$	0.512 (0.152)	0.328 (0.304)	0.708 (0.333)	0.730 (0.313)
$b^{lastChoiceGPMemory}$	-0.358 (0.0679)	-0.165 (0.117)	-0.260 (0.144)	-0.233 (0.127)
b^{memory}	0.0880 (0.0215)	0.245 (0.132)	0.196 (0.0802)	0.182 (0.0782)
Main effects of experiences in the previous 90 days				
$b^{histMLtimeDiff}$	-0.136 (0.0242)	-0.216 (0.0392)	-0.280 (0.0532)	-0.270 (0.0535)
$b^{histGPtimeDiff}$	-0.00206 (0.00719)	-0.00206 (0.0116)	0.00725 (0.0150)	0.00150 (0.0146)
Main effects of experience of the last trip in the previous 90 days				
$b^{lastTripMLDiff}$	-0.0112 (0.0452)	-0.00382 (0.0930)	0.0277 (0.104)	0.0398 (0.0970)
$b^{lastTripGPDiff}$	0.00526 (0.0101)	0.0147 (0.0204)	0.0250 (0.0228)	0.0175 (0.0204)
Interaction effects of choices in the previous 90 days				
$b^{toll,loyal90}$	-0.220 (0.0295)	-0.533 (0.0729)	-1.21 (0.227)	-0.643 (0.130)
$b^{time,loyal90}$	-0.158 (0.0219)	-0.0870 (0.0377)	-0.571 (0.159)	-0.128 (0.0598)

Table 4.5: Estimated state dependence effects

standard errors away from zero. However, this estimate is not as unintuitive as it seems as the corresponding variable $s_{nm}^{hadMLtrip90}$ is by definition correlated with other state-dependent variables. When a person's history in the previous 90 days changes from not having ML trip to having one, their s_{nm}^{loyal} must increase $ln(2)-ln(1) = 0.693$ (see its definition in Table 4.1), which makes the overall effect less negative, not to mention that if this change comes from the previous 30 days, $s_{nm}^{loyal30}$ and $s_{nm}^{hadMLtrip30}$ will also increase.

For the effects of last choice in the previous 90 days, the parameter not interacted with memory effect, $b^{lastChoiceML}$, is close to zero in terms of the standard errors. The parameter interacted with memory effects $b^{lastChoiceMLMemory}$ and $b^{lastChoiceGPMemory}$ have expected signs and are in general more distant from zero. The memory effect b^{memory} is estimated to be positive which means more distant last choices have less effect.

The effect of ML experiences in the previous 90 days ($b^{histMLtimeDiff}$) has a negative sign, meaning if the actual travel time in those ML trips were longer than expected, the traveler would be less likely to use ML. On the other hand, the effect of GP experiences ($b^{histGPtimeDiff}$) is very close to zero. This makes sense because the travelers would be disappointed if they had large experienced travel time on the ML as they are tolled. As the GP are free, such disappointment might not occur or might only have minimal effects on a new choice. The additional effects of previous ML and GP experiences ($b^{lastMLtimeDiff}$ and $b^{lastGPtimeDiff}$) are discovered to be practically zero as well.

For the interaction terms, the choices in the previous 90 days affect toll and time sensitivities. A traveler with higher ratio of ML usage is less sensitive to both toll and travel time.

Finally, to analyze the overall state-dependence effects, we compute the change in the aggregate ML market share in the testing data with respect to perturbations of each observation's previous trip history, presented in Table 4.6. With perturbations, the four models all suggest that there is a positive state dependence—travelers who used ML more in the past have higher utility in continue using it. However, the

estimated magnitudes of the state dependence effects are different across models.

Pertubations	**Predicted changes in managed lanes demand [%]**			
	Flat Logit	**Logit Mixture No Correction**	**Logit Mixture Wooldridge**	**Logit Mixture Control Function**
Previous choice changed to ML	+38.4	+28.2	+14.2	+16.9
Previous choice changed to GP	-16.8	-11.5	-7.88	-8.47
+ 1 ML trip 30 days ago	+20.1	+16.5	+8.82	+10.3
+ 1 GP trip 30 days ago	-16.2	-14.3	-9.39	-10.4
+ 1 ML trip 90 days ago	+14.0	+13.9	+4.92	+6.54
+ 1 GP trip 90 days ago	-9.98	-11.0	-6.38	-6.89
Numbers are % changes in proportion to base case (original test data) Computed among travelers who have at least one trip in the previous 90 days				

Table 4.6: Comparison of overall state dependence effects on prediction

Specifically, the flat logit suggests the largest state dependence. This is not a surprise as in this case the omitted unobserved heterogeneity is statistically misinterpreted as state dependence, which is widely known as *spurious state dependence* [65]. Comparing the logit mixtures, the one that does not correct for initial condition estimats the largest state dependence effects. This is also as expected as the initial conditions are endogenous and the same direction of bias is observed in the Monte Carlo experiments of chapter 3. Comparing the Wooldridge's method and Control Function, they both estimate smaller state dependence effects compared to the flat logit and logit mixture without initial condition correction. The Wooldridge method estimates overall smaller effects of choices in the previous 90 and 30 days, which are results of its reversed signs of $b^{hadMLtrip90}$ and $b^{hadGPtrip90}$ estimates.

Unobserved heterogeneity

The unobserved heterogeneity is represented by $\zeta_n \sim N(\mu, \Omega_b)$ for inter-heterogeneity and $\eta_{nm} \sim N(0, \Omega_w)$ for intra-heterogeneity.

Without initial condition correction, the population distribution of ζ_n is directly estimated. With the Wooldridge's method or Control Function, the conditional distribution of ζ_n on the initial conditions are estimated. For these two methods, we acquire the estimates of unconditional (population) distribution as explained and verified in

subsection 3.3.3, which evaluates the population distribution based on the parameter estimates of the conditional distribution in Equation 4.12 and Equation 4.14, and the sample distribution of explanatory variables in those equations. Estimates of standard errors are acquired based on the posterior distribution of parameters in Equation 4.12 and Equation 4.14.

The estimates of $N(\mu, \Omega_b)$ is presented in Table 4.7. The estimates by Wooldridge's method and Control Function are overall close considering the standard errors. Across all methods, the variances are significantly different from zero, which suggest the large extent of unobserved inter-heterogeneity. The *No Correction* appears to underestimate the variances. A positive correlation between ζ_n^{ASC} and ζ_n^{toll} is discovered, suggesting a traveler who is more sensitive to toll prefers ML more when all the utility computed on attributes are equal. A positive correlation between ζ_n^{toll} and ζ_n^{time} is discovered, suggesting a traveler who is more sensitive to toll is also more sensitive to travel time. Estimates of the conditional distribution—Equation 4.12 for Wooldridge and Equation 4.14 for Control Function—are presented in Appendix B.

The estimate of $N(0, \Omega_w)$ is shown in Table 4.8. Ω_w is specified to be a diagonal matrix, and as explained eariler η_{nm}^{ASC} is normalized to zero for identification. The variances appear to be significantly different from zero, suggesting the existence of intra-heterogeneity.

Time-of-day effects

This section presents and analyzes the estimated Fourier series in Equation 4.2. The estimated parameters are in Table 4.9 and the overall effect is plotted in Figure 4-4. Clearly, travelers prefer ML during the AM and PM peak periods. This could be explained by trip purpose and expectations of congestion levels. During the AM and PM peak, the proportion of commuters should be much higher than leisure travelers. Commuters would want to arrive on time in the morning and get home quickly in the evening, and hence favor the congestion-free and more reliable ML. As trip purpose is not observed, its average variations are captured by the time-of-day variable. Further, in general, travelers would expect the GP during peak hours to be congested and some

Parameter	Flat Logit	Logit Mixture No Correction	Logit Mixture Wooldridge	Logit Mixture Control Function
Population mean				
ζ_n^{ASC}	-0.837 (0.0861)	-0.906 (0.0715)	-1.25 (0.134)	-1.16 (0.0961)
ζ_n^{toll}	-3.88 (0.541)	-4.40 (0.257)	-4.76 (0.400)	-4.65 (0.301)
ζ_n^{time}	-2.06 (0.0822)	-2.20 (0.107)	-3.01 (0.273)	-2.32 (0.146)
$\zeta_n^{DPspeed}$	-3.46 (0.0713)	-5.06 (0.283)	-5.24 (0.433)	-4.75 (0.324)
Population variance				
ζ_n^{ASC}	0	1.46 (0.189)	4.66 (0.780)	3.33 (0.485)
ζ_n^{toll}	0	1.58 (0.277)	2.85 (0.689)	2.88 (0.545)
ζ_n^{time}	0	0.845 (0.142)	2.16 (0.501)	1.42 (0.261)
$\zeta_n^{DPspeed}$	0	3.84 (0.743)	4.22 (0.994)	3.96 (0.770)
Population covariance				
$\zeta_n^{ASC}, \zeta_n^{toll}$	0	0.663 (0.145)	1.29 (0.386)	1.02 (0.284)
$\zeta_n^{ASC}, \zeta_n^{time}$	0	-0.182 (0.119)	-0.575 (0.240)	-0.0728 (0.169)
$\zeta_n^{ASC}, \zeta_n^{DPspeed}$	0	-0.166 (0.352)	-0.165 (0.595)	0.332 (0.471)
$\zeta_n^{toll}, \zeta_n^{time}$	0	-0.861 (0.177)	1.67 (0.464)	1.59 (0.320)
$\zeta_n^{toll}, \zeta_n^{DPspeed}$	0	-0.461 (0.457)	-1.22 (0.781)	-0.418 (0.678)
$\zeta_n^{time}, \zeta_n^{DPspeed}$	0	-0.291 (0.381)	-0.786 (0.666)	-0.300 (0.770)

Table 4.7: Estimated unobserved inter-heterogeneity

Parameter	Logit Mixture No Correction	Logit Mixture Wooldridge	Logit Mixture Control Function
Variance			
η_{nm}^{toll}	0.345 (0.0989)	0.574 (0.220)	0.578 (0.164)
η_{nm}^{time}	0.115 (0.0351)	0.298 (0.119)	0.109 (0.0335)
$\eta_{nm}^{DPspeed}$	2.20 (0.620)	2.42 (0.814)	1.13 (0.538)

Table 4.8: Estimated unobserved intra-heterogeneity

of them might decided to use ML without checking real-time travel information.

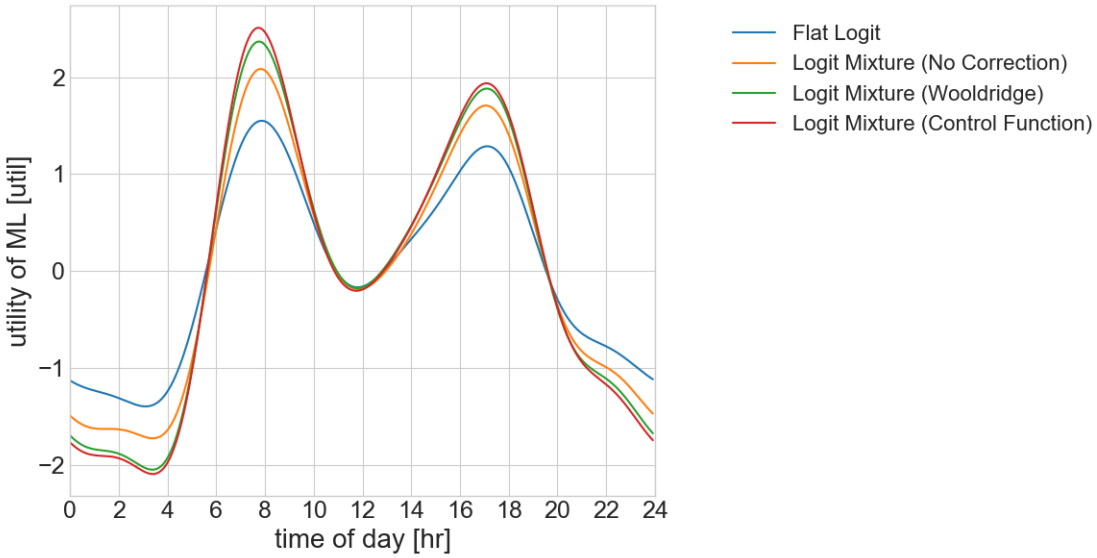

Figure 4-4: Overall time-of-day effects

Toll, time, and speed sensitivities

The toll sensitivity function is specified in Equation 4.4. The corresponding parameters are shown in Table 4.10. The box-cox parameter is larger than 1, meaning that the marginal disutility of toll increases as toll increases. Travelers with higher frequency are toll-sensitive, which is likely a reflection of unobserved budget constraints. Loyal travelers are less toll-sensitive.

The time sensitivity function has been specified in Equation 4.5. The corresponding parameters are shown in Table 4.11. Travelers with higher trip frequency and lower loyalty, and who had no trip in previous 90 days are more time-sensitive. These travelers are likely the ones who check travel time before making the choice. Travelers are more time-sensitive during peak hours and night compared to midday.

The estimated distributions of value of time—willingness to pay for travel time saving—is shown in Figure 4-5. As the marginal disutility of toll increases as toll increases, the marginal willingness to pay decreases as time saving increases. The flat logit omits significant amounts of heterogeneity.

Parameter	Flat Logit	Logit Mixture No Correction	Logit Mixture Wooldridge	Logit Mixture Control Function
b_1^{sin}	-0.199 (0.0278)	-0.288 (0.0419)	-0.314 (0.0479)	-0.316 (0.0480)
b_2^{sin}	-0.312 (0.0356)	-0.401 (0.0509)	-0.489 (0.0632)	-0.473 (0.0607)
b_3^{sin}	0.0440 (0.0341)	0.0855 (0.0460)	0.0553 (0.0549)	0.0579 (0.0509)
b_4^{sin}	0.110 (0.0296)	0.160 (0.0392)	0.227 (0.0492)	0.200 (0.0449)
b_5^{sin}	-0.729 (0.0243)	-0.107 (0.0345)	-0.103 (0.0423)	-0.101 (0.0392)
b_6^{sin}	0.00590 (0.0185)	-0.0300 (0.0268)	-0.0366 (0.0331)	-0.0316 (0.0310)
b_1^{cos}	-0.924 (0.0543)	-1.19 (0.0704)	-1.40 (0.0997)	-1.36 (0.0849)
b_2^{cos}	-0.658 (0.0434)	-0.850 (0.0563)	-1.02 (0.0775)	-0.962 (0.0696)
b_3^{cos}	0.523 (0.0437)	0.693 (0.0559)	0.804 (0.0713)	0.776 (0.0663)
b_4^{cos}	0.0543 (0.0258)	0.0450 (0.0373)	0.0822 (0.0453)	0.0822 (0.0432)
b_5^{cos}	-0.0835 (0.0251)	-0.157 (0.0358)	-0.195 (0.0428)	-0.178 (0.0403)
b_6^{cos}	-0.0408 (0.0179)	-0.0308 (0.0267)	-0.0420 (0.0317)	-0.0514 (0.0308)

Table 4.9: Estimated time-of-day effects

Parameter	Flat Logit	Logit Mixture No Correction	Logit Mixture Wooldridge	Logit Mixture Control Function
b^{boxcox}	2.26 (0.236)	2.32 (0.0854)	2.33 (0.101)	2.32 (0.0875)
$b^{toll,freq}$	1.25 (0.228)	2.43 (0.393)	2.33 (0.715)	2.51 (0.489)
$b^{toll,loyal90}$	-0.220 (0.0295)	-0.533 (0.729)	-1.21 (0.227)	-0.643 (0.130)
$b^{toll,noTrip}$	-0.548 (0.0795)	0.280 (0.125)	0.296 (0.254)	0.487 (0.215)
mean(ζ_n^{toll})	-3.88 (0.541)	-4.40 (0.257)	-4.76 (0.400)	-4.65 (0.301)
var(ζ_n^{toll})	0	1.58 (0.277)	2.85 (0.689)	2.88 (0.545)
var(η_{nm}^{toll})	0	0.345 (0.0989)	0.574 (0.220)	0.578 (0.164)

Table 4.10: Estimated toll sensitivity function

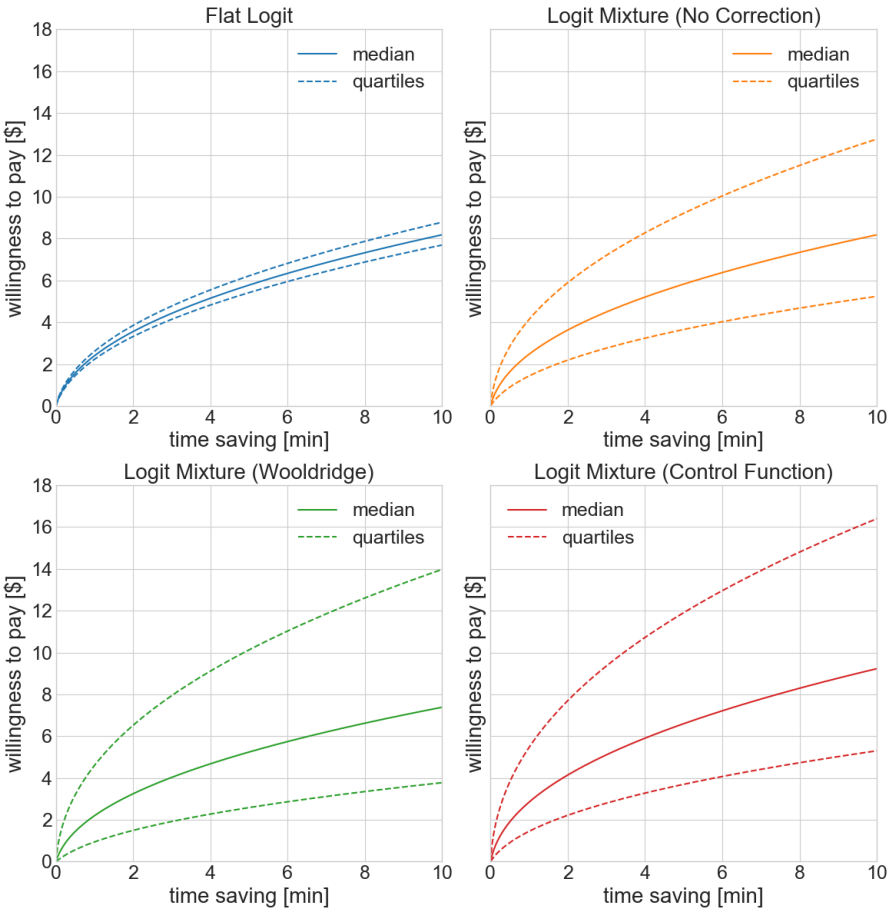

Figure 4-5: Estimated value of time distributions

Parameter	Flat Logit	Logit Mixture No Correction	Logit Mixture Wooldridge	Logit Mixture Control Function
$b^{time,freq}$	1.18 (0.145)	2.54 (0.300)	1.54 (0.559)	2.12 (0.353)
$b^{time,loyal90}$	-0.158 (0.0219)	-0.0870 (0.0377)	-0.571 (0.159)	-0.128 (0.0598)
$b^{time,noTrip}$	-0.276 (0.0947)	-0.0395 (0.134)	0.618 (0.340)	0.619 (0.264)
$b^{time,night}$	0.409 (0.117)	0.235 (0.122)	0.110 (0.104)	0.216 (0.134)
$b^{time,AM}$	0.188 (0.0758)	0.198 (0.0784)	0.391 (0.0769)	0.271 (0.0799)
$b^{time,PM}$	0.151 (0.0867)	0.106 (0.0914)	0.282 (0.0835)	0.216 (0.0843)
mean(ζ_n^{time})	-2.06 (0.0822)	-2.20 (0.107)	-3.01 (0.273)	-2.32 (0.146)
var(ζ_n^{time})	0	0.845 (0.142)	2.16 (0.501)	1.42 (0.261)
var(η_{nm}^{time})	0	0.115 (0.0351)	0.298 (0.119)	0.109 (0.0335)

Table 4.11: Estimated time sensitivity function

The decision point speed sensitivity function has been specified in Equation 4.6. The corresponding parameters are shown in Table 4.12. Larger unobserved heterogeneity and lower mean are found compared to the toll and time sensitivity, suggesting some travelers use decision point speed to make the choice while some do not.

Parameter	Flat Logit	Logit Mixture No Correction	Logit Mixture Wooldridge	Logit Mixture Control Function
mean($\zeta_n^{DPspeed}$)	-3.46 (0.0713)	-5.06 (0.283)	-5.24 (0.433)	-4.75 (0.324)
var($\zeta_n^{DPspeed}$)	0	3.84 (0.743)	4.22 (0.994)	3.96 (0.770)
var($\eta_{nm}^{DPspeed}$)	0	2.20 (0.620)	2.42 (0.814)	1.13 (0.538)

Table 4.12: Estimated speed sensitivity function

4.5.3 Prediction

The prediction performance on the testing data is shown in Table 4.13. For the logit mixture models, predictions are performed based on the personalized posterior

parameter distribution from the previously observed trips of the same traveler. The detailed procedure is described in subsection 5.2.2 and [44]. Across all models, the predictions are better for travelers from whom we observe more trips. For the flat logit, this is due to that the state-dependent variables based on more frequent previous trips become more predictive. For the logit mixture models, this trend is also a result of improved parameter personalization as more trips are observed. The logit mixture models perform better than the flat logit model. The corrected logit mixture models perform slightly better than the one without correction.

Note that the testing data here is the month after training data, so the training and testing data have similar traffic conditions and tolling policy. This is not as ideal as testing data from completely different distributions of exogenous attributes (which we do not have). As shown in [52], if the training and testing data follow the same data generation process, an endogenous model might predict better as the misinterpreted correlation could exist in both data. Therefore, we expect the corrected logit mixture models to perform much better for the analysis of tolling algorithm.

	Flat Logit	**Logit Mixture No Correction**	**Logit Mixture Wooldridge**	**Logit Mixture Control Function**
Avg. predicted choice probability	0.7906	0.8026	0.8041	0.8041
Accuracy	0.8535	0.8549	0.8553	0.8560

Table 4.13: Prediction performance on testing data

4.6 Conclusions

This chapter developed a comprehensive model for the choice between managed lanes and general purpose lanes based on empirical data.

Both significant state dependence and unobserved heterogeneity are found from empirical data. By comparing different modeling assumptions of the state dependence and unobserved heterogeneity, omission of unobserved heterogeneity or the initial condition problem lead to spuriously overstated state dependence. The predicted impact of past choices on market share is about doubled compared to the models with

proper unobserved heterogeneity and initial condition corrections. The Wooldridge's method and Control Function method for initial condition correction overall give similar results.

It was also found that choice data under dynamic pricing are subject to price endogeneity. A Hausman-type instrument—toll on the opposite direction—is found useful for correction.

Chapter 5

Personalized Toll Optimization with Long-Term Objectives

5.1 Introduction

In chapter 4, we analyzed how travelers choose between managed lanes (ML) and general purpose lanes (GP), and discovered significant preference heterogeneity and state dependence. From a tolling perspective, the discovered heterogeneity further motivates the potential of personalized pricing that were discussed in chapter 1, namely that personalized pricing would effectively improve the capture rate of ML and hence better satisfy the interests of the operator, the travelers, as well as the regulator. Further, the state-dependent choice behavior suggests the need to consider a long-term objective for the impact of current pricing decisions on future choices of the travelers.

This chapter culminates the thesis with the development of a personalized real-time prediction-based pricing system for managed lanes, to better achieve comprehensive short- and long-term operation objectives. As has been presented in chapter 1, Figure 5-1 illustrates how the proposed personalized tolling system would interact with travelers. In addition to the displayed toll, personalized discounts are offered upon arrivals of travelers who wish to receive them and have downloaded a specialized mobile app. We refer to these travelers with the app as the subscribers, and others as non-subscribers.

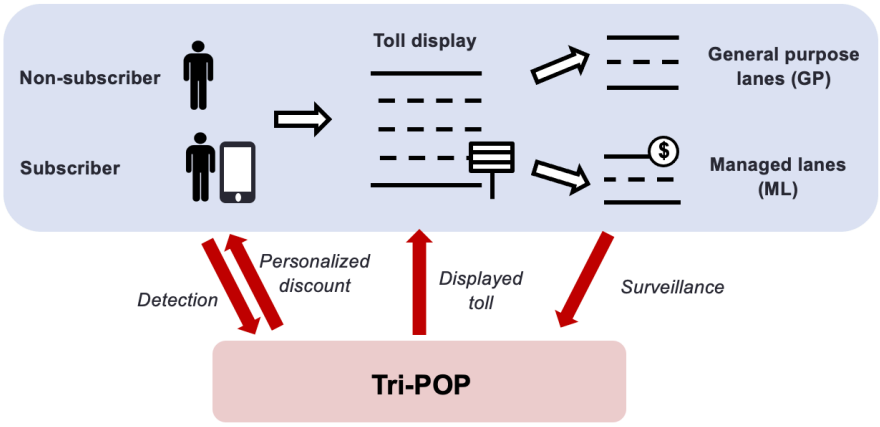

Figure 5-1: Proposed personalized tolling system: Overview

In real time, the personalized tolling algorithm needs to jointly optimize the displayed toll and personalized discounts. To this end, our method is based on an online bi-level optimization paradigm that combines three key online capabilities: prediction, optimization and personalization. This paradigm is hence termed *Tri-POP* [19].

The key contribution of this chapter is the application of Tri-POP to ML personalized pricing with a multi-component objective for the benefits of all stakeholders, where detailed choice behaviors with unobserved heterogeneity and state dependence are considered based on chapter 4. Our development advances [115] which considered the same bi-level formulation to ML personalized pricing but only with revenue as a single-component objective and did not consider the detailed choice behaviors.

This chapter first presents the methodology of designing the proposed tolling algorithm with Tri-POP, followed by a closed-loop simulation case study investigating its performance.

5.2 Methodology

5.2.1 Overview

For effective real-time optimization of the displayed toll and personalized discounts, Tri-POP exploits the bi-level nature of the decision variables—displayed toll at the

system level and discounts at the individual level—and formulates the operation problem into two connected sub-problems with consistent objectives: system optimization and user optimization.

Figure 5-2 shows the bi-level architecture of Tri-POP. The system optimization is triggered periodically (e.g., every 5 minutes, termed as a roll period) to optimize the displayed toll and a discount control parameter based on traffic prediction. It works within a rolling horizon framework where the optimization is performed on a horizon including the next three roll periods (e.g., next 15 minutes, Figure 5-3). The optimized discount control parameter is fed to user optimization to consider traveler interactions and achieve the system objective at the individual level. The user optimization is triggered upon detection of each subscriber to offer a tailored discount based on individual-level choice prediction and the discount control parameter.

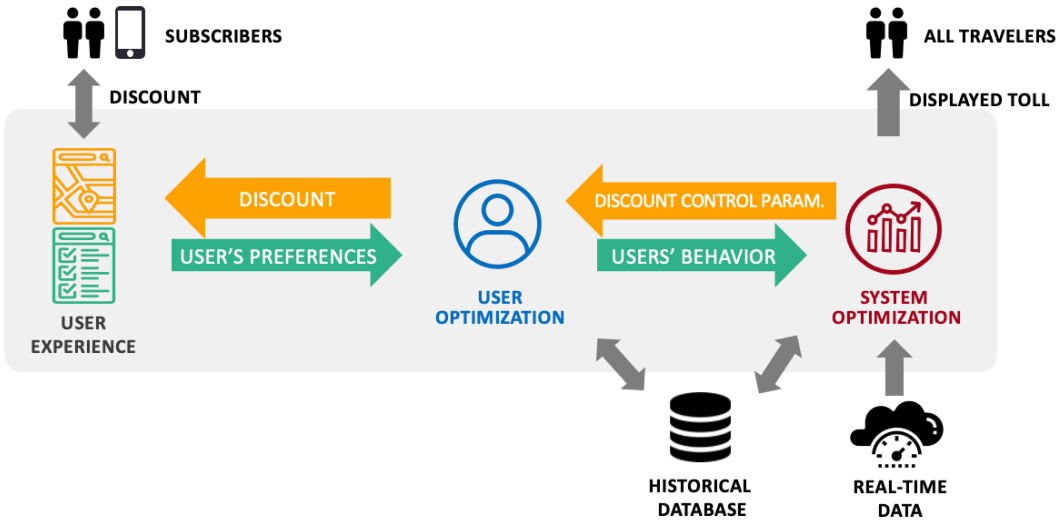

Figure 5-2: Tri-POP: Overall framework

The optimization problems are formulated and solved based on individual- and system-level predictive models. Individual-level behavior prediction is supported by the one developed in chapter 4. The system-level traffic predictions are generated by a simulation-based dynamic traffic assignment (DTA) system. One key feature of Tri-POP is that these predictive models are updated (calibrated) with real-time data from the mobile discount app and network surveillance in an online setting.

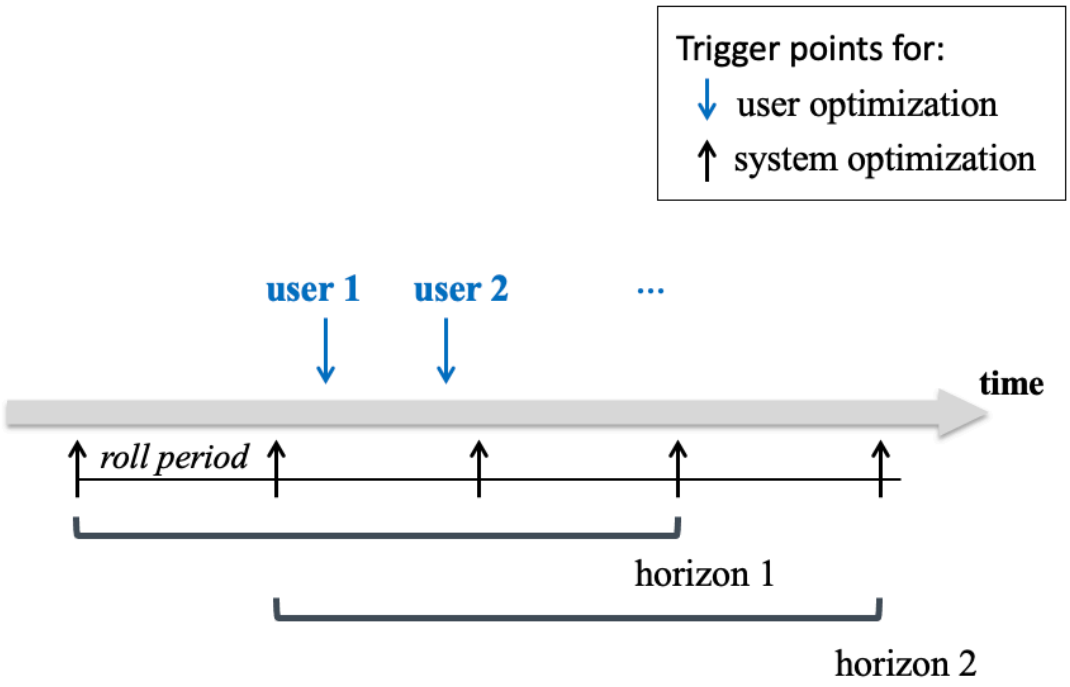

Figure 5-3: Tri-POP in action

The analytics involved in Tri-POP are developed in a series of studies summarized in [19], which includes the individual-specific choice prediction to be outlined in subsection 5.2.2 and the system-level traffic prediction to be outlined in subsection 5.2.3. A key contribution—the design of multi-component objectives—is discussed in the formulations of system and user optimizations in subsection 5.2.3 and subsection 5.2.4.

5.2.2 Online Estimation and Prediction of Choices

The choice model for whether a traveler uses ML is introduced in chapter 4. Both system and user optimizations are formulated based on its predictions, as will become clear in subsection 5.2.3 and subsection 5.2.4. For better predictions, the model predicts based on individual-level parameters that are updated as more data become available from a given user. To this end, we adopt the online estimation and prediction framework by [22, 44]. The fact that user preferences keep being updated and used for system and user optimizations are reflected by the green arrows in Figure 5-2.

We first summarize the choice model with a general utility specification. A traveler n makes trip m and considers a binary choice between ML and GP. The probability of choosing ML, denoted as π_{nm}, is given by the logit formula in Equation 5.1, where V represents the systematic utility function of ML. X_{nm} is a vector representing trip attributes (e.g., toll rate, travel time saving, decision point speed) including an intercept. β_{nm} is a vector of corresponding sensitivity functions.

$$\pi_{nm} = 1/(1 + e^{-V(X_{nm},\beta_{nm})}) \tag{5.1}$$

β_{nm} is specified as Equation 5.2, a linear function of S_{nm} that includes observed characteristics (e.g., state-dependent variables) and contextual variables (e.g., time of day), coefficient matrix b, and trip-specific random parameter vector η_{nm}. We specify η_{nm} to follow two hierarchical levels of distribution: $\eta_{nm} \sim N(\zeta_n, \Omega_w)$ that represents unobserved preference variations at individual level and $\zeta_n \sim N(\mu, \Omega_b)$ that represents those at the population level. This notation differs from chapter 4 that uses η_{nm} to denote the deviates of trip-specific preference from ζ_n. The two are equivalent mathematically and we change the notation here for consistency with [22, 44].

$$\beta_{nm} = bS_{nm} + \eta_{nm}, \qquad \eta_{nm} \sim N(\zeta_n, \Omega_w), \qquad \zeta_n \sim N(\mu, \Omega_b) \tag{5.2}$$

There are three levels of unknown parameters:

- Population-level parameters: b, μ, Ω_b Ω_w
- Individual-level parameters: ζ_n
- Trip-level parameters: η_{nm}

Two interacting estimation procedures with Gibbs Sampling are used:

- Offline estimation: It updates (estimates) all the parameters. It uses all the observed trips and is computationally expensive. It is only performed periodically such as once a week.

- Online estimation: It updates (estimates) only ζ_n and η_{nm}. Population parameters b, Ω_b Ω_w are fixed to values from last offline estimation. When a new trip is made by a traveler, online estimation is triggered only for them based on their data. As such, online estimation is computationally cheap, highly scalable, and hence manageable in real time.

Choice probability prediction of a new trip (denoted as $M+1$) is based on the latest population-level parameters from offline estimation $\hat{b}$, and the latest posterior draws of η_{nm} of previous observations from online estimation (denoted as $\eta_n^r, r \in \{1, ..., R\}$ where R is the number of draws) as Equation 5.3.

$$\pi_{n(M+1)} = \frac{1}{R} \sum_{r=1}^{R} \frac{1}{1 + e^{-V(X_{n(M+1)}, \hat{b} S_{n(M+1)} + \eta_n^r)}} \tag{5.3}$$

5.2.3 System Prediction and Optimization

To be proactive, Tri-POP optimizes the system-level decision variables—displayed tolls and a discount control parameter—based on real-time traffic predictions on a rolling horizon. In this section, we first introduce our method for system prediction, and then the optimization formulations.

System Prediction

For real-time traffic prediction, we rely on DynaMIT 2.0, a simulation-based dynamic traffic assignment system with online calibration of supply, demand and choice model parameters [25]. It utilizes a rolling horizon framework, and is triggered periodically (every 5 minutes, a roll period). In each execution cycle, it performs traffic state estimation of the previous interval, and predicts the state of the system for the next 3 intervals.

System optimization is performed on the second and third prediction intervals allowing for execution time. To evaluate the objective function on given values for the displayed tolls and discount control parameter, prediction intervals are executed with those candidate values implemented in P2 (O1) and P3 (O2). For example, in

cycle 2 of Figure 5-4, the values of tolls and the discount control parameter for P1 are their previously optimized and applied values from cycle 1, and their values for P2 (O1) and P3 (O2) are their candidate values for the current cycle. These are illustrated in Figure 5-4.

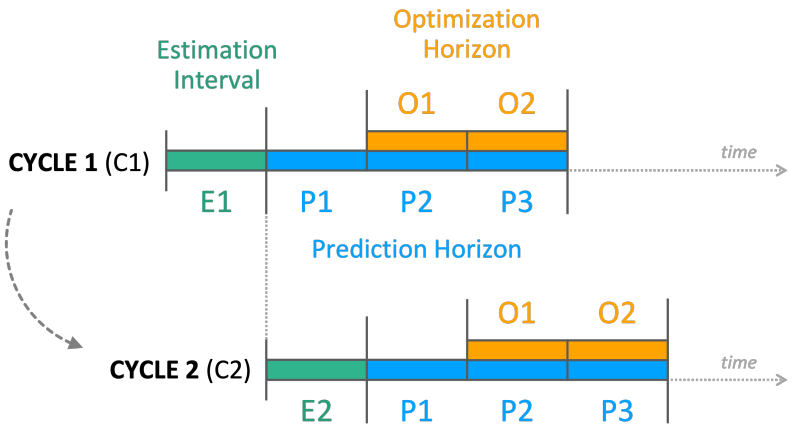

Figure 5-4: System prediction and optimization with rolling horizons

To achieve desirable prediction accuracy and hence better optimization of system objectives, DynaMIT uses online calibration that adjusts its simulation parameters in real-time to match the simulated and observed surveillance data. Specifically, the online calibration problem is formulated as a state space model and solved using Extended Kalman Filter (EKF) [114].

System Optimization Formulation

Notations for the system optimization are summarized in Table 5.1

The system optimization solves a simulation-based optimization problem based on traffic prediction. Its input, output and constraints are first summarized as follows:

- Input
  - historical demand, supply and preference estimates
  - real-time data from network surveillance
- Output
  - displayed toll (decision variable p^D)

notation	description
p^D	displayed toll rates matrix; dimension equals the number of optimization intervals by number of toll segments
x	discount control parameter vector; dimension equals the number of optimization intervals
$\mathbb{O}_{t_0}$	set of optimization intervals at real-world time t_0
$\mathbb{N}_t$	set of simulated travelers at optimization interval t
n	individual index
a_n	subscription status; 1 if n is a subscriber, 0 otherwise
d_n^*	discount given to simulated user; by user optimization for subscribers and 0 for non-subscribers
z_n	system objective evaluated at individual n
$t(n)$	arrival time interval when n enters corridor (detected)
$k(n)$	n's origin-destination pair (destination is inferred)
$p^D_{t(n),k(n)}$	displayed price for the ML path to anticipated destination of n; output from system optimization
$x_{t(n)}$	discount control parameter for the arrival interval of n
π_n	n's predicted probability to choose ML
ΔR_n^F	expected revenue improvement from n in future 90 days if they choose ML for the current trip
$R_n^{F\|ML}$	expected revenue from n in future 90 days if they choose ML for the current trip
$R_n^{F\|GP}$	expected revenue from n in future 90 days if they choose GP for the current trip
δ^W	welfare policy hyperparameter
$N_{t(n)}$	predicted number of travelers in interval t(n)
δ^V	customer retention policy hyperparameter
m_n	n's expenditure on ML in the past 90 days
T	route attributes (e.g. travel time, decision point speed) vector
B_n	choice model parameters and characteristics
U^{ML}	ML speed vector
D	O-D demand matrix
H	supply parameters matrix
p^{cap}	toll cap
U^{LB}	lower bound on ML speed

Table 5.1: Notations for system and user optimization

  - discount control parameter (decision variable x)
  - traffic prediction

- Constraint: maximum toll and ML speed requirement

At real-world time t_0, the system optimization optimizes the displayed toll p^D and discount control parameter x based on simulations of the next 15 minutes by DynaMIT. As explained earlier, the optimization intervals $\mathbb{O}_{t_0}$ are the next 5 to 15 minutes, which leaves the first 5 minutes of the prediction horizon as execution time. Each simulated traveler n in the optimization intervals is associated with subscription status ($a_n = 1$ if subscribed). The simulated discount d_n^* is offered by the user optimization if n is a subscriber, and otherwise set to zero.

The system objective is defined in Equation 5.4, as the sum of z_n over all the simulated travelers in the optimization intervals. z_n is the system objective value evaluated at each individual, as a function of the simulated discount d_n^*, the displayed toll $p^D_{t(n),k(n)}$ of their arrival time $t(n)$ and origin-destination pair $k(n)$, and the subscription status a_n. z_n is in the form of expectation over n's choice probability π_n. The objective function if n chooses ML is defined as a sum of four components, explained below.

$$\begin{aligned} &\max_{x,p^D} \sum_{t\in\mathbb{O}_{t_0}} \sum_{n\in\mathbb{N}_t} z_n(d_n^*, p^D_{t(n),k(n)}, a_n) \\ \text{where} \qquad &z_n = \pi_n[(1-d_n^*)p^D_{t(n),k(n)} + \Delta R_n^F + \delta^W \frac{1}{N_{t(n)}} + a_n \delta^V m_n] \end{aligned} \tag{5.4}$$

Objective components:

- **Short-term revenue** $(1-d_n^*)p^D_{t(n),k(n)}$ is the revenue to be collected for the current trip equals the toll rate offered to n.
- **Future revenue improvement** ΔR_n^F is the expected future revenue improvement if traveler n chooses ML for the current trip as opposed to GP, calculated by Equation 5.5 with the respective *conditional future revenue* $R_n^{F|ML}$ and $R_n^{F|GP}$. The future revenue depends on the current choice because of state-

dependent travel behavior.

$$\Delta R_n^F = R_n^{F|ML} - R_n^{F|GP} \tag{5.5}$$

$R_n^{F|ML}$ and $R_n^{F|GP}$ need to be computed based on future trip projections. Given a future horizon (e.g., next 90 days), we assume that the future trip-making (frequency, trip attributes) to be the same as the observed personal history (e.g., past 90 days), but with new future choices to be simulated with the choice model conditional on the current choice being ML or GP.

For example, a person with three trips in the previous 90 days respectively 60, 40 and 20 days ago, is assumed to travel and encounter the same choice situations in the 30 (=-60+90), 50 (=-40+90) and 70 (=-20+90) days from now. To improve the quality of future projections for them to reflect the most recent conditions, trip attributes of recent days could be matched to projected future trips instead of directly using the exact historical attributes.

To compute $R_n^{F|ML}$, we simulate choices and revenue in the future horizon assuming ML is selected for current trip. To compute $R_n^{F|GP}$, we do the same except assuming GP is selected for current trip. The random seed is fixed to be the same for the simulations of $R_n^{F|ML}$ and $R_n^{F|GP}$ to reduce simulation variance.

- **Capture rate bonus** $\delta^W \frac{1}{N_t(n)}$ is a bonus term for capture rate with a policy parameter δ^W. It allows operators to shift some focus from revenue to social welfare at their discretion.
- **Subscriber lifetime value** $a_n \delta^V m_n$ is designed to retain high-value customers measured by their expenditure in the previous 90 days (m_n). Commonly used in marketing, a customer's lifetime value is defined as their expenditure until they no longer consider ML in their choice set or have quit using the corridor. If a subscriber constantly receives high prices and hence, has a relatively lower probability of using ML, it is more likely that they would become inactive sooner thereby reducing their lifetime value. Therefore, $\delta^V m_n$ captures the impact of current price (choice) on a customer's lifetime value. m_n reflects the value

of a customer per time period. δ^V is a policy hyperparameter that reflects the influence of current price on the customer's lifetime value and the level of emphasis that the operator desires. From a pure optimization perspective, $\delta^V m_n$ could be understood as a personalized capture rate bonus (δ^W) for the loyal customers that is proportional to m_n.

The full optimization problem is presented in Equation 5.6.

$$
\begin{aligned}
&\max_{x,p^D} \sum_{t\in\mathbb{O}_{t_0}} \sum_{n\in\mathbb{N}_t} z_n(d_n^*, p^D_{t(n),k(n)}, a_n) \\
&\text{where} \qquad z_n = \pi_n[(1-d_n^*)p^D_{t(n),k(n)} + \Delta R_n^F + \delta^W \frac{1}{N_{t(n)}} + a_n \delta^V m_n] \\
s.t \quad &\forall n \qquad d_n^* = a_n * \mathrm{UO}(x_{t(n)}, p^D_{t(n),k(n)}, \Delta R_n^F, T, B_n, N_{t(n)}) \\
&\forall n \qquad \pi_n = \mathrm{choiceprob}(d_n^*, p^D_{t(n),k(n)}, T, B_n) \\
&(U^{ML}, T) = \mathrm{traffic}(\pi_n \forall n, D, H) \\
&\forall t \qquad p_t^D \le p^{cap}, \qquad U_t^{ML} \ge U^{LB}
\end{aligned}
\tag{5.6}
$$

The first constraint with UO(·) reflects that the simulated discounts are from the user optimization. Note that in this problem, by design, the discount control parameter affects the system objective only through user optimization, the way of which will be outlined in the next section. The second constraint with choiceprob(·) reflects that π_n is the choice probability computed for a simulated traveler (Equation 5.3). The third constraints with traffic(·) reflects that the objective is evaluated by traffic prediction simulated with DynaMIT.

Further, we consider two regulatory constraints that commonly appear in ML facilities operations: a cap (upper bound) on displayed toll ($p_t^D \le p^{cap}$) and a lower bound on ML speed ($U_t^{ML} \ge U^{LB}$). The toll cap is enforced through the feasible region of decision variables. The ML speed requirement is implemented as a very large penalty on the objective value.

Under ML congestion, the system enters a *mandatory mode* where the system optimization is skipped and the toll is raised as a function of the excessive demand and speed violations to ensure that the ML become uncongested quickly, in which case no

discounts are offered (equivalent of $x \to \infty$ as will be shown in subsection 5.2.4). This mechanism is based on existing regulation agreements and discussions with private operators. It is implemented but not encountered in the case study.

The system optimization is solved with a simple grid search algorithm for computation considerations. The grid size could be determined based on available computation resources. More sophisticated methods could be used to improve performance such as genetic algorithms or Bayesian optimization.

5.2.4 User Optimization

For a subscriber indexed by n entering the corridor at $t(n)$ with origin-destination pair $k(n)$, user optimization solves for a personalized discount d_n^*. Its input, output and constraints are first summarized as follows:

- Input
  - predicted network condition (from system optimization)
  - displayed toll (from system optimization)
  - discount control parameter (from system optimization)
  - traveler-specific behavioral information including preference estimates and trip history
- Output: personalized discount (decision variable d_n)
- Constraint: $0 \leq d_n \leq 1$

We consider the optimization problem defined in Equation 5.7. The objective function is a personalization of the system objective. It is in the form of expectation over n's choice probability π_n that is computed by the online prediction procedure in subsection 5.2.2. The objective function if n chooses ML is defined as a sum of five components, where first four components are the same as z_n in the system optimization.

$$\max_{d_n} \pi_n(d_n, p^D_{t(n),k(n)})[(1-d_n)p^D_{t(n),k(n)} + \Delta R^F_n + \delta^W \frac{1}{N_t(n)} + \delta^V m_n - x_{t(n)} p^D_{t(n),k(n)}] \quad (5.7)$$

The added fifth component $x_{t(n)}p^D_{t(n),k(n)}$ captures the loss of system objective—externality. With a limited capacity of supply, the choice of n affects other travelers' choices, and we need to take this into account when optimizing the discount for a specific individual. A lower discount to n might incur a loss to the system objective because more travelers on ML reduce the difference in traffic conditions between ML and GP, and hence decrease the attractiveness of ML. To achieve desirable system-level performance, we need to consider the loss of system objective caused by n performing a ML trip. This loss is unknown, and we model it to be proportional to the displayed toll $p^D_{t(n),k(n)}$, as $p^D_{t(n),k(n)}$ carries OD and congestion information. The proportionality factor $x_{t(n)}$ is the discount control parameter solved from the system optimization problem which should estimate its optimal value for system objective.

To solve the user optimization, we experimented with the Newton method for the first order condition as used in [115]. However, this method is observed to have similar results but slower than a grid search of the discount up to two decimal points—a reasonable precision to show to a subscriber—leveraging vectorized operations for simultaneous evaluations of the grid. This observation could also be potentially due to the fact that the objective function has very flat regions as the choice model contains significant unobserved heterogeneity. The grid search is adopted in the case study.

5.3 Case Study

We test the proposed pricing system in a closed-loop simulation environment, where a microscopic traffic simulator, SimMobility Short-Term [20] is used as a digital twin of a ML facility in the real world. This setting is shown in Figure 5-5.

By design, SimMobility Short-Term and DynaMIT (in Tri-POP) are both traffic simulators, but with different purposes and models. DynaMIT is designed for real-time predictions of traffic and optimizations of control policies. Therefore, for real-time performance, DynaMIT uses mesoscopic simulation models for queueing and the relationships among traffic flow, speed, and density. On the other hand, SimMobility Short-Term is designed to be a high-fidelity digital urban laboratory, so

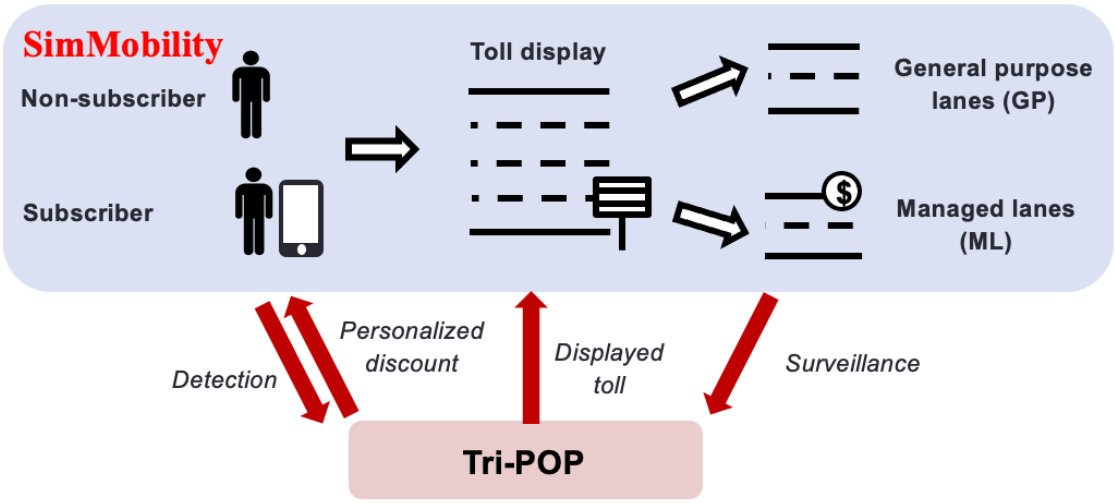

Figure 5-5: Closed-loop simulation environment

it simulates detailed driving behaviors of individual drivers, which is more realistic yet of higher computation cost. These differences explain why Tri-POP, as a real-time optimization system, uses DynaMIT, and SimMobility Short-Term is used in the closed-loop experiments as a surrogate for the real world.

5.3.1 Network and Data

We consider the managed lanes facility shown in Figure 5-6, which is the same network where the data for choice model estimation is collected in chapter 4.

The network consists of three toll segments, corresponding to three displayed tolls to be managed and optimized (see the legend in Figure 5-6). The displayed tolls from different ramps within the same toll segment are converted with fixed factors depending on the distance of ML usage. In our study, based on availability of calibration data, we limit our scope to the westbound direction, and consider the scope of the operation problem as optimizing the displayed tolls on segment 2 and 3 (the horizontal corridor in Figure 5-6), while considering the toll on segment 1 to be the same as existing tolling policy. The considered network has 74 origin-destination pairs and 90 sensors that provide count and speed measurements every 5 minutes.

One month of sensor data and toll under the existing tolling policy are made available to us. As incident data are not available, we detect the probable incidents

Figure 5-6: Case study network

based on flow and speed drops from time-of-day- and day-of-week-specific averages. The measurements from time periods with suspected incidents are then imputed with the compared averages.

To simplify the calibration process and scope of the study, the demand and supply of SimMobility is calibrated towards average sensor measurements across weekdays. Further, the choice data in chapter 4 (of a sample of actual travelers) are used to construct the synthetic population database for simulation. The travelers are selected based on trip frequency and time of day to match the calibrated average demand. Each simulated traveler hence is associated with a trip history from an actual traveler. More details regarding the setup of SimMobility and Tri-POP parameters are presented in subsection C.0.1 of Appendix C.

In order to simulate scenarios with discounts, we need to know who are the subscribers. Unfortunately, no data on the subscription choice are available. Therefore, the model is specified purely under assumptions that are deemed reasonable by us, and calibrated for a 25% penetration rate among all travelers.

Specifically, the subscription probability is determined by a Gompertz curve in

Equation 5.8. Gompertz curve is commonly used in growth analysis, whose shape could be more flexibly specified compared to the logit and probit curves. The variables enter this subscription model are $s_n^{tripsML}$ and $s_n^{tripsGP}$ respectively for the ML and GP trips that traveler n performed during the pervious 90 days under the existing scenario.

$$\begin{aligned} &P_n(subscribe) = a\, exp(-b\, exp(-s_n)) \\ &\text{where } s_n = c_1 s_n^{tripsML} + c_2 s_n^{tripsGP} \end{aligned} \tag{5.8}$$

The model has four parameters a, b, $c1$ and $c2$. a is the asymptote of the subscription probability as $s_n \to \infty$. As we do not want travelers in any case to deterministically subscribe, a is set to 0.95. b, c_1 and c_2 jointly determine the shape of the probability curve. After some exploration and calibrating for a 25% penetration rate, we set $b = 2.65$, $c_1 = 0.3$ and $c_2 = 0.05$ which gives the subscription probability as Figure 5-7. The ratio of c_1 and c_2 are determined to make the two variables to have similar influence.

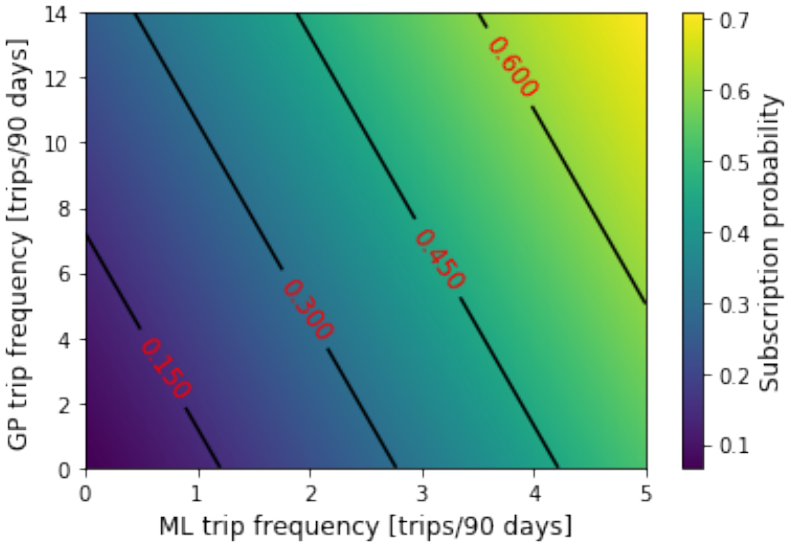

Figure 5-7: Subscription probability

5.3.2 Scenario Design

To investigate the benefit of our proposed system, we consider four scenarios with different tolling policies:

- *Base case*: existing toll, no discounts
- Three scenarios with Tri-POP:
  - *Scenario A*: optimized toll, no discounts (system optimization only)
  - *Scenario B*: existing toll, optimized discounts (user optimization only)
  - *Scenario C*: optimized toll, optimized discounts (system and user optimization combined, full Tri-POP)

As the demand and supply in simulation are calibrated towards an average weekday, the existing toll is considered to be the average existing toll across the corresponding days.

5.3.3 Selection of Policy Hyperparameters

The policy hyperparameters include the welfare hyperparameter δ^W that controls the weight of capture rate in the objective, and the customer retention hyperparameter δ^V that controls the weight of subscriber lifetime values. In this section, we present the effects of their values on the performance of Tri-POP scenario C where Tri-POP is in full effect, and discuss their selections.

As the tolling policy would be determined by the operator, we consider the overall selection criterion is to improve performances in other aspects without significant revenue loss. The selection of hyperparameter is ultimately a judgement of the operator and ours serves as a typical example. The different results under various values of hyperparameters showcase the flexibility of the system.

Selection of Welfare Policy Hyperparameter δ^W

For this analysis, we experiment δ^W at 0, 1250, 2500, 3750 and 5000, with the other hyperparameter δ^V being 0.5. Because the application of δ^W to peak periods (6 to

10 AM, and 3:30 to 7 PM) causes more revenue loss, and that in those period the capture rate is already high, we only set the nonzero values of δ^W to off-peak periods.

The performance is presented in Table 5.2. Overall, Tri-POP is able to increase revenue, increase ML usage, and reduce peak-hour congestion all at the same time. A further discussion of this is provided in the comparison across scenarios in subsection 5.3.4. As δ^W increases, the toll decreases, the revenue decreases and ML usage (in counts, equivalent to capture rate as total demand is fixed) increases. For various values of δ^W, the changes in peak-hour travel time are small, because nonzero δ^W is only applied to off-peak periods and therefore only affects the very beginning of peak hours.

The trade-off between revenue and ML usage is visualized in Figure 5-8. Clearly, the loss of revenue is minimal with a very small δ^W, but significantly increases for $\delta^W = 3750$ and 5000 after an inflection at 2500. This is further explained with a visualization of displayed toll in Figure 5-9. The higher values of δ^W start to result in significant toll drops during the mid-day. As our selection criterion is based on containing revenue loss, the optimal value of δ^W is selected to be 2500. A larger δ^W and its application to the peak periods would be preferred if more focus on the improvement of ML usage is desired.

Scenario	**Short-term revenue**	**Future revenue improv.**	**Long-term revenue**	**ML usage**	**Peak-hour travel time**	**Average price charged**	
						Non-sub.	**Subscriber**
$\delta^W = 0$	+2.88	+73.5	+19.3	+5.79	-10.7	+28.9	-34.6
$\delta^W = 1250$	+2.33	+74.5	+19.1	+7.03	-11.0	+27.3	-36.1
$\delta^W = 2500$	+2.14	+75.2	+19.1	+7.64	-10.7	+26.2	-36.5
$\delta^W = 3750$	+0.45	+76.2	+18.0	+8.37	-10.8	+22.4	-37.5
$\delta^W = 5000$	-0.58	+75.6	+17.1	+8.94	-11.8	+20.3	-38.5

numbers are % changes in proportion to base case (existing toll, no discounts)
Long-term revenue = short-term revenue + future revenue improvement (second component of objective)
Peak-hour travel time is computed for 6 – 10 AM (the most congested period)
Tri-POP (C), optimized toll, optimized discounts offered to 25% subscribers

Table 5.2: Performance under various δ^W

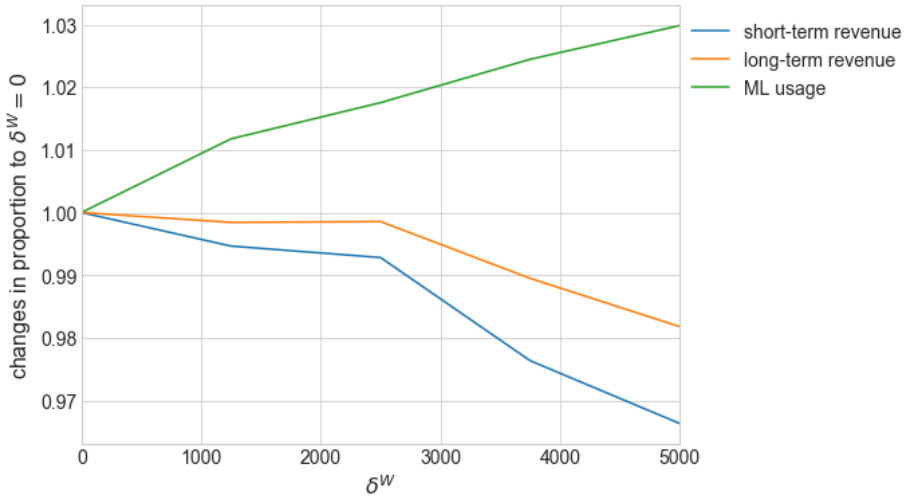

Figure 5-8: Revenue and ML usage under various δ^W

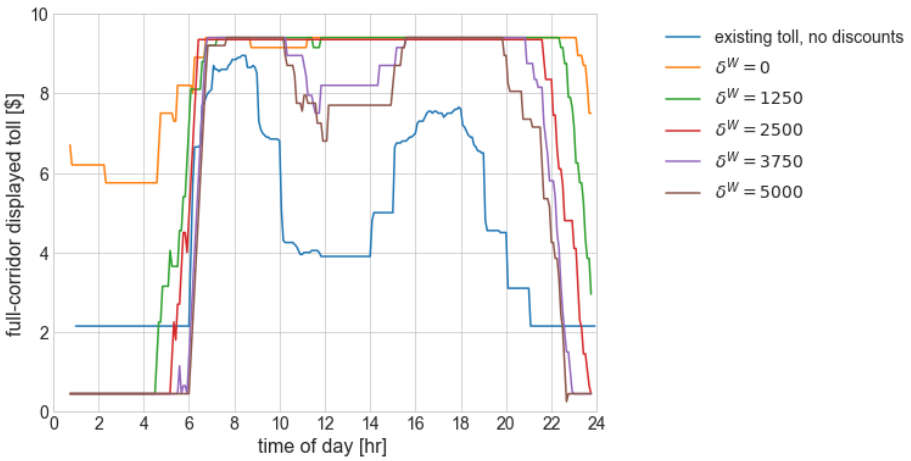

Figure 5-9: Displayed toll under various δ^W

Selection of Customer Retention Policy Hyperparameter δ^V

For this analysis, we experiment δ^V at 0, 0.25, 0.5, and 1, with δ^W being 2500.

The customer retention consideration could be understood as a subscriber-specific capture rate bonus (the δ_W just discussed) that is proportional to their past expenditure. A larger value of δ^V dictates relatively lower toll to high-value customers for their retention. On the other hand, these high-value customers are most likely the ones from whom we could acquire more revenue, so a higher value of δ^V would inevitable incur revenue loss. The rationale behind δ^V's inclusion is that if the loyal customers are always getting much higher toll, they are likely to feel being treated unequally and stop using ML or the corridor at all (churn). So, an ideal value of δ^V needs to be determined based on the observed churn rate or complaints in the field. Lacking this feedback, the criterion for δ^V is to achieve a more balanced profile of presented toll without excessive revenue loss.

The impact of δ^V on the distribution of toll presented to subscribers is shown in Figure 5-10. First, even under the existing toll with no discounts, high-value customers are getting higher toll as they are more likely to appear during the peak hours. Then, as expected, this trend is largely accentuated with Tri-POP (δ^V=0) that does not consider customer retention. An increasing value of δ^V works to balance the profile of presented toll across levels of past usage. The trade-offs in revenue are summarized in Table 5.3. As expected, δ^V decreases the price charged to the subscriber and revenue. The optimal values selected in this case is $\delta^V = 0.5$, as it provides the most balanced toll profile without have less short-term revenue compared to the base case.

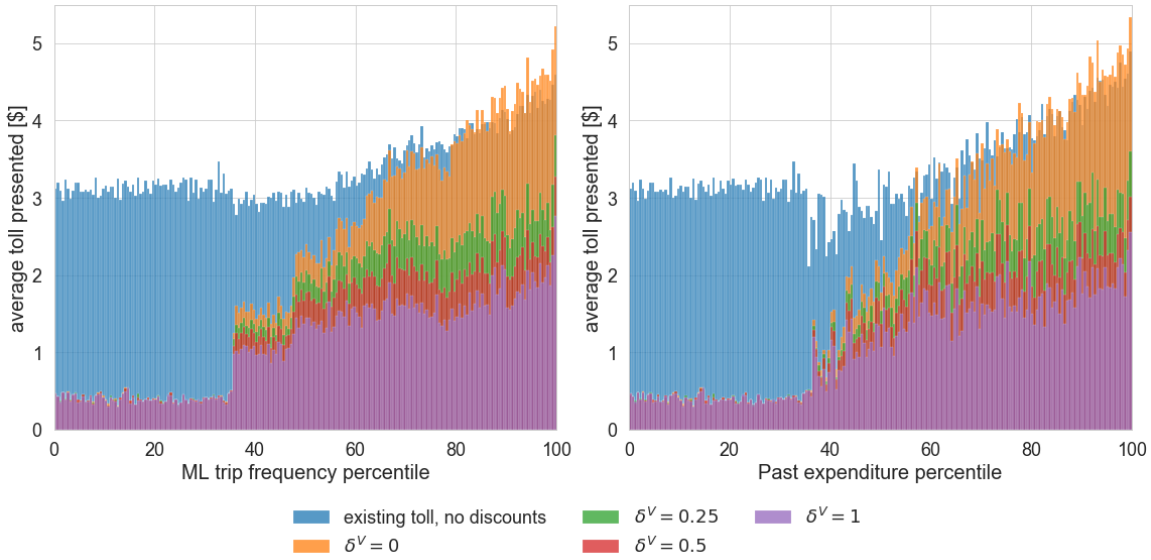

Figure 5-10: Toll presented to subscribers under various δ^V

Scenario	Short-term revenue	Future revenue improv.	Long-term revenue	ML usage	Peak-hour travel time	Average price charged	
						Non-sub.	Subscriber
$\delta^V = 0$	+8.30	+68.3	+22.2	+5.38	-9.86	+27.3	-23.7
$\delta^V = 0.25$	+4.34	+68.8	+19.3	+6.76	-11.1	+26.3	-31.5
$\delta^V = 0.50$	+2.14	+75.2	+19.1	+7.64	-10.7	+26.2	-36.5
$\delta^V = 1$	-2.22	+76.1	+16.0	+8.06	-11.1	+24.6	-43.3

numbers are % changes in proportion to base case (existing toll, no discounts)
Long-term revenue = short-term revenue + future revenue improvement (second component of objective)
Peak-hour travel time is computed for 6 – 10 AM (the most congested period)
Tri-POP (C), optimized toll, optimized discounts offered to 25% subscribers

Table 5.3: Performance under various δ^V

5.3.4 Comparison of Tolling Policies

For the following results, we use the selected policy hyperparameter $\delta^W = 2500$ and $\delta^V = 0.5$. Different selections of these hyperparameter across the Tri-POP scenarios could be further investigated.

An overview of results is presented in Table 5.4. Compared to the base case, the system optimization only (Scenario A) improves revenue and decreases ML usage, which is a result of the revenue-focus selection of δ^W. On the other hand, the discounts by user optimization (Scenario B) are able to maintain long-term revenue under the existing toll, while increasing ML usage and reducing congestion. Comparing the effects of system and user optimization, it is clear that discounts by the user optimization specifically work towards a reconciliation of the interests of travelers and the operator. The combined system and user optimization (Scenario C) increase long-term revenue, increase ML usage and reduce peak-hour congestion all at the same time.

Scenario	**Short-term revenue**	**Future revenue improv.**	**Long-term revenue**	**ML usage**	**Peak-hour travel time**	**Average price charged**	
						Non-sub.	**Subscriber**
A: opt. toll no discounts	+12.6	+27.4	+16.0	-7.13	+2.82	+25.6	+14.4
B: existing toll opt. discounts	-10.2	+42.2	+2.0	+13.5	-11.9	-0.1	-44.0
C: opt. toll opt. discounts	+2.14	+75.2	+19.1	+7.64	-10.7	+26.2	-36.5

numbers are % changes in proportion to base case (existing toll, no discounts)
Long-term revenue = short-term revenue + future revenue improvement (second component of objective)
Peak-hour travel time is computed for 6 – 10 AM (the most congested period)
Optimized discounts offered to 25% subscribers

Table 5.4: Performance comparison across Tri-POP scenarios

Figure 5-11 shows the average toll presented by the time of day. Overall, the optimized tolls are higher compared to the existing tolls, which explains the revenue improvements. Further, more interestingly, under the same mechanism for displayed toll, discounts mainly reduce the average toll during the AM peak. This is because for the direction we simulated, in general, AM peak corresponds to the period with more regular travelers with high trip frequencies. They have higher future revenue

potential and hence are offered with more discounts. A very nice outcome of these high discounts is the congestion reduction during this most congested period, which is visualized in Figure 5-12 that shows the average speed across all travelers by time of day. The future revenue consideration is designed for optimal long-term revenue, but it naturally leads to congestion reductions as regular travelers appear at the congested period.

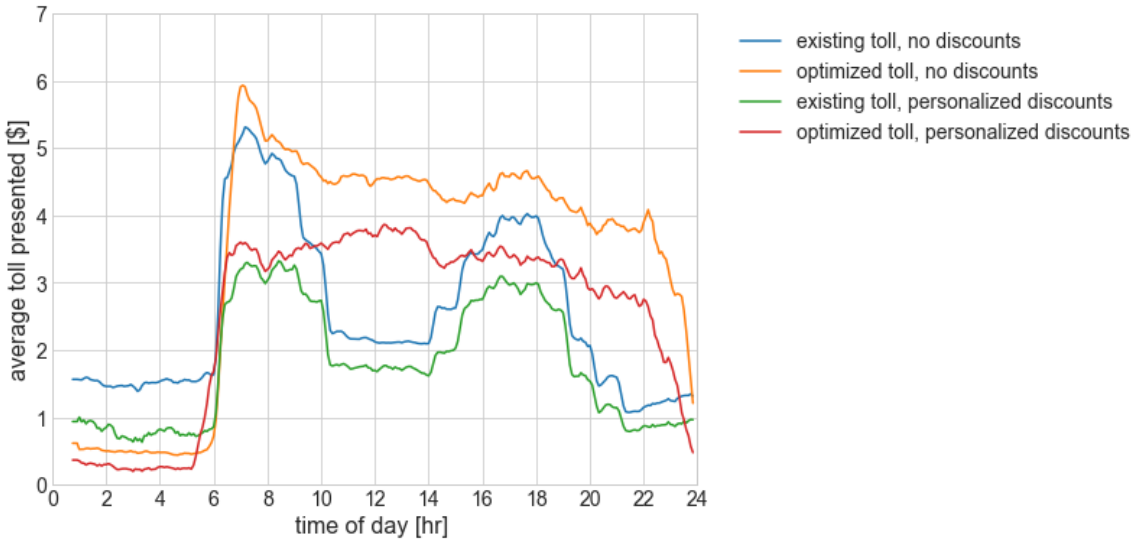

Figure 5-11: Average toll presented by time of day

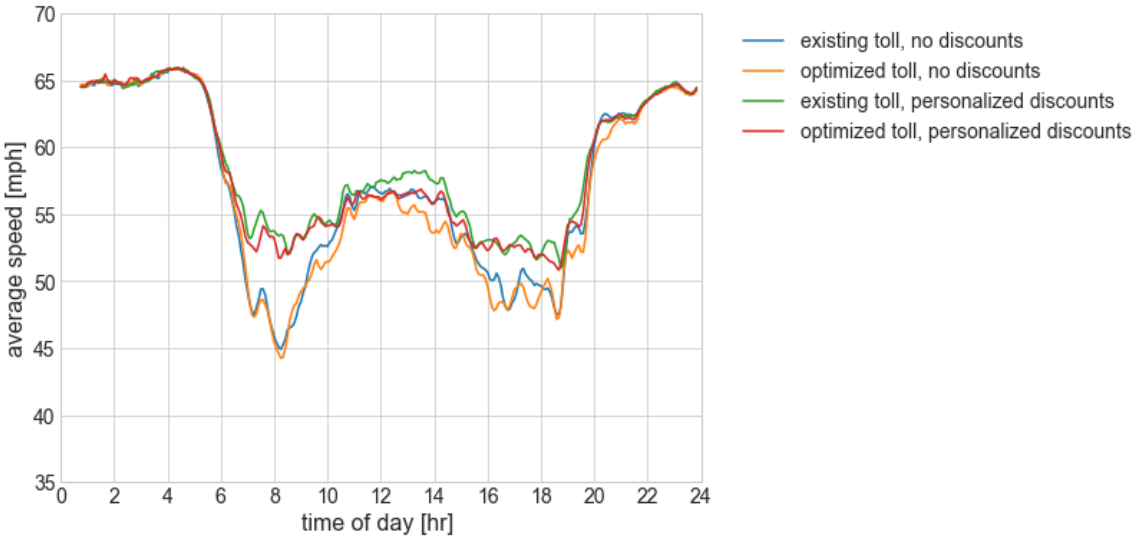

Figure 5-12: Average speed by time of day

Further, as we investigate the performance of personalized pricing, it is important

to analyze the distribution of toll, ML usage, travel time, and net benefit among travelers, for us to understand who benefit and who lose under different scenarios, and how personalized tolling would affect equity.

First, we would like to see how the benefits vary across travelers with different values of time, as the value of time should be positively correlated with the traveler's income that is unobserved. Second, we would like to see how the benefits vary with the traveler's previous GP frequency (number of GP trips in the previous 90 days), where we would expect that the travelers with higher previous GP frequency receive more benefit as the long-term-oriented tolling algorithm should give them higher discount for their conversion.

The distributions of toll presented to all travelers are visualized in Figure 5-13 and Figure 5-14. Under no discounts (left of the figures), the different toll levels are results of the variations in traveler characteristics by the time of day. Under discounts (right of the figures), Figure 5-13 shows that the travelers with lower values of time are presented lower tolls, because these travelers are less likely to use ML. Figure 5-14 shows that the travelers with more GP trips in the previous 90 days are presented lower tolls. There are three reasons: first, these travelers are less likely to use ML; second, they have greater future revenue potential; third, based on the subscription model, they are more likely to be subscribers (when everything else including ML trip frequencies are equal)—this is a result of our assumption but is logical.

The distributions of ML usage are visualized in Figure 5-15 and Figure 5-16. The idea of these visualizations comes from the Lorenz curve for the analysis of income inequality [47]. Because the horizontal axes are essentially sorted travelers, a straight line of cumulative usage would indicate uniform usage across the population. In Figure 5-15, the four usage curves are all convex with respect to travelers' values of time, meaning that the travelers with higher values of time use ML more. Under scenarios with discounts, as the travelers with lower values of time are presented lower tolls, we can see that the ML usage improvements come from these travelers (curvature differences appear at the left of horizontal axis). This confirms our prior belief that personalized tolling, if done properly, would open the managed lanes to more trav-

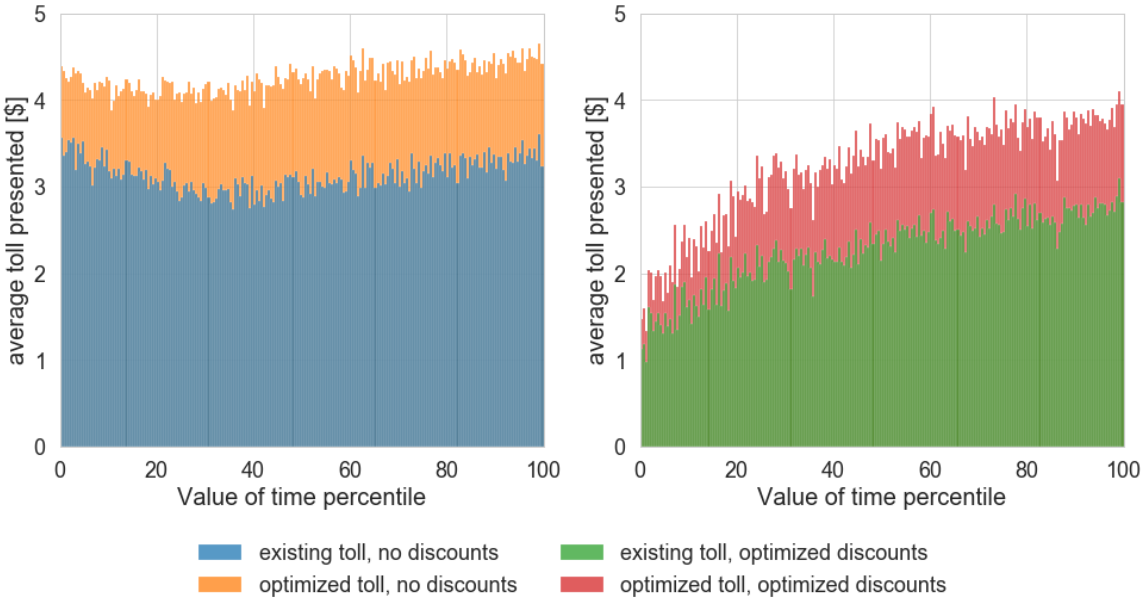

Figure 5-13: Toll presented by value of time

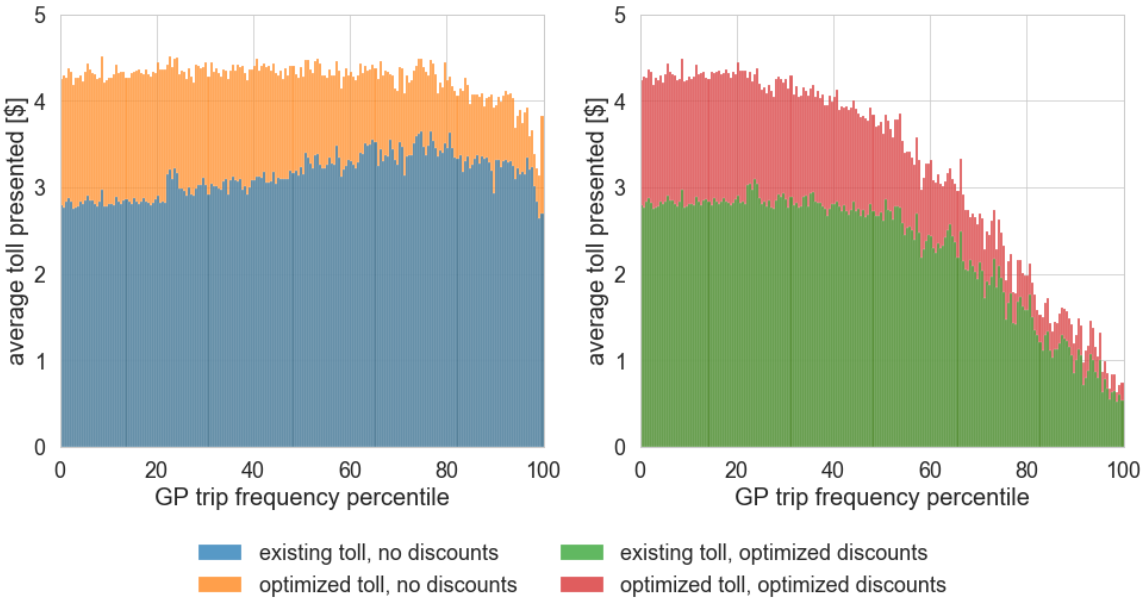

Figure 5-14: Toll presented by GP trip frequency

elers that are less wealthy. Similarly, Figure 5-16 shows that without discounts the travelers with more GP trips in the previous 90 days are less likely to use ML, but are successfully converted to ML users under scenarios with discounts.

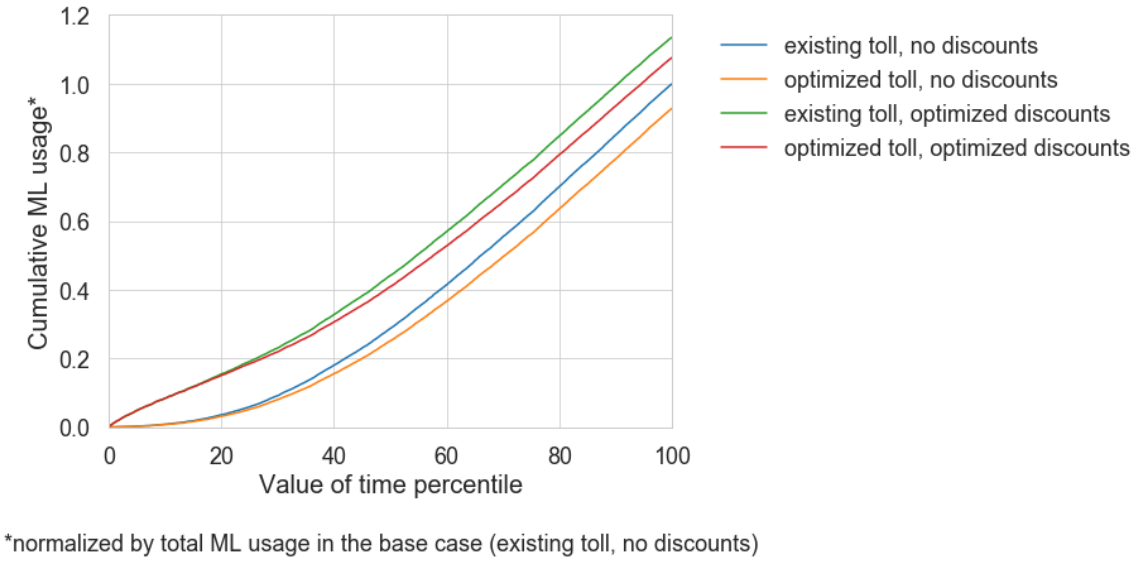

*normalized by total ML usage in the base case (existing toll, no discounts)

Figure 5-15: ML usage by value of time

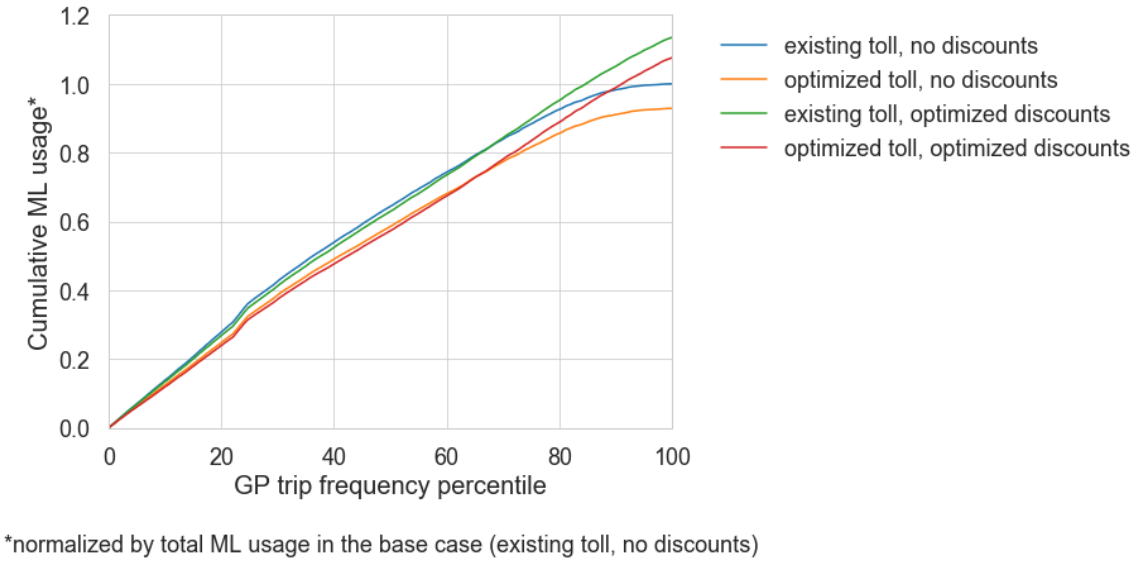

*normalized by total ML usage in the base case (existing toll, no discounts)

Figure 5-16: ML usage by GP trip frequency

Next, the distributions of travel time are visualized in Figure 5-17 and Figure 5-18. Comparing before and after discounts, overall the travelers that enjoy most travel time reductions are the ones who switch from GP to ML, and the other GP travelers

because ML is not congested in all scenarios. We compute these distributions among peak travelers with the through OD (the origin-destination pairs from the rightmost to leftmost on Figure 5-6). Figure 5-17 shows that discounts generate travel time reductions that are slightly more for travelers with lower value of time. Figure 5-18 shows that the travel time reductions are more for travelers with higher GP trip frequency.

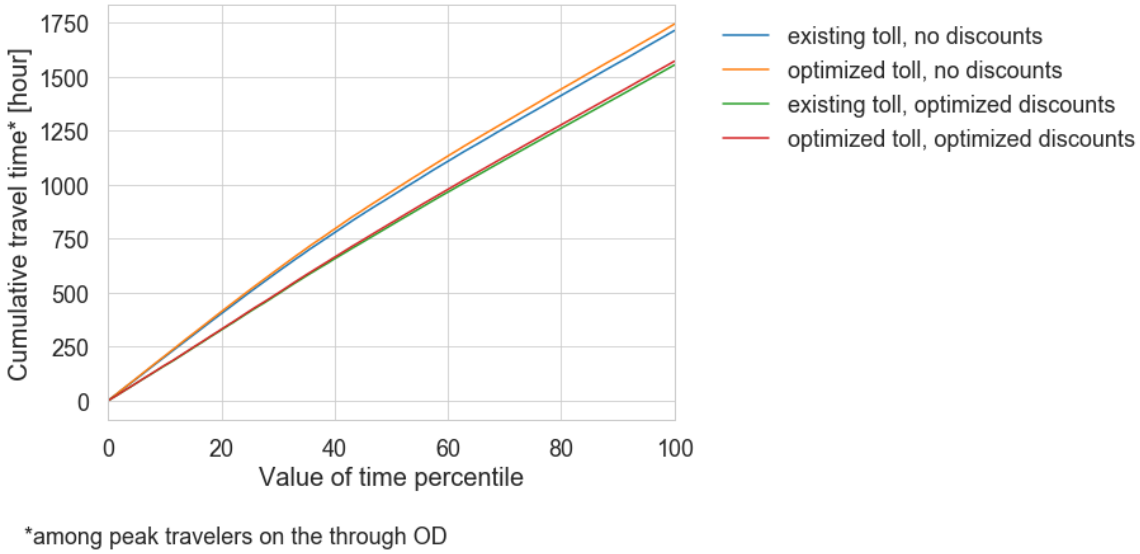

Figure 5-17: Travel time by value of time

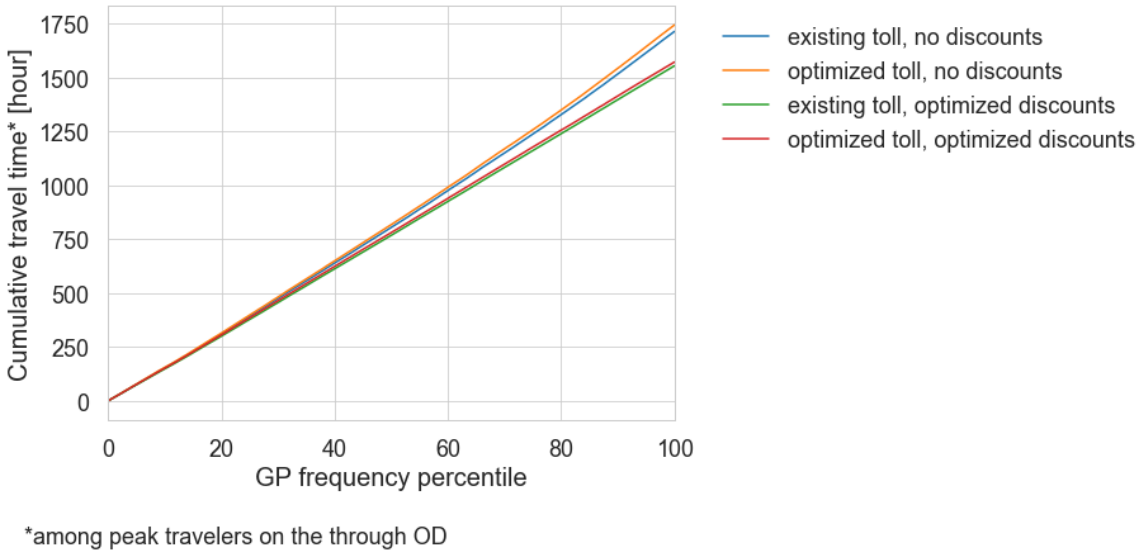

Figure 5-18: Travel time by GP trip frequency

Finally, we analyze the distribution of net benefits to travelers under the Tri-POP scenarios. The net benefit to a traveler is the change in the expected maximum utility (computed with the logsum formula [26]) relative to the base case. It is expressed in equivalent minutes in the following analysis. Its distribution by traveler's value of time is shown in the following slides for four groups, where the peak refers to the most congested hours (6 - 10 AM):

- Peak subscribers
- Peak non-subscribers
- Off-peak subscribers
- Off-peak non-subscribers

The distributions of net benefit during peak hours (to the first two groups) are presented in Figure 5-19 and Figure 5-20. Figure 5-19 shows the cumulative net benefit where the curvatures indicate the most benefited value-of-time segments. Overall, the optimized tolls without discounts provide less benefits compared to existing tolls as they are higher. With discounts, the peak subscribers (left of Figure 5-19) benefit from the reductions of toll and congestion, especially the ones with lower value of time. In addition, the discounts also benefit the peak non-subscribers (right of Figure 5-19) as they reduce congestion.

Figure 5-20 presents the same data but changes the vertical axis to the cumulative moving average. For sorted data points $x_1, ..., x_n$, the cumulative moving average to the t^{th} data point is $(x_1 + ... + x_t)/t$. Therefore, in this figure, the height of a curve at the 20^{th} percentile is the average net benefit for all the travelers with values of time below or equal to the 20^{th} value of time percentile. At the 100^{th}, the height is simply the average net benefit across population. A decreasing slope of cumulative moving average means that travelers with higher values of time benefit less, and vice versa. Note that a declining cumulative moving average does not necessarily mean that the corresponding travelers lose, but just that their benefits are less. The signs of benefits (winning or losing) to a specific percentile could be more clearly see from the slopes in previous cumulative plots (Figure 5-19). The purpose of showing

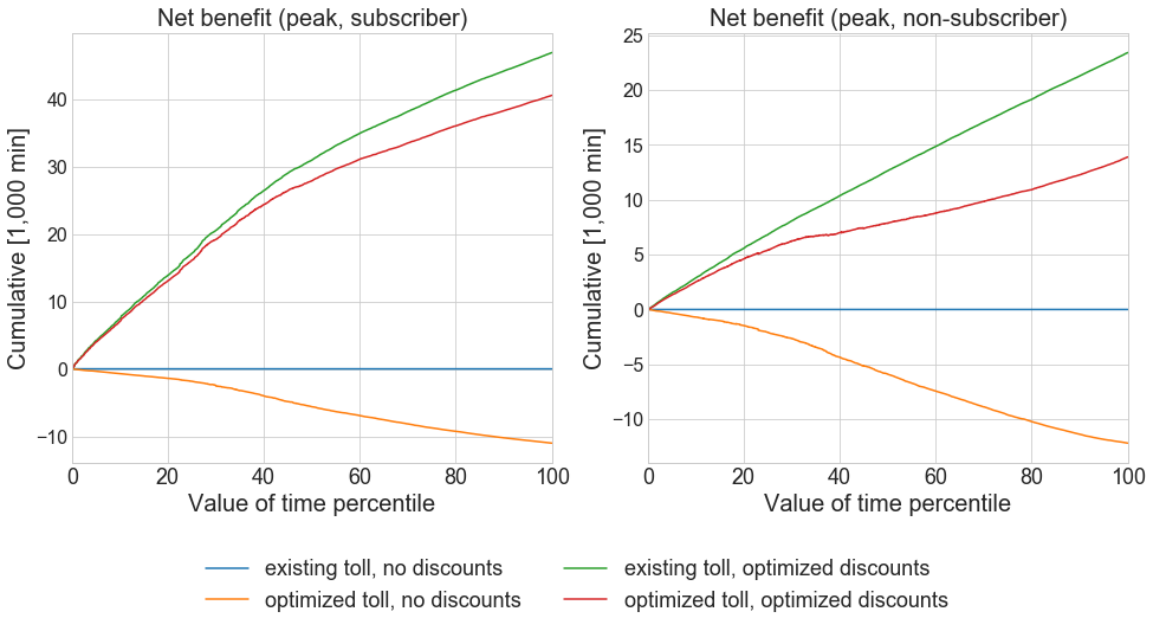

Figure 5-19: Cumulative net benefit during peak

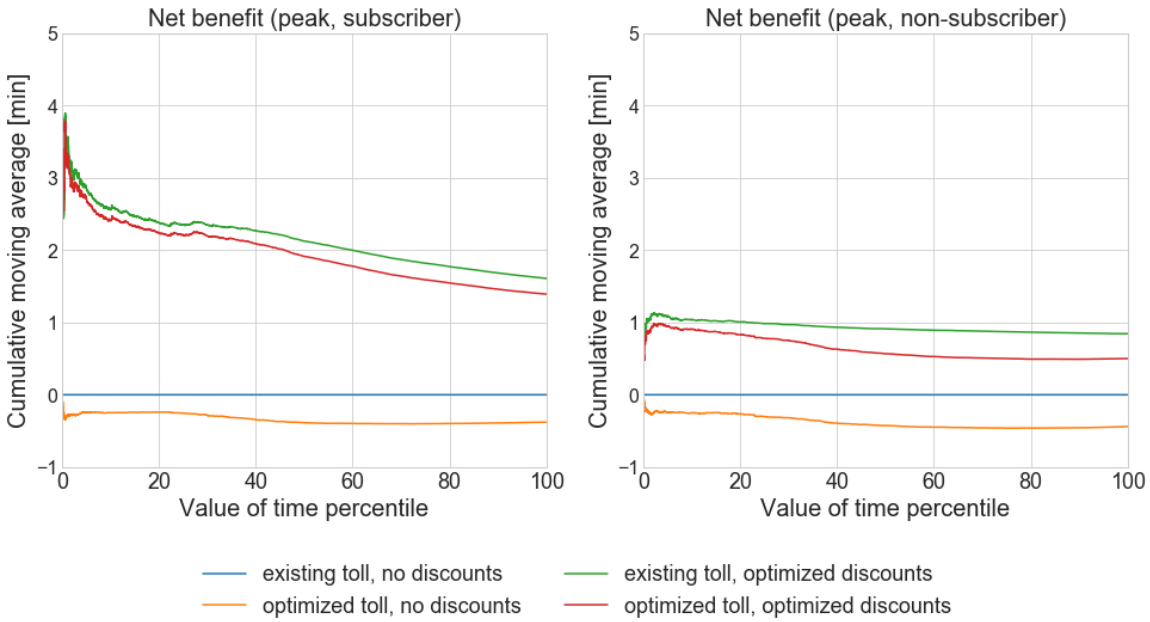

Figure 5-20: Cumulative average net benefit during peak

cumulative moving average is to directly compare average benefit across scenarios. With discounts, it is clear that the peak subscribers receive more benefit compared to non-subscribers. Among peak subscribers, the clearly declining slopes of scenarios with discounts demonstrate again that the discounts benefit especially travelers with lower values of time.

With the same visualization methods, the distributions of net benefit during off-peak are presented in Figure 5-21 and Figure 5-22. As there is lower congestion in the off-peak compared to peak, there are overall less benefit with discounts. Even so, the subscribers benefit because of the lower tolls they are presented. For the non-subscribers, although the optimized toll and discounts make them lose compared to existing toll with no discounts, discounts still benefit them compared to optimized toll with no discounts.

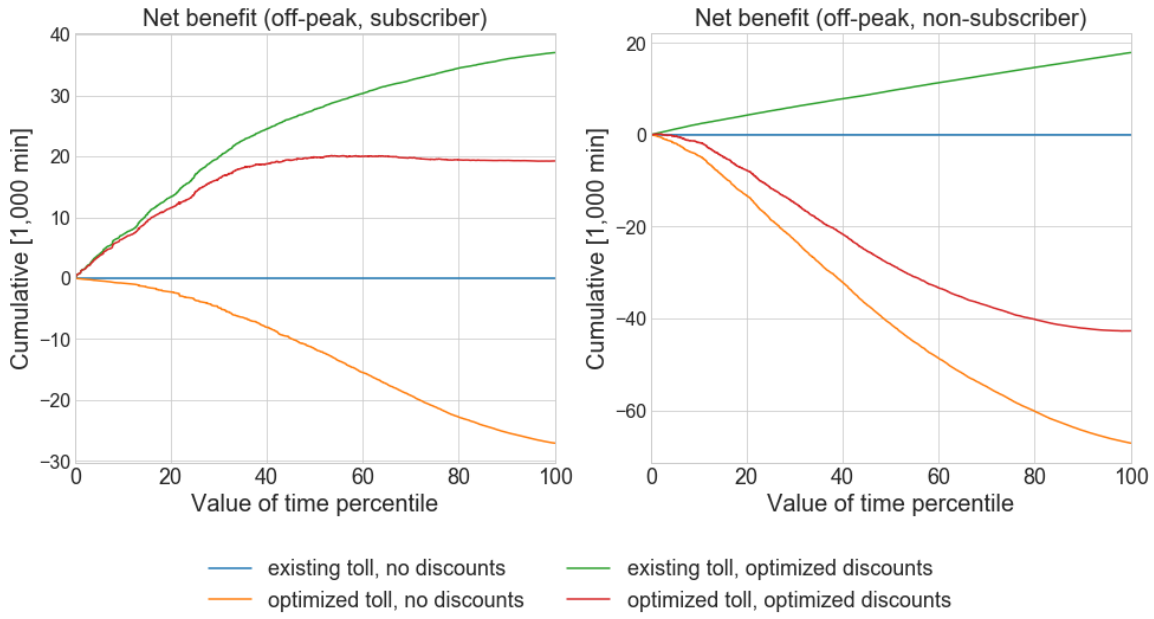

Figure 5-21: Cumulative net benefit during off-peak

In summary, subscribers benefit from personalized discounts, especially the ones with lower values of time. This feature improves the equity of managed lanes facilities that are sometimes criticized for serving the rich. Non-subscribers also benefit from congestion reduction. The benefit of discounts is larger during peak hours where the congestion is higher. Subscribers benefit more than non-subscribers, as they

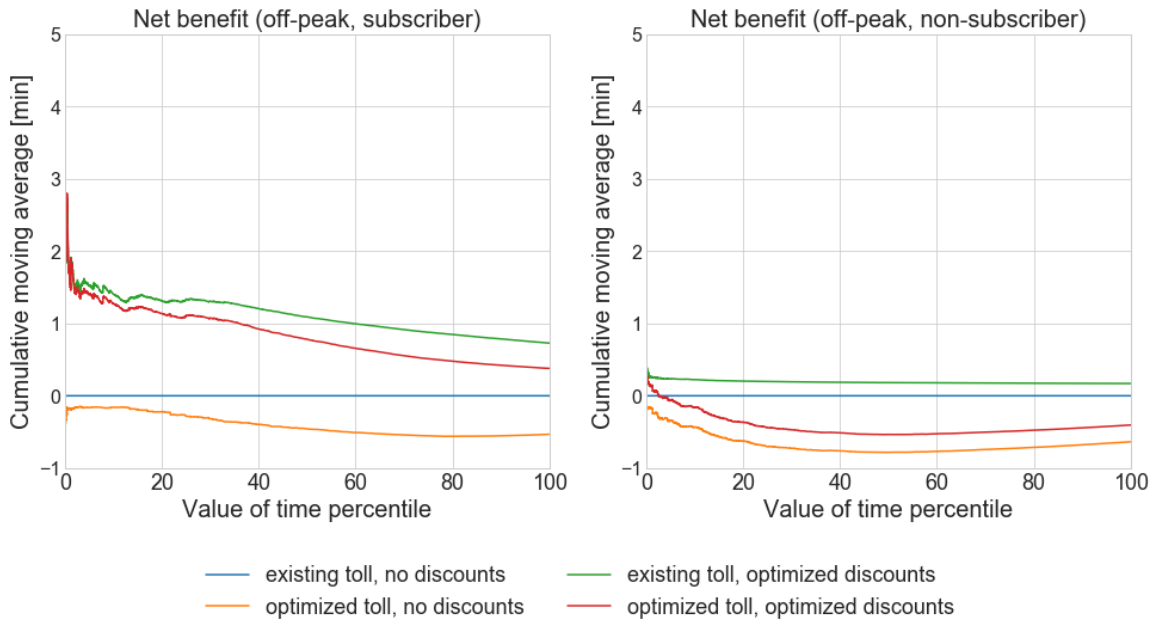

Figure 5-22: Cumulative average net benefit during off-peak

receive discounted tolls—this is not a concern as the non-subscribers could improve their benefit simply by subscribing, which actually is beneficial for increasing the subscription rate.

5.4 Conclusions

This chapter develops a personalized real-time prediction-based pricing system that jointly optimizes displayed toll and personalized discounts. The formulation is based on the Tri-POP online bi-level optimization paradigm that combines prediction, optimization and personalization. Two connected optimization problems are solved: system optimization that is solved every 5 minutes for displayed toll and a discount control parameter, and user optimization that is solved upon arrivals of subscribers for personalized discounts. The system optimization problem is based on simulations of real-time traffic predictions within which the simulated subscribers receive discounts by user optimization. The user optimization problem is based on individual-specific choice predictions and the discount control parameter that is optimized from system optimization to consider the system objective.

A key contribution is our design of a multi-component objective that includes short-term revenue, future revenue improvement from increased loyalty, capture rate, and subscriber lifetime value for customer retention. The consideration of future revenue improvement is based on the discovered state-dependent choice behaviors in chapter 4 where travelers previous ML usage structurally increases their probability of using the ML, which motivates lower price in exchange for future revenue potential. The inclusion of capture rate with a policy hyperparameter allows the operator to shift focus towards social welfare and promote ML usage. The case study shows that it could improve capture rate under minimal costs of revenue. The consideration of subscriber lifetime value mitigates the undesirable pattern that more loyal subscribers are presented higher toll because of their tendency to keep using ML.

A closed-loop simulation case study based on data from a real facility shows and dissects the performance of Tri-POP. Optimized tolls from system optimization is shown to improve revenue. Optimized discounts from user optimization is shown to increase ML usage and reduce congestion. Combined system and user optimizations increase long-term revenue, increase ML usage, and reduce congestion.

Under discounts, the lower tolls benefit subscribers, while the congestion reduction benefit all travelers. Further, discounts encourage ML usage by travelers with lower values of time who are less likely to use ML under no discounts. Higher net benefits are also observed to subscribers with lower value of time. This indicates that personalized tolling based on individual-specific preferences are able to improve equity on ML.

In the case study, the weights (hyperparameters) of different objective components are chosen with a primary focus on revenue. The proposed system could be further tested under different criteria for their determinations, which would further showcase the flexibility of our framework.

Chapter 6

Conclusion

6.1 Summary of Contributions

This thesis investigates the tolling algorithm on managed lanes (ML) that are tolled and in parallel to general purpose lanes (GP). The objective of this thesis is to develop a personalized adaptive tolling algorithm that meets the interests of the operator, the travelers and the regulator. For this purpose, chapter 3 and chapter 4 develop a comprehensive managed lanes choice model to understand how travelers choose between ML and GP, with a focus on the proper quantifications of heterogeneity and state dependence that are crucial in personalized pricing. It is shown that improper modeling assumptions tend to overstate the state dependence, which could make the operator overinvest in customer loyalty. Then, chapter 5 develops the proposed tolling algorithm based on Tri-POP, an online bi-level optimization framework that combines prediction, optimization and personalization. The contributions are summarized chapter by chapter in the following paragraphs.

Chapter 3 investigates the initial condition problem in the estimation of dynamic choice model with random parameters—the workhorse model for quantifying unobserved heterogeneity and state dependence. The initial condition problem is a special form of endogeneity that is hard to avoid and causes overestimation of the state dependence. Our contribution is that we propose a Control Function solution that is applicable to the general case of random parameters and multinomial choice. The pro-

posed method and widely used current methods are compared in Monte Carlo studies where we found improvements of the Control Function over Wooldridge's Method. These two methods appear to be inferior than the Heckman's method for estimating the population variances of random parameters, but are comparable for estimating the population means and simpler to use.

With revealed preferences data, chapter 4 develops a comprehensive dynamic choice model with random parameters for managed lanes choices. The Wooldridge's method and Control Function corrections for the initial condition problem both are applied and conclude the presence of significant unobserved heterogeneity and state dependence. We show the dangers of omitting unobserved heterogeneity or improper treatment of the initial condition problem, which largely overstate the state dependence. In the literature of managed lanes behaviors, this work is the first to distinguish between state dependence and unobserved heterogeneity, and hence uncover what drive the commonly observed high correlation among choices by the same traveler. Further, price endogeneity under dynamic pricing is found and corrected, which is the first to address this in managed lanes choice models to the best of my knowledge.

Chapter 5 develops the personalized adaptive tolling algorithm. An online bi-level optimization problem is formulated based on Tri-POP that jointly optimizes the displayed toll and personalized discounts in an online setting. The key contribution is the design of a multi-component objective with flexible policy hyperparameters. It considers short-term revenue, the impact on future revenue based on the state-dependent choice behavior, capture rate, and loyal customer retention. Through closed-loop simulation studies, the developed algorithm is shown to increase long-term revenue, increase ML usage, and reduce congestion in the corridor. From an equity perspective, the personalized discounts based on individual preferences are shown to encourage ML usage by travelers with lower value of time, and benefit them relatively more. This would help to change the impressions that ML mainly serve the wealthy travelers.

Overall, this research shows that personalized discounts can benefit both the operator and the travelers, and are therefore very useful in addressing the interests of

the operator, the travelers, and the regulator. It challenges the traditional view of personalized pricing being a tool only for revenue generation.

6.2 Future Research Directions

For the initial condition problem treated in chapter 3, the remaining research problem is seeking further bias reductions and hopefully consistent estimators. We think that the Control Function still has untapped potentials, considering its convenience and flexibility. Further flexible specifications are worth trying. In addition, the Monte Carlo studies could be extended to multinomial choices to investigate the performance of different solutions.

For the modeling of managed lanes travel behavior, first, more thorough selections could be performed on the definitions of state-dependent variables, and analyze how those definitions would change the estimated effects. Second, the Heckman's correction could be applied in comparison to the Wooldridge's method and the Control Function. Third, compared to the adopted normality assumptions on unobserved heterogeneity, more flexible distribution assumptions and latent class could be experimented. One popular theory is that there exists a class of travelers who do not factor toll into their decisions as the toll is paid by someone else (i.e., a company car, corporate reimbursement policies). It would be interesting to see the estimated share of these travelers after the price endogeneity has been corrected.

For the personalized tolling algorithm with Tri-POP, different methods could be explored to reduce the real-time computation in system optimization, as the current formulation with Dynamic Traffic Assignment (DTA) system requires real-time traffic simulations. This is not an easy task as cautions are required to not lose the theory-driven tractability of the DTA system. Tolling significantly affects road congestion and arbitrary tolls by black-box models are especially harmful for the public acceptance of road pricing. One possible idea is model-based reinforcement learning, where the system dynamics of traffic simulation models could be incorporated into a reinforcement learning model via offline interactions between the simulator and

the learning agent [99]. Other related ideas include the recent proposal by [82] that solves the system optimization problem based on a metamodel that is specified to incorporate traffic dynamics and trained with simulations.

Further, a lot more research could be done into the adoption and attrition behaviors under personalized pricing, as well as the perception and acceptance towards it. These questions are important for validating the benefit and feasibility of personalized pricing, and to answer them specific data need to be collected from stated preference surveys or field experiments.

Appendix A

Supplementary Results for the Initial Condition Problem

	True Value	No Correction	Heckman's	Wooldridge's (Full Cov.)	CF (Full Cov.)	Wooldridge's (Diag. Cov.)	CF (Diag. Cov.)
Population mean							
ζ_n^{scale}	1	0.866 (0.0632)	0.992 (0.0741)	1.01 (0.0821)	1.00 (0.0789)	1.01 (0.0789)	1.00 (0.0724)
ζ_n^{d}	1.5	2.14 (0.0531)	1.48 (0.0504)	1.50 (0.0709)	1.49 (0.0572)	1.48 (0.0526)	1.47 (0.0476)
ζ_n^{ASC}	-0.5	-0.836 (0.0309)	-0.487 (0.0374)	-0.502 (0.0382)	-0.499 (0.0358)	-0.493 (0.0330)	-0.495 (0.0326)
ζ_n^{time}	0	-0.00173 (0.0338)	0.00389 (0.0321)	0.0139 (0.0379)	0.0164 (0.0325)	0.0118 (0.0384)	0.0135 (0.0331)
Population variance							
ζ_n^{scale}	0.5	0.458 (0.0928)	0.506 (0.112)	0.602 (0.149)	0.567 (0.137)	0.570 (0.121)	0.544 (0.112)
ζ_n^{d}	0.5	1.14 (0.111)	0.485 (0.109)	0.576 (0.158)	0.504 (0.132)	0.472 (0.0936)	0.427 (0.0922)
ζ_n^{ASC}	1	0.419 (0.0519)	1.06 (0.0983)	1.04 (0.112)	1.00 (0.0962)	1.03 (0.0977)	0.989 (0.0860)
ζ_n^{time}	1	1.16 (0.0841)	1.00 (0.0716)	0.991 (0.0863)	0.958 (0.0823)	0.986 (0.0808)	0.951 (0.0756)
60 repetitions, 5 observed choices, 5000 individuals							

Table A.1: Dataset 1 estimates with full covariance matrices

	No Correction	Heckman's	Wooldridge's (Full Cov.)	CF (Full Cov.)	Wooldridge's (Diag. Cov.)	CF (Diag. Cov.)
Population mean						
ζ_n^{scale}	0.148	0.0746	0.0829	0.0791	0.0794	0.0725
ζ_n^{d}	0.643	0.0541	0.0710	0.0588	0.0569	0.0558
ζ_n^{ASC}	0.337	0.0397	0.0382	0.0358	0.0337	0.0329
ζ_n^{time}	0.0339	0.0323	0.0404	0.0365	0.0401	0.0358
Population variance						
ζ_n^{scale}	0.102	0.113	0.180	0.153	0.140	0.121
ζ_n^{d}	0.651	0.110	0.175	0.132	0.0978	0.118
ζ_n^{ASC}	0.584	0.115	0.120	0.0962	0.101	0.0867
ζ_n^{time}	0.181	0.0716	0.0868	0.0926	0.0820	0.0903
60 repetitions, 5 observed choices, 5000 individuals						

Table A.2: Dataset 1 RMSE with full covariance matrices

Appendix B

Supplementary Results for Managed Lanes Travel Behavior Modeling

Variable	**Coefficient Estimate**	**Standard Error**
Intercept	1.61	0.0179
$x_{nm}^{toll^*}$	1.28	0.0107
$x_{nm}^{timeSaving}$	0.0930	0.000947
$x_{nm}^{DPspeed}$	0.00232	0.000367
$sin(2\pi x_{nm}^{tod})$	0.210	0.00442
$sin(4\pi x_{nm}^{tod})$	-0.5494	0.00189
$sin(6\pi x_{nm}^{tod})$	0.3498	0.00279
$sin(8\pi x_{nm}^{tod})$	0.3332	0.00207
$sin(10\pi x_{nm}^{tod})$	-0.1542	0.00208
$sin(12\pi x_{nm}^{tod})$	-0.1748	0.00178
$cos(2\pi x_{nm}^{tod})$	-0.7996	0.00665
$cos(4\pi x_{nm}^{tod})$	-0.6980	0.00479
$cos(6\pi x_{nm}^{tod})$	0.7978	0.00362
$cos(8\pi x_{nm}^{tod})$	-0.2057	0.00168
$cos(10\pi x_{nm}^{tod})$	-0.2430	0.00196
$cos(12\pi x_{nm}^{tod})$	0.0847	0.00195
Adjusted R^2	0.933	

Table B.1: Estimates of the Control Function first step for price endogeneity correction

Parameter	Estimate	Parameter	Estimate
ASC		*Toll*	
$\alpha^{ASC,0}$	-1.17 (0.265)	$\alpha^{toll,0}$	-4.21 (0.384)
$\alpha^{ASC,logOdds}$	0.374 (0.0931)	$\alpha^{toll,logOdds}$	0.476 (0.144)
$\alpha^{ASC,onlyML}$	2.11 (0.310)	$\alpha^{toll,onlyML}$	0.529 (0.333)
$\alpha^{ASC,onlyGP}$	-0.777 (0.233)	$\alpha^{toll,onlyGP}$	-0.727 (0.378)
$\alpha^{ASC,noTrip}$	-0.0740 (0.262)	$\alpha^{toll,noTrip}$	-0.668 (0.403)
$\alpha^{ASC,avgTSoverToll}$	-0.938 (0.194)	$\alpha^{toll,avgTSoverToll}$	-0.275 (0.248)
$\alpha^{ASC,avgTSoverTollAll}$	0.287 (0.198)	$\alpha^{toll,avgTSoverTollAll}$	-0.0192 (0.246)
Time		*DPspeed*	
$\alpha^{time,0}$	-0.824 (0.246)	$\alpha^{DPspeed,0}$	-4.46 (0.573)
$\alpha^{time,logOdds}$	0.372 (0.123)	$\alpha^{DPspeed,logOdds}$	0.0743 (0.0915)
$\alpha^{time,onlyML}$	-0.116 (0.336)	$\alpha^{DPspeed,onlyML}$	-0.571 (0.0356)
$\alpha^{time,onlyGP}$	-1.49 (0.369)	$\alpha^{DPspeed,onlyGP}$	-0.957 (0.329)
$\alpha^{time,noTrip}$	-2.87 (0.514)	$\alpha^{DPspeed,noTrip}$	0.620 (0.504)
$\alpha^{time,avgTSoverToll}$	-1.10 (0.239)	$\alpha^{DPspeed,avgTSoverToll}$	1.24 (0.565)
$\alpha^{time,avgTSoverTollAll}$	-0.0233 (0.233)	$\alpha^{DPspeed,avgTSoverTollAll}$	-1.84 (0.721)

Table B.2: Conditional distribution of ζ_n by Wooldridge (fixed parameters)

	ASC	Toll	Timesaving	DPspeed
ASC	3.78 (0.594)	0.919 (0.293)	-0.832 (0.204)	-0.254 (0.545)
Toll	0.919 (0.293)	2.56 (0.607)	1.32 (0.355)	-1.25 (0.774)
Timesaving	-0.832 (0.204)	1.32 (0.355)	1.35 (0.248)	-0.717 (0.632)
DPspeed	-0.254 (0.545)	-1.25 (0.774)	-0.717 (0.632)	3.78 (0.927)

Table B.3: Conditional distribution of ζ_n by Wooldridge (covariance matrix)

Parameter	Estimate	Parameter	Estimate
ASC		*Toll*	
$\gamma^{ASC,0}$	-1.39 (0.128)	$\gamma^{toll,0}$	-4.46 (0.270)
$\gamma^{ASC,control}$	1.15 (0.174)	$\gamma^{toll,control}$	-0.123 (0.278)
$\gamma^{ASC,noTrip}$	0.361 (0.125)	$\gamma^{toll,noTrip}$	-0.374 (0.263)
Time		*DPspeed*	
$\gamma^{time,0}$	-1.80 (0.112)	$\gamma^{DPspeed,0}$	-4.87 (0.307)
$\gamma^{time,control}$	0.277 (0.188)	$\gamma^{DPspeed,control}$	0.378 (0.151)
$\gamma^{time,noTrip}$	-1.10 (0.263)	$\gamma^{DPspeed,noTrip}$	0.215 (0.393)

Table B.4: Conditional distribution of ζ_n by Control Function (fixed parameters)

	ASC	Toll	Timesaving	DPspeed
ASC	2.94 (0.416)	1.07 (0.247)	-0.0857 (0.150)	0.201 (0.450)
Toll	1.07 (0.247)	2.80 (0.522)	1.48 (0.302)	-0.390 (0.671)
Timesaving	-0.0857 (0.150)	1.48 (0.302)	1.06 (0.194)	-0.276 (0.510)
DPspeed	0.201 (0.450)	-0.390 (0.671)	-0.276 (0.510)	3.87 (0.767)

Table B.5: Conditional distribution of ζ_n by Control Function (covariance matrix)

Appendix C

Supplementary Results for Personalized Toll Optimization

C.0.1 Setting Up the Closed-Loop Environment

To set up the closed-loop simulation, there are overall two tasks. First, we need to calibrate SimMobility, for it to mimic the real-world conditions. Second, we need to prepare the parameters in the pricing system Tri-POP.

Calibration of SimMobility Short-Term

Calibration is the process of adjusting simulation parameters to minimize the discrepancy between observed and simulated sensor measurements. To simplify the calibration process, we first compute observed measurements across one week with the least irregular flow and speed drops, and then try to match these measurements so that we have the simulation parameters for an average day. The following three groups of parameters in SimMobility Short-Term are calibrated, explained one by one as follows:

- *Driving behavior models*: SimMobility Short-Term uses comprehensive driving behavior models to capture the reaction time, car following and lane changing behaviors of drivers. The model parameters are calibrated with SPSA [76] that minimizes the measurements discrepancy based on gradients computed from

SimMobility simulations with perturbed parameters. There are more than 100 parameters in these models, which makes the calibration problem challenging for SPSA due to the noise in gradient. To reduce the dimension of calibration, based on evidence in [41], we only calibrate a subset of important parameters that are likely to vary from study to study. In addition, we noticed that the calibration of parameter heterogeneity among different ODs has a major effects on matching different levels of congestion at different on- and off-ramps.

- *Trips with origin, destination, start time*: we represent the trips as an origin-destination (OD) matrix and calibrate it with the W-SPSA algorithm that improves the the efficiency of SPSA [76]. W-SPSA is particularly suitable for OD calibration as it utilizes structural knowledge of the network via adjusting the simulation-based gradient so that the measurement discrepancy on a particular sensor is only attributed to OD pairs that have paths passing it.

- *Route choice model*: the route choice model is from chapter 4 where the model estimation data includes a subset of ODs on the network. Therefore, to use the model, a new set of gantry-specific constants are incorporated to the model to capture the ML preference difference among ODs associated with different on-ramps. To calibrate the model efficiently without repetitively running SimMobility, we record the route attributes faced by each traveler during the simulation, and minimize the ML capture rate discrepancy between observed and simulated choices only based on these records. This approximation allows us to compute the analytical gradient with the choice model, unlike SPSA and W-SPSA.

The calibration results, i.e. the matching between simulated and observed sensor measurements, are shown in subsection C.0.2. Overall, we are able to capture the traffic and congestion patterns on the corridor.

Preparation of Tri-POP Parameters

Tri-POP's predictive models—the personalized choice model and the DTA system in DynaMIT—need to be learnt from the real world, which in this study means SimMobility. To facilitate the closed-loop study, we assume Tri-POP to have overall good but not perfect knowledge of the parameters in these predictive models. This is not an unreasonable assumption as in reality Tri-POP would be exposed to vast amount of data from the site of study, the process of which is yet difficult to simulate within a short period of time. The specific assumptions as listed as follows:

- *Personalized choice model*: Tri-POP (both in user optimization and system optimization) uses the true fixed parameters, and the random individual-specific parameters are learnt from 6 months of choice data with the procedure outlined in subsection 5.2.2.

- *Demand OD matrix*: the system optimization by DynaMIT uses a demand matrix generated by introducing noise into the actual demand in SimMobility. The level of noise is computed from day-to-day variations in the observed sensor data from the actual facility.

- *Supply parameter*: the system optimization by DynaMIT uses supply parameters calibrated based on the observed sensor data from the actual facility.

- *Online calibration parameters*: as outlined in subsection 5.2.3, DynaMIT online calibrates the above-mentioned simulation parameters as part of Tri-POP's online operation. The online calibration procedure involves parameters that specify the underlying process of how the simulation parameters evolve over time. These parameters for online calibration are estimated on the observed sensor data from the actual facility.

C.0.2 Calibration Results

To visualize the level of matching between simulated and observed sensor measurements of count and speed, the westbound corridor considered in the study is divided

into 9 parts, from upstream to downstream. In each parts, the sensor measurements from ML and GP are respectively grouped into averages.

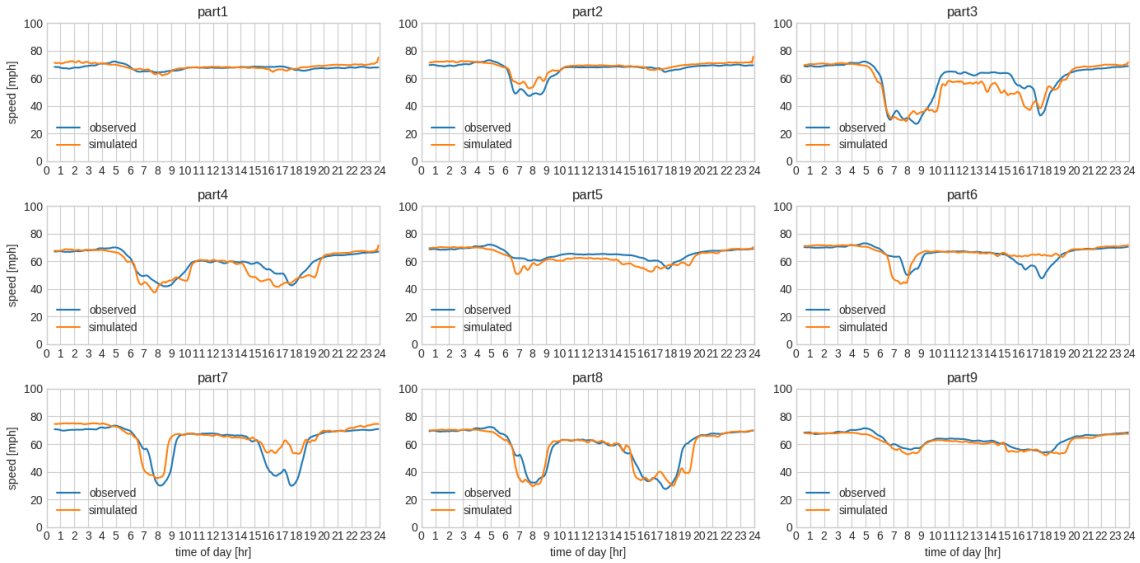

Figure C-1: Calibration for closed-loop: simulated versus observed speed (GP)

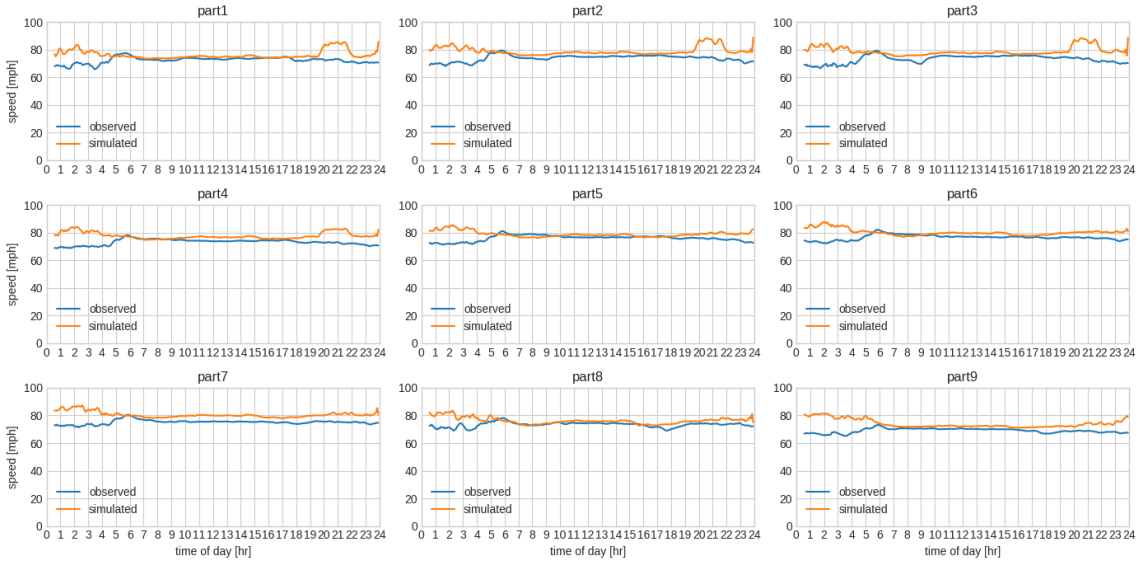

Figure C-2: Calibration for closed-loop: simulated versus observed speed (ML)

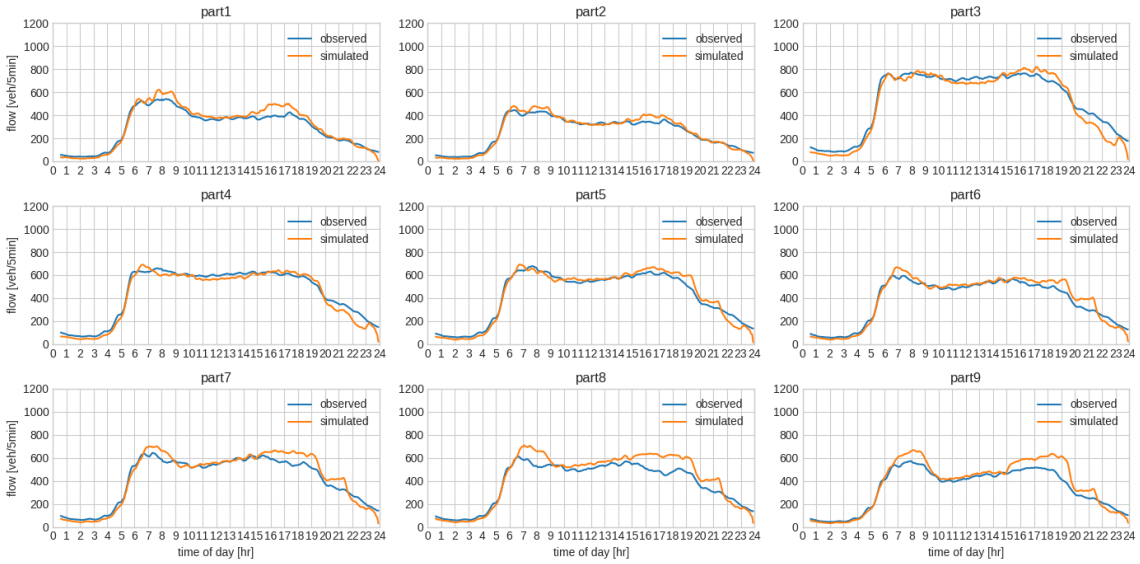

Figure C-3: Calibration for closed-loop: simulated versus observed flow (GP)

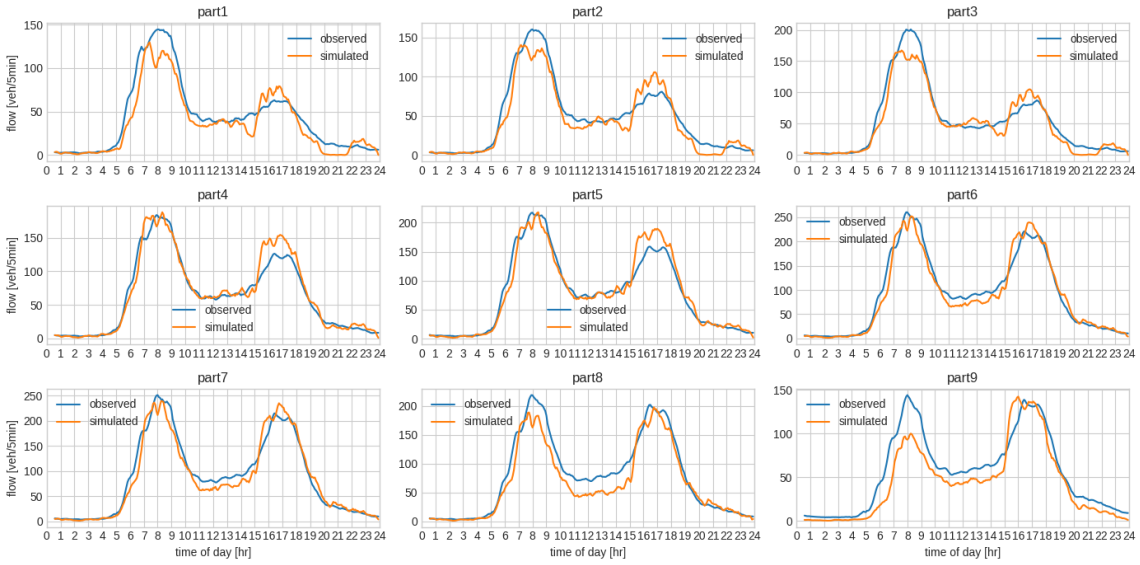

Figure C-4: Calibration for closed-loop: simulated versus observed flow (ML)

Bibliography

[1] Boston's 'soul-crushing' traffic creeping back after pandemic dip. https://www.bostonherald.com/2021/05/31/bostons-soul-crushing-traffic-creeping-back-after-pandemic-dip/. Accessed 2021-08-17.

[2] Building Lyft's marketing automation platform. https://eng.lyft.com/lyft-marketing-automation-b43b7b7537cc. Accessed 2021-02-26.

[3] Design build finance operate maintain (DBFOM) toll concessions. https://www.fhwa.dot.gov/ipd/p3/defined/new_build_facilities/dbfom_toll_concessions.aspx. Accessed 2021-11-12.

[4] Georgia officials mark 10 years since opening of first peach pass lanes in Gwinnett. https://www.gwinnettdailypost.com/local/georgia-officials-mark-10-years-since-opening-of-first-peach-pass-lanes-in-gwinnett/article_1c0e6270-230b-11ec-9d87-3bfbef7a73f8.html. Accessed 2021-11-12.

[5] Inrix: Congestion costs each American nearly 100 hours, $1,400 a year. https://inrix.com/press-releases/2019-traffic-scorecard-us/. Accessed 2021-08-17.

[6] Inrix: Downtown travel plummets 44% in 2020 amid COVID-19 pandemic. https://inrix.com/press-releases/2020-traffic-scorecard-us/. Accessed 2021-08-17.

[7] N.Y.C. roads are busy again, and so are traffic reporters. https://www.nytimes.com/2021/05/29/nyregion/city-traffic-pre-covid.html. Accessed 2021-08-17.

[8] Traffic is terrible again. here's how to get it closer to spring 2020 levels. https://www.latimes.com/business/story/2021-07-22/los-angeles-traffic-congestion-commute-pandemic. Accessed 2021-08-17.

[9] Where GoToll works. https://www.gotoll.com/where-gotoll-works. Accessed 2021-12-25.

[10] Youssef M Aboutaleb, Mazen Danaf, Yifei Xie, and Moshe Ben-Akiva. Discrete choice analysis with machine learning capabilities. *arXiv preprint arXiv:2101.10261*, 2021.

[11] Wiktor L Adamowicz. Habit formation and variety seeking in a discrete choice model of recreation demand. *Journal of Agricultural and Resource Economics*, pages 19–31, 1994.

[12] Victor Aguirregabiria and Aviv Nevo. Recent developments in empirical io: Dynamic demand and dynamic games. *Advances in economics and econometrics*, 3:53–122, 2013.

[13] Murray Aitkin and Marco Alfò. Longitudinal analysis of repeated binary data using autoregressive and random effect modelling. *Statistical Modelling*, 3(4):291–303, 2003.

[14] Alpaslan Akay. Finite-sample comparison of alternative methods for estimating dynamic panel data models. *Journal of Applied Econometrics*, 27(7):1189–1204, 2012.

[15] Greg M Allenby and Peter E Rossi. Marketing models of consumer heterogeneity. *Journal of econometrics*, 89(1-2):57–78, 1998.

[16] Greg M Allenby and Peter E Rossi. Hierarchical Bayes models. *The handbook of marketing research: Uses, misuses, and future advances*, pages 418–440, 2006.

[17] Salvatore Ammirato, Alberto Michele Felicetti, Roberto Linzalone, Antonio Palmiro Volpentesta, and Giovanni Schiuma. A systematic literature review of revenue management in passenger transportation. *Measuring Business Excellence*, 2020.

[18] Wiji Arulampalam and Mark B Stewart. Simplified implementation of the heckman estimator of the dynamic probit model and a comparison with alternative estimators. *Oxford bulletin of economics and statistics*, 71(5):659–681, 2009.

[19] Bilge Atasoy, Carlos Lima de Azevedo, Arun Prakash Akkinepally, Ravi Seshadri, Fang Zhao, Maya Abou-Zeid, and Moshe Ben-Akiva. Smart mobility via prediction, optimization and personalization. In *Demand for Emerging Transportation Systems*, pages 227–265. Elsevier, 2020.

[20] Carlos Lima Azevedo, Neeraj Milind Deshmukh, Balakumar Marimuthu, Simon Oh, Katarzyna Marczuk, Harold Soh, Kakali Basak, Tomer Toledo, Li-Shiuan Peh, and Moshe E Ben-Akiva. Simmobility short-term: An integrated microscopic mobility simulator. *Transportation Research Record*, 2622(1):13–23, 2017.

[21] Carlos Lima Azevedo, Ravi Seshadri, Song Gao, Bilge Atasoy, Arun Prakash Akkinepally, Eleni Christofa, Fang Zhao, Jessika Trancik, and Moshe Ben-Akiva. Tripod: sustainable travel incentives with prediction, optimization, and personalization. In *Proceedings of the Transportation Research Record 97th Annual Meeting*, 2018.

[22] Felix Becker, Mazen Danaf, Xiang Song, Bilge Atasoy, and Moshe Ben-Akiva. Bayesian estimator for logit mixtures with inter-and intra-consumer heterogeneity. *Transportation Research Part B: Methodological*, 117:1–17, 2018.

[23] Moshe Ben-Akiva and Maya Abou-Zeid. Methodological issues in modelling time-of-travel preferences. *Transportmetrica A: Transport Science*, 9(9):846–859, 2013.

[24] Moshe Ben-Akiva, Mark Bradley, Takayuki Morikawa, Julian Benjamin, Thomas Novak, Harmen Oppewal, and Vithala Rao. Combining revealed and stated preferences data. *Marketing Letters*, 5(4):335–349, 1994.

[25] Moshe Ben-Akiva, Haris N Koutsopoulos, Constantinos Antoniou, and Ramachandran Balakrishna. Traffic simulation with dynamit. In *Fundamentals of traffic simulation*, pages 363–398. Springer, 2010.

[26] Moshe E Ben-Akiva, Steven R Lerman, Steven R Lerman, et al. *Discrete choice analysis: theory and application to travel demand*, volume 9. MIT press, 1985.

[27] Moshe Emanuel Ben-Akiva, Daniel McFadden, Kenneth Train, et al. *Foundations of stated preference elicitation: Consumer behavior and choice-based conjoint analysis*. Now, 2019.

[28] Chandra R Bhat and Saul Castelar. A unified mixed logit framework for modeling revealed and stated preferences: formulation and application to congestion pricing analysis in the San Francisco Bay area. *Transportation Research Part B: Methodological*, 36(7):593–616, 2002.

[29] Michel Bierlaire. Biogeme: A free package for the estimation of discrete choice models. In *Swiss transport research conference*, number CONF, 2003.

[30] Richard Blundell and James L Powell. Endogeneity in nonparametric and semiparametric regression models. 2001.

[31] Transportation Research Board, Engineering National Academies of Sciences, and Medicine. *Guidelines for Implementing Managed Lanes*. The National Academies Press, Washington, DC, 2016.

[32] Maria Börjesson, Elisabetta Cherchi, and Michel Bierlaire. Within-individual variation in preferences: equity effects of congestion charges. *Transportation research record*, 2382(1):92–101, 2013.

[33] Maria Börjesson, Jonas Eliasson, and A Levander. The value of time of car drivers choosing route: evidence from the Stockholm congestion charging trial. In *2007 European Transport Conference, Leiden, Netherlands*, page 14, 2007.

[34] Daniel A Brent and Austin Gross. Dynamic road pricing and the value of time and reliability. *Journal of Regional Science*, 58(2):330–349, 2018.

[35] David Brownstone, Arindam Ghosh, Thomas F Golob, Camilla Kazimi, and Dirk Van Amelsfort. Drivers' willingness-to-pay to reduce travel time: evidence from the San Diego I-15 congestion pricing project. *Transportation Research Part A: Policy and Practice*, 37(4):373–387, 2003.

[36] Mark W Burris. Application of variable tolls on congested toll road. *Journal of transportation engineering*, 129(4):354–361, 2003.

[37] Mark W Burris and Sruthi Ashraf. Tracking the impact of a toll increase on managed lane travel behavior. *Transportation Research Record*, 2673(2):779–788, 2019.

[38] Mark W Burris and John F Brady. Unrevealed preferences: unexpected traveler response to pricing on managed lanes. *Transportation Research Record*, 2672(5):23–32, 2018.

[39] Ahmet Birol Çavdar and Nilgün Ferhatosmanoğlu. Airline customer lifetime value estimation using data analytics supported by social network information. *Journal of Air Transport Management*, 67:19–33, 2018.

[40] Danhong Cheng, Wan Li, and Sherif Ishak. Accounting for travel time reliability and trip purpose in an agent-based approach to toll pricing with dynamic feedback control: case study on I-95 managed-lanes corridor. *Transportation Research Record*, 2470(1):131–141, 2014.

[41] Biagio Ciuffo and Carlos Lima Azevedo. A sensitivity-analysis-based approach for the calibration of traffic simulation models. *IEEE Transactions on Intelligent Transportation Systems*, 15(3):1298–1309, 2014.

[42] Koray Cosguner, Tat Y Chan, and PB Seetharaman. Behavioral price discrimination in the presence of switching costs. *Marketing Science*, 36(3):426–435, 2017.

[43] Mazen Danaf, Bilge Atasoy, and Moshe Ben-Akiva. Logit mixture with inter and intra-consumer heterogeneity and flexible mixing distributions. *Journal of choice modelling*, 35:100188, 2020.

[44] Mazen Danaf, Felix Becker, Xiang Song, Bilge Atasoy, and Moshe Ben-Akiva. Online discrete choice models: Applications in personalized recommendations. *Decision Support Systems*, 119:35–45, 2019.

[45] André de Palma and Robin Lindsey. Traffic congestion pricing methodologies and technologies. *Transportation Research Part C: Emerging Technologies*, 19(6):1377–1399, 2011.

[46] Jing Dong, Hani S Mahmassani, Sevgi Erdoğan, and Chung-Cheng Lu. State-dependent pricing for real-time freeway management: Anticipatory versus reactive strategies. *Transportation Research Part C: Emerging Technologies*, 19(4):644–657, 2011.

[47] Robert Dorfman. A formula for the gini coefficient. *The review of economics and statistics*, pages 146–149, 1979.

[48] Jean-Pierre Dubé, Günter J Hitsch, and Peter E Rossi. State dependence and alternative explanations for consumer inertia. *The RAND Journal of Economics*, 41(3):417–445, 2010.

[49] Jean-Pierre Dubé, Günter J Hitsch, Peter E Rossi, and Maria Ana Vitorino. Category pricing with state-dependent utility. *Marketing Science*, 27(3):417–429, 2008.

[50] Jean-Pierre Dubé and Sanjog Misra. Personalized pricing and customer welfare. *Available at SSRN 2992257*, 2019.

[51] Jeffrey A. Dubin and Daniel L. McFadden. An econometric analysis of residential electric appliance holdings and consumption. *Econometrica*, 52(2):345–362, 1984.

[52] Peter Ebbes, Dominik Papies, and Harald J Van Heerde. The sense and nonsense of holdout sample validation in the presence of endogeneity. *Marketing Science*, 30(6):1115–1122, 2011.

[53] Tülin Erdem. A dynamic analysis of market structure based on panel data. *Marketing science*, 15(4):359–378, 1996.

[54] Amy Finkelstein. E-ztax: Tax salience and tax rates. *The Quarterly Journal of Economics*, 124(3):969–1010, 2009.

[55] Ali Reza Fotouhi. The initial conditions problem in longitudinal binary process: A simulation study. *Simulation Modelling Practice and Theory*, 13(7):566–583, 2005.

[56] Matthew Gibson and Maria Carnovale. The effects of road pricing on driver behavior and air pollution. *Journal of Urban Economics*, 89:62–73, 2015.

[57] C Angelo Guevara. Overidentification tests for the exogeneity of instruments in discrete choice models. *Transportation Research Part B: Methodological*, 114:241–253, 2018.

[58] C Angelo Guevara and Daniel Polanco. Correcting for endogeneity due to omitted attributes in discrete-choice models: the multiple indicator solution. *Transportmetrica A: Transport Science*, 12(5):458–478, 2016.

[59] C Angelo Guevara, Yue Tang, and Song Gao. The initial condition problem with complete history dependency in learning models for travel choices. *Transportation research procedia*, 23:758–771, 2017.

[60] Cristian Angelo Guevara and Moshe Ben-Akiva. Endogeneity in residential location choice models. *Transportation research record*, 1977(1):60–66, 2006.

[61] Cristian Angelo Guevara and Moshe Ben-Akiva. Addressing endogeneity in discrete choice models: Assessing control-function and latent-variable methods. In *Choice Modelling: The State-of-the-art and The State-of-practice*. Emerald Group Publishing Limited, 2010.

[62] Samarth Gupta, Ravi Seshadri, Bilge Atasoy, A Arun Prakash, Francisco Pereira, Gary Tan, and Moshe Ben-Akiva. Real-time predictive control strategy optimization. *Transportation research record*, 2674(3):1–11, 2020.

[63] Sunil Gupta, Dominique Hanssens, Bruce Hardie, Wiliam Kahn, V Kumar, Nathaniel Lin, Nalini Ravishanker, and S Sriram. Modeling customer lifetime value. *Journal of service research*, 9(2):139–155, 2006.

[64] Jerry A Hausman and Timothy F Bresnahan. *Valuation of New Goods under Perfect and Imperfect Competition*. University of Chicago Press, 2008.

[65] James J Heckman. Heterogeneity and state dependence. In *Studies in labor markets*, pages 91–140. University of Chicago Press, 1981.

[66] James J Heckman. *The incidental parameters problem and the problem of initial conditions in estimating a discrete time-discrete data stochastic process and some Monte Carlo evidence*. MIT press, 1981.

[67] Stephane Hess, Elizabeth R Greene, C Stacey Falzarano, and Mark Muriello. Pay to drive in my bus lane: a stated choice analysis for the proposed Lincoln Tunnel HOT lane into Manhattan. *Transport Policy*, 18(5):649–656, 2011.

[68] Stephane Hess and John M Rose. Allowing for intra-respondent variations in coefficients estimated on repeated choice data. *Transportation Research Part B: Methodological*, 43(6):708–719, 2009.

[69] Md Sakoat Hossan, Hamidreza Asgari, and Xia Jin. Investigating preference heterogeneity in value of time (VOT) and value of reliability (VOR) estimation for managed lanes. *Transportation Research Part A: Policy and Practice*, 94:638–649, 2016.

[70] Michael Janson and David Levinson. HOT or not: Driver elasticity to price on the MnPASS HOT lanes. *Research in Transportation Economics*, 44:21–32, 2014.

[71] Nathan Kallus and Angela Zhou. Fairness, welfare, and equity in personalized pricing. In *Proceedings of the 2021 ACM Conference on Fairness, Accountability, and Transparency*, pages 296–314, 2021.

[72] Antonis F Lentzakis, Ravi Seshadri, Arun Akkinepally, Vinh-An Vu, and Moshe Ben-Akiva. Hierarchical density-based clustering methods for tolling zone definition and their impact on distance-based toll optimization. *Transportation Research Part C: Emerging Technologies*, 118:102685, 2020.

[73] Robin Lindsey. Do economists reach a conclusion? *Econ Journal Watch*, 3(2):292–379, 2006.

[74] Xiaoyue Liu, Guohui Zhang, Yunteng Lao, and Yinhai Wang. Quantifying the attractiveness of high-occupancy toll lanes with traffic sensor data under various traffic conditions. *Transportation research record*, 2229(1):102–109, 2011.

[75] Yingyan Lou, Yafeng Yin, and Jorge A Laval. Optimal dynamic pricing strategies for high-occupancy/toll lanes. *Transportation Research Part C: Emerging Technologies*, 19(1):64–74, 2011.

[76] Lu Lu. W-SPSA: an efficient stochastic approximation algorithm for the off-line calibration of dynamic traffic assignment models, 2013.

[77] Pierre-Carl Michaud and Konstantinos Tatsiramos. Fertility and female employment dynamics in Europe: the effect of using alternative econometric modeling assumptions. *Journal of Applied Econometrics*, 26(4):641–668, 2011.

[78] Alfonso Miranda et al. Dynamic probit models for panel data: A comparison of three methods of estimation. In *United Kingdom Stata Users' Group Meetings*, volume 11, 2007.

[79] BPS Murthi and Sumit Sarkar. The role of the management sciences in research on personalization. *Management Science*, 49(10):1344–1362, 2003.

[80] Jerzy Neyman and Elizabeth L Scott. Consistent estimates based on partially consistent observations. *Econometrica: Journal of the Econometric Society*, pages 1–32, 1948.

[81] Chris D Orme. Two-step inference in dynamic non-linear panel data models. *Unpublished paper, University of Manchester*, 2001.

[82] Carolina Osorio and Bilge Atasoy. Efficient simulation-based toll optimization for large-scale networks. *Transportation Science*, 55(5):1010–1024, 2021.

[83] Venktesh Pandey and Stephen D Boyles. Dynamic pricing for managed lanes with multiple entrances and exits. *Transportation Research Part C: Emerging Technologies*, 96:304–320, 2018.

[84] Venktesh Pandey, Evana Wang, and Stephen D Boyles. Deep reinforcement learning algorithm for dynamic pricing of express lanes with multiple access locations. *Transportation Research Part C: Emerging Technologies*, 119:102715, 2020.

[85] Sunil Patil, Mark Burris, and W Douglass Shaw. Travel using managed lanes: An application of a stated choice model for Houston, Texas. *Transport Policy*, 18(4):595–603, 2011.

[86] Amil Petrin and Kenneth Train. A control function approach to endogeneity in consumer choice models. *Journal of marketing research*, 47(1):3–13, 2010.

[87] Arthur Cecil Pigou. *The economics of welfare*. Palgrave Macmillan, 1920.

[88] Sophia Rabe-Hesketh and Anders Skrondal. Avoiding biased versions of wooldridge's simple solution to the initial conditions problem. *Economics Letters*, 120(2):346–349, 2013.

[89] Peter E Rossi, Greg M Allenby, and Rob McCulloch. *Bayesian statistics and marketing*. John Wiley & Sons, 2012.

[90] Peter E Rossi, Robert E McCulloch, and Greg M Allenby. The value of purchase history data in target marketing. *Marketing Science*, 15(4):321–340, 1996.

[91] Sandeep Saharan, Seema Bawa, and Neeraj Kumar. Dynamic pricing techniques for intelligent transportation system in smart cities: A systematic review. *Computer Communications*, 150:603–625, 2020.

[92] Wafaa Saleh and Gerd Sammer. *Travel demand management and road user pricing: success, failure and feasibility*. Routledge, 2016.

[93] Peter Seele, Claus Dierksmeier, Reto Hofstetter, and Mario D Schultz. Mapping the ethicality of algorithmic pricing: A review of dynamic and personalized pricing. *Journal of Business Ethics*, 170(4):697–719, 2021.

[94] Benjamin Reed Shiller et al. *First degree price discrimination using big data*. Brandeis Univ., Department of Economics, 2013.

[95] Anders Skrondal and Sophia Rabe-Hesketh. Handling initial conditions and endogenous covariates in dynamic/transition models for binary data with unobserved heterogeneity. *Journal of the Royal Statistical Society: Series C (Applied Statistics)*, 63(2):211–237, 2014.

[96] Kenneth A Small, Clifford Winston, and Jia Yan. Uncovering the distribution of motorists' preferences for travel time and reliability. *Econometrica*, 73(4):1367–1382, 2005.

[97] Adam Smith. *The wealth of nations*. 1776.

[98] Mark B Stewart. The interrelated dynamics of unemployment and low-wage employment. *Journal of applied econometrics*, 22(3):511–531, 2007.

[99] Richard S Sutton and Andrew G Barto. *Reinforcement learning: An introduction*. MIT press, 2018.

[100] Tomer Toledo, Omar Mansour, and Jack Haddad. Simulation-based optimization of HOT lane tolls. *Transportation Research Procedia*, 6:189–197, 2015.

[101] Tomer Toledo and Shayma Sharif. The effect of information on drivers' toll lane choices and travel times expectations. *Transportation Research Part F: Traffic Psychology and Behaviour*, 62:149–159, 2019.

[102] Kenneth E Train. *Discrete choice methods with simulation*. Cambridge university press, 2009.

[103] JI Van der Rest, Alan M Sears, Li Miao, and Lorna Wang. A note on the future of personalized pricing: cause for concern. *Journal of Revenue and Pricing Management*, 19(2):113–118, 2020.

[104] J Miguel Villas-Boas and Russell S Winer. Endogeneity in brand choice models. *Management science*, 45(10):1324–1338, 1999.

[105] Joan L Walker, Moshe Ben-Akiva, and Denis Bolduc. Identification of parameters in normal error component logit-mixture (NECLM) models. *Journal of Applied Econometrics*, 22(6):1095–1125, 2007.

[106] Michael D Wittman and Peter P Belobaba. Customized dynamic pricing of airline fare products. *Journal of Revenue and Pricing Management*, 17(2):78–90, 2018.

[107] Nick Wood, Trey Baker, Maarit Moran, Gavin Pritchard, Timothy J Lomax, Max Steadman, Brianne Glover, Brian Dell, et al. Managed lanes in texas: a review of the application of congestion pricing. 2016.

[108] Jeffrey M Wooldridge. Simple solutions to the initial conditions problem in dynamic, nonlinear panel data models with unobserved heterogeneity. *Journal of applied econometrics*, 20(1):39–54, 2005.

[109] Jeffrey M Wooldridge. Control function methods in applied econometrics. *Journal of Human Resources*, 50(2):420–445, 2015.

[110] Yifei Xie, Mazen Danaf, Carlos Lima Azevedo, Arun Prakash Akkinepally, Bilge Atasoy, Kyungsoo Jeong, Ravi Seshadri, and Moshe Ben-Akiva. Behavioral modeling of on-demand mobility services: general framework and application to sustainable travel incentives. *Transportation*, 46(6):2017–2039, 2019.

[111] Mengmeng Ye. Dynamic pricing for managed lanes: Synthesis of current best practices and framework for integration with connected and automated vehicles, 2017.

[112] Yafeng Yin and Yingyan Lou. Dynamic tolling strategies for managed lanes. *Journal of Transportation Engineering*, 135(2):45–52, 2009.

[113] Guohui Zhang, Xiaolei Ma, and Yinhai Wang. Self-adaptive tolling strategy for enhanced high-occupancy toll lane operations. *IEEE Transactions on Intelligent Transportation Systems*, 15(1):306–317, 2013.

[114] Haizheng Zhang, Ravi Seshadri, A Arun Prakash, Constantinos Antoniou, Francisco C Pereira, and Moshe Ben-Akiva. Improving the accuracy and efficiency of online calibration for simulation-based dynamic traffic assignment. *Transportation Research Part C: Emerging Technologies*, 128:103195, 2021.

[115] Yundi Zhang. *Real-time personalized toll optimization based on traffic predictions*. PhD thesis, Massachusetts Institute of Technology, 2019.

[116] Yundi Zhang, Bilge Atasoy, Arun Akkinepally, and Moshe Ben-Akiva. Dynamic toll pricing using dynamic traffic assignment system with online calibration. *Transportation Research Record*, 2673(10):532–546, 2019.